Universidad de Valladolid

ESCUELA DE INGENIERÍAS INDUSTRIALES

UNIVERSIDAD DE VALLADOLID

ESCUELA DE INGENIERIAS INDUSTRIALES

Máster en ingeniería industrial

# Reversible solid oxide cell as energy storage system


Autor:

Abad Moreno, Felipe Jose

Blanca Giménez Olavarría

Università degli studi di Perugia


Valladolid, Junio 2016.

TFM REALIZADO EN PROGRAMA DE INTERCAMBIO

---

TÍTULO: Reversible solid oxide cell as energy storage system

ALUMNO: Felipe Jose Abad Moreno

FECHA: 23/06/2016

CENTRO: Dipartimento di Ingegneria industriale

TUTOR: Giovanni Cinti

## Resumen:

El objetivo principal de este trabajo fin de master es analizar la operación de una pila de combustible de óxido sólido como sistema de almacenamiento de energía. El sistema recibe el nombre de reSOC por las siglas en inglés (reversible solid oxide cell). La misma pila trabaja como electrolizador para producir hidrogeno mediante energía eléctrica, y como pila de combustible para producir energía eléctrica mediante hidrogeno. El estudio sobre la operación del sistema se ha realizado en el laboratorio de pila de combustible (fclab) de la università degli studi di Perugia. El trabajo consta de una introducción sobre pilas de combustible y sobre el proceso de electrolisis, una descripción detallada del banco de pruebas donde se realiza la simulación, y de una descripción numérica y gráfica de los ensayos realizados en el sistema, haciendo hincapié en los resultados y conclusiones obtenidos respecto a la operación y diseño del mismo.

**Palabras clave:** Pila, combustible, hidrogeno, electrolisis, almacenamiento.

## Abstract:

The main goal of this master thesis is to evaluate the operation of a solid oxide fuel cell as energy storage system. The system is called reSOC (reversible solid oxide cell). The same cell works as an electrolyzer to produce hydrogen from electric energy (SOEC), and as a fuel cell to produce electric energy from hydrogen (SOFC). The study of the system operation has been done in the fuel cell laboratory (fclab) of the università degli studi di Perugia. The thesis consists of an introduction about fuel cells and the electrolysis process, a detailed description of the test rig where the simulation has been performed, and a numeric and graphic description of the essays made in the system, making reference to the results and conclusions obtained regarding the operation and design of the system.

**Keywords:** Cell, fuel, hydrogen, electrolysis, storage.

# Contents

# List of Figures

# 1. Introduction

The first section of this thesis is a summary of literature review of different aspects of the system tested in the laboratory. The section is divided in three subsections which represent both operating modes of the stack as well as the main goal of the system. The first one makes reference to fuel cells in general, from the operating principle, applications, theoretical background, etc. The second one talks about the two kinds of electrolyzers and a comparative summary among them. The last subsection makes reference to the importance of energy storage and why reSOC can be so useful, theoretical aspects of reSOC are also explained.

## 1.1. Fuel cells

Fuel cells are electrochemical devices that convert chemical energy in fuels into electrical energy directly, producing power with high efficiency and low environmental impact.

Because the intermediate steps of producing heat and mechanical work typical of most conventional power generation methods are avoided, fuel cells are not limited by thermodynamic limitations of heat engines such as the Carnot efficiency. In addition, because combustion is avoided, fuel cells produce power with minimal pollutant emission. However, unlike batteries the reductant and oxidant in fuel cells must be continuously replaced to allow continuous operation. Fuel cells bear significant resemblance to electrolyzers. In fact, some fuel cells operate in reverse as electrolyzers, yielding a reversible fuel cell that can be used for energy storage.

Though fuel cells could, in principle, process a wide variety of fuels and oxidants, of most interest today are those fuel cells that use common fuels (or their derivatives) or hydrogen as a reductant, and ambient air as the oxidant.

Fuel cell power systems comprise a number of components grouped in two:

- Stacks, in which individual cells are modularly combined by electrically connecting the cells to form units with the desired output capacity. Electrochemical reactions take place in single cells.
- Balance of plant which comprises components that provide feedstream conditioning (including a fuel processor if needed), thermal management, and electric power conditioning among other ancillary and interface functions [1].

### 1.1.1. Fuel cell Structure

Single cell

Single cell forms the core of a fuel cell. These devices convert the chemical energy contained in a fuel electrochemically into electrical energy. The basic physical structure,

or building block, of a fuel cell consists of an electrolyte layer in contact with an anode and a cathode on either side. A schematic representation of a unit cell with the reactant/product gases and the ion conduction flow directions through the cell is shown in figure 1.

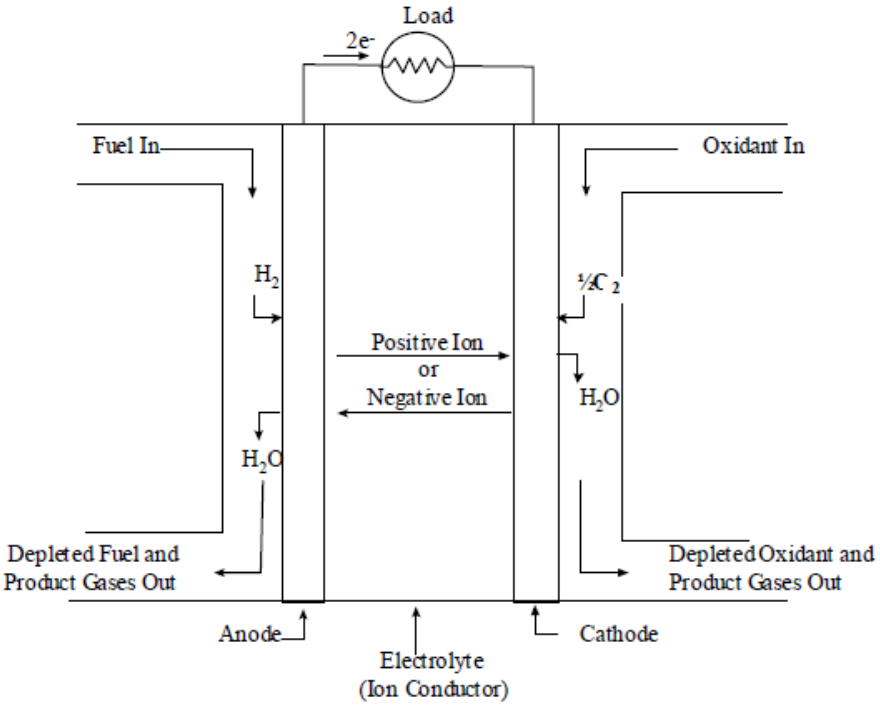


*Figure 1: Schematic of an Individual Fuel Cell*

In a typical fuel cell, fuel is fed continuously to the anode (negative electrode) and an oxidant (often oxygen from air) is fed continuously to the cathode (positive electrode). The electrochemical reactions take place at the electrodes to produce an electric current through the electrolyte, while driving a complementary electric current that performs work on the load. Although a fuel cell is similar to a typical battery in many ways, it differs in several respects. The battery is an energy storage device in which all the energy available is stored within the battery itself (at least the reductant). The battery will cease to produce electrical energy when the chemical reactants are consumed (i.e., discharged). A fuel cell, on the other hand, is an energy conversion device in which fuel and oxidant are supplied continuously. In principle, the fuel cell produces power for as long as fuel is supplied.

Fuel cells are classified according to the choice of electrolyte and fuel, which in turn determine the electrode reactions and the type of ions that carry the current across the electrolyte. In theory, any substance capable of chemical oxidation that can be supplied continuously (as a fluid) can be burned galvanically as fuel at the anode of a fuel cell. Similarly, the oxidant can be any fluid that can be reduced at a sufficient rate. Though the direct use of conventional fuels in fuel cells would be desirable, most fuel cells under development today use gaseous hydrogen, or a synthesis gas rich in hydrogen, as a fuel. Hydrogen has a high reactivity for anode reactions, and can be produced chemically from a wide range of fossil and renewable fuels, as well as via

electrolysis. For similar practical reasons, the most common oxidant is gaseous oxygen, which is readily available from air. For space applications, both hydrogen and oxygen can be stored compactly in cryogenic form, while the reaction product is only water [1].

## Fuel Cell Stacking

For most practical fuel cell applications, unit cells must be combined in a modular fashion into a cell stack to achieve the voltage and power output level required for the application. Generally, the stacking involves connecting multiple unit cells in series via electrically conductive interconnects. Different stacking arrangements have been developed.

The most common fuel cell stack design is the so-called planar-bipolar arrangement (figure 2 depicts a PAFC). Individual unit cells are electrically connected with interconnects. Because of the configuration of a flat plate cell, the interconnect becomes a separator plate with two functions:

- To provide an electrical series connection between adjacent cells, specifically for flat plate cells.
- To provide a gas barrier that separates the fuel and oxidant of adjacent cells.

In many planar-bipolar designs, the interconnect also includes channels that distribute the gas flow over the cells. The planar-bipolar design is electrically simple and leads to short electronic current paths (which help to minimize cell resistance) [1].

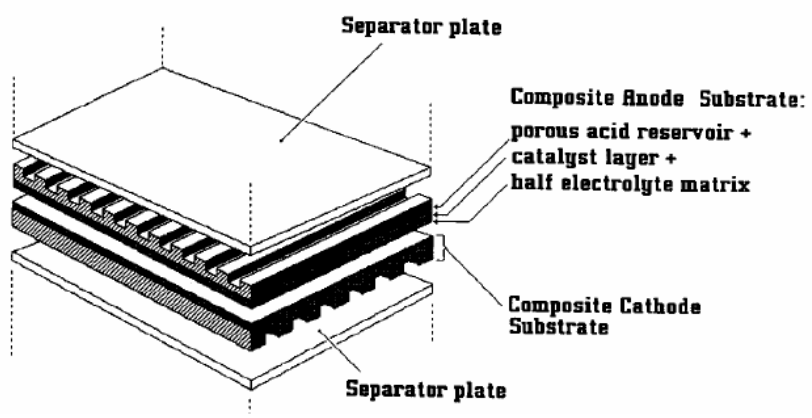


*Figure 2: Expanded View of a Basic Fuel Cell Unit in a Fuel Cell Stack*

## Fuel Cell Systems

In addition to the stack, practical fuel cell systems require several other sub-systems and components; the so-called balance of plant (BoP). Together with the stack, the BoP forms the fuel cell system. The precise arrangement of the BoP depends heavily on the fuel cell type, the fuel choice, and the application. In addition, specific operating conditions and requirements of individual cell and stack designs determine the characteristics of the BoP. Still, most fuel cell systems contain:

- Fuel preparation. Except when pure fuels (such as pure hydrogen) are used, fuel preparation is required, usually involving the removal of impurities and thermal conditioning. In addition, many fuel cells that use fuels other than pure hydrogen require fuel processing, such as reforming, in which the fuel is reacted with some oxidant (usually steam or air) to form a hydrogen-rich anode feed mixture.
- Air supply. In most practical fuel cell systems, this includes air compressors or blowers as well as air filters.
- Thermal management. All fuel cell systems require careful management of the fuel cell stack temperature.
- Water management. Water is needed in some parts of the fuel cell, while overall water is a reaction product. To avoid having to feed water in addition to fuel, and to ensure smooth operation, water management systems are required in most fuel cell systems.
- Electric power conditioning equipment. Since fuel cell stacks provide a variable DC voltage output that is typically not directly usable for the load, electric power conditioning is typically required.

While perhaps not the focus of most development effort, the BoP represents a significant fraction of the weight, volume, and cost of most fuel cell systems.

Figure 3 shows a simple rendition of a fuel cell power plant. Beginning with fuel processing, a conventional fuel (natural gas, other gaseous hydrocarbons, methanol, naphtha, or coal) is cleaned, then converted into a gas containing hydrogen. Energy conversion occurs when dc electricity is generated by means of individual fuel cells combined in stacks or bundles. A varying number of cells or stacks can be matched to a particular power application. Finally, power conditioning converts the electric power from dc into regulated dc or ac for consumer use [1].

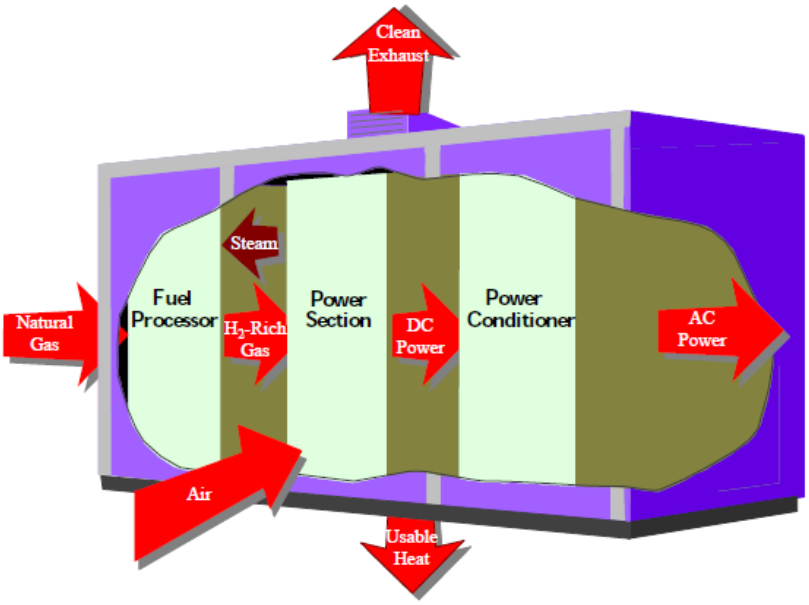


*Figure 3: Fuel Cell Power Plant Major Processes*

### 1.1.2. Fuel Cell Types

A variety of fuel cells are in different stages of development. The most common classification of fuel cells is by the type of electrolyte used in the cells and includes 1) polymer electrolyte fuel cell (PEFC), 2) alkaline fuel cell (AFC), 3) phosphoric acid fuel cell (PAFC), 4) molten carbonate fuel cell (MCFC), and 5) solid oxide fuel cell (SOFC). Broadly, the choice of electrolyte dictates the operating temperature range of the fuel cell. The operating temperature and useful life of a fuel cell dictate the physicochemical and thermomechanical properties of materials used in the cell components (electrodes, electrolyte, interconnect, current collector, etc.). Aqueous electrolytes are limited to temperatures of about 200°C or lower because of their high vapour pressure and rapid degradation at higher temperatures. The operating temperature also plays an important role indicating the degree of fuel processing required. In low-temperature fuel cells, all the fuel must be converted to hydrogen prior to entering the fuel cell. In addition, the anode catalyst in low temperature fuel cells (mainly platinum) is strongly poisoned by CO. In high-temperature fuel cells, CO and even $CH_4$ can be internally converted to hydrogen or even directly oxidized electrochemically. Table 1 provides an overview of the key characteristics of the main fuel cell types.

Although all kind of fuel cells are described below, this thesis is only focused on solid oxide fuel cell (SOFC), whose main characteristic are described in detail in later sections [1].

*Table 1: Summary of Major Differences of the Fuel Cell Types*

| | PEFC | AFC | PAFC | MCFC | SOFC |
|---|---|---|---|---|---|
| **Electrolyte** | Hydrated Polymeric Ion Exchange Membranes | Mobilized or Immobilized Potassium Hydroxide in asbestos matrix | Immobilized Liquid Phosphoric Acid in SiC | Immobilized Liquid Molten Carbonate in $LiAlO_2$ | Perovskites (Ceramics) |
| **Electrodes** | Carbon | Transition metals | Carbon | Nickel and Nickel Oxide | Perovskite and perovskite / metal cermet |
| **Catalyst** | Platinum | Platinum | Platinum | Electrode material | Electrode material |
| **Interconnect** | Carbon or metal | Metal | Graphite | Stainless steel or Nickel | Nickel, ceramic, or steel |
| **Operating temperature** | 40 – 80°C | 65°C – 220°C | 205°C | 650°C | 600-1000°C |
| **Charge Carrier** | H+ | OH- | H+ | CO3= | O= |
| **External reformer for hydrocarbon** | Yes | Yes | Yes | No, for some fuels | No, for some fuels and |

| | | | | | |
|---|---|---|---|---|---|
| **fuels** | | | | | cell designs |
| **External shift conversion of CO to hydrogen** | Yes, plus purification to remove trace CO | Yes, plus purification to remove CO and $CO_2$ | Yes | No | No |
| **Prime Cell Components** | Carbon-based | Carbon-based | Graphite-based | Stainless-based | Ceramic |
| **Product Water management** | Evaporative | Evaporative | Evaporative | Gaseous Product | Gaseous Product |
| **Product heat management** | Process Gas + Liquid Cooling Medium | Process Gas + Electrolyte Circulation | Process Gas + Liquid cooling medium or steam generation | Internal Reforming + Process Gas | Internal Reforming + Process Gas |

The overall reactions for various types of fuel cells are presented in table 2.

*Table 2: Electrochemical Reactions in Fuel Cells*

| Fuel Cell | Anode Reaction | Cathode Reaction |
|---|---|---|
| Polymer Electrolyte and Phosphoric Acid | $H_2 \rightarrow 2H^+ + 2e^-$ | $\frac{1}{2}O_2 + 2H^+ + 2e^- \rightarrow H_2O$ |
| Alkaline | $H_2 + 2(OH)^- \rightarrow 2H_2O + 2e^-$ | $\frac{1}{2}O_2 + H_2O + 2e^- \rightarrow 2(OH)^-$ |
| Molten Carbonate | $H_2 + CO_3^- \rightarrow H_2O + CO_2 + 2e^-$<br>$CO + CO_3^- \rightarrow 2CO_2 + 2e^-$ | $\frac{1}{2}O_2 + CO_2 + 2e^- \rightarrow CO_3^-$ |
| Solid Oxide | $H_2 + O^= \rightarrow H_2O + 2e^-$<br>$CO + O^= \rightarrow CO_2 + 2e^-$<br>$CH_4 + 4O^= \rightarrow 2H_2O + CO_2 + 8e^-$ | $\frac{1}{2}O_2 + 2e^- \rightarrow O^=$ |

## Polymer Electrolyte Fuel Cell (PEFC)

The electrolyte in this fuel cell is an ion exchange membrane (fluorinated sulfonic acid polymer or other similar polymer) that is an excellent proton conductor. The only liquid in this fuel cell is water; thus, corrosion problems are minimal. Typically, carbon electrodes with platinum electro-catalyst are used for both anode and cathode and with either carbon or metal interconnects.

Water management in the membrane is critical for efficient performance; the fuel cell must operate under conditions where the by-product water does not evaporate faster than it is produced because the membrane must be hydrated. Because of the limitation on the operating temperature imposed by the polymer, usually less than 100°C, but more typically around 60 to 80°C. , and because of problems with water balance, a $H_2$-rich gas with minimal or no CO (a poison at low temperature) is used. Higher catalyst loading (Pt in

most cases) than that used in PAFCs is required for both the anode and cathode. Extensive fuel processing is required with other fuels, as the anode is easily poisoned by even trace levels of CO, sulphur species, and halogens.

PEFCs are being pursued for a wide variety of applications, especially for prime power for fuel cell vehicles (FCVs). As a consequence of the high interest in FCVs and hydrogen, the investment in PEFC over the past decade easily surpasses all other types of fuel cells combined. Although significant development of PEFC for stationary applications has taken place, many developers now focus on automotive and portable applications [1].

## Alkaline Fuel Cell (AFC)

The electrolyte in this fuel cell is concentrated (85 wt percent) KOH in fuel cells operated at high temperature (~250°C), or less concentrated (35 to 50 wt percent) KOH for lower temperature (<120°C) operation. The electrolyte is retained in a matrix (usually asbestos), and a wide range of electro-catalysts can be used (Ni, Ag, metal oxides, spinels, and noble metals). The fuel supply is limited to non-reactive constituents except for hydrogen. CO is a poison, and $CO_2$ will react with the KOH to form $K2CO_3$, thus altering the electrolyte. Even the small amount of $CO_2$ in air must be considered a potential poison for the alkaline cell. Generally, hydrogen is considered as the preferred fuel for AFC, although some direct carbon fuel cells use (different) alkaline electrolytes.

The AFC was one of the first modern fuel cells to be developed, it has enjoyed considerable success in space applications, but its terrestrial application has been challenged by its sensitivity to $CO_2$. Still, some developers in the U.S. and Europe pursue AFC for mobile and closed-system (reversible fuel cell) applications [1].

## Phosphoric Acid Fuel Cell (PAFC)

Phosphoric acid, concentrated to 100 percent, is used as the electrolyte in this fuel cell, which typically operates at 150 to 220°C. At lower temperatures, phosphoric acid is a poor ionic conductor, and CO poisoning of the Pt electro-catalyst in the anode becomes severe. The relative stability of concentrated phosphoric acid is high compared to other common acids; consequently the PAFC is capable of operating at the high end of the acid temperature range (100 to 220°C). In addition, the use of concentrated acid (100 percent) minimizes the water vapour pressure so water management in the cell is not difficult. The matrix most commonly used to retain the acid is silicon carbide, and the electro-catalyst in both the anode and cathode is Pt.

PAFCs are mostly developed for stationary applications. Both in the U.S. and Japan, hundreds of PAFC systems were produced, sold, and used in field tests and demonstrations. It is still one of the few fuel cell systems that are available for purchase [1].

### Molten Carbonate Fuel Cell (MCFC)

The electrolyte in this fuel cell is usually a combination of alkali carbonates, which is retained in a ceramic matrix of $LiAlO_2$. The fuel cell operates at 600 to 700°C where the alkali carbonates form a highly conductive molten salt, with carbonate ions providing ionic conduction. At the high operating temperatures in MCFCs, Ni (anode) and nickel oxide (cathode) are adequate to promote reaction. Noble metals are not required for operation, and many common hydrocarbons fuels can be reformed internally.

The focus of MCFC development has been larger stationary and marine applications, where the relatively large size and weight of MCFC and slow start-up time are not an issue. MCFCs are under development for use with a wide range of conventional and renewable fuels. MCFC-like technology is also considered for DCFC. After the PAFC, MCFCs have been demonstrated most extensively in stationary applications [1].

### Solid Oxide Fuel Cell (SOFC)

The electrolyte in this fuel cell is a solid, nonporous metal oxide, usually Y2O3-stabilized $ZrO_2$. The cell operates at 600-1000°C where ionic conduction by oxygen ions takes place. Typically, the anode is Co-$ZrO_2$ or Ni-$ZrO_2$ cermet, and the cathode is Sr-doped LaMnO3.

Early on, the limited conductivity of solid electrolytes required cell operation at around 1000°C, but more recently thin-electrolyte cells with improved cathodes have allowed a reduction in operating temperature to 650 – 850°C. Some developers have been attempting to push a SOFC operating temperature even lower, which has allowed the development of compact and high-performance SOFC, which utilized relatively low-cost construction materials.

Concerted stack development efforts have considerably advanced the knowledge and development of thin-electrolyte planar SOFC. As a consequence of the performance improvements, SOFCs are now considered for a wide range of applications, including stationary power generation, mobile power, auxiliary power for vehicles, and specialty applications [1].

This fuel cell is the main topic of this thesis because is one of the most developed cells nowadays, so it is developed in detail in later sections.

## 1.1.3. Fuel cell applications

The major applications for fuel cells are as stationary electric power plants, including cogeneration units; as motive power for vehicles, and as on-board electric power for space vehicles or other closed environments. Derivative applications will be summarized.

## Stationary Electric Power

One characteristic of fuel cell systems is that their efficiency is nearly unaffected by size. This means that small, relatively high efficient power plants can be developed, thus avoiding the higher cost exposure associated with large plant development. As a result, initial stationary plant development has been focused on several hundred kW to low MW capacity plants. Smaller plants (several hundred kW to 1 to 2 MW) can be sited at the user's facility and are suited for cogeneration operation. Larger, dispersed plants (1 to 10 MW) are likely to be used for distributed generation. The plants are fuelled primarily with natural gas. Once these plants are commercialized and price improvements materialize, fuel cells will be considered for large base-load plants because of their high efficiency. The base-load plants could be fuelled by natural gas or coal. The fuel product from a coal gasifier, once cleaned, is compatible for use with fuel cells. Systems integration studies show that high temperature fuel cells closely match coal gasifier operation [1].

## Distributed Generation

Distributed generation involves small, modular power systems that are sited at or near their point of use. The typical system is less than 30 MW, used for generation or storage, and extremely clean. Examples of technologies used in distributed generation include gas turbines and reciprocating engines, biomass-based generators, solar power and photovoltaic systems, fuel cells, wind turbines, micro-turbines, and flywheel storage devices.

Fuel cells, one of the emerging technologies in distributed generation, have been hindered by high initial costs. However, costs are expected to decline as manufacturing capacity and capability increase and designs and integration improve. The fuel cell systems offer many potential benefits as a distributed generation system. They are small and modular, and capital costs are relatively insensitive to scale. This makes them ideal candidates for diverse applications where they can be matched to meet specific load requirements. The systems are unobtrusive, with very low noise levels and negligible air emissions. These qualities enable them to be placed close to the source of power demand. Fuel cells also offer higher efficiencies than conventional plants. The efficiencies can be enhanced by using the quality waste heat derived from the fuel cell reactions for combined heat and power and combined-cycle applications [1].

## Vehicle Motive Power

Since the late 1980s, there has been a strong push to develop fuel cells for use in light-duty and heavy-duty vehicle propulsion. A major drive for this development is the need for clean, efficient cars, trucks, and buses that operate on conventional fuels (gasoline, diesel), as well as renewable and alternative fuels (hydrogen, methanol, ethanol, natural gas, and other hydrocarbons). With hydrogen as the on-board fuel, these would be zero-emission vehicles. With on-board fuels other than hydrogen, the fuel cell systems would use an appropriate fuel processor to convert the fuel to hydrogen, yielding vehicle power trains with very low acid gas emissions and high efficiencies. Further, such

vehicles offer the advantages of electric drive and low maintenance because of few moving parts.

The major activity in transportation fuel cell development has focused on the polymer electrolyte fuel cell (PEFC) [1].

### 1.1.4. Fuel cell performance

The purpose of this section is to describe the chemical and thermodynamic relations governing fuel cells and how operating conditions affect their performance.

The maximum electrical work (Wel) obtainable in a fuel cell operating at constant temperature and pressure is given by the change in Gibbs free energy (ΔG) of the electrochemical reaction:

$$Wel = \Delta G = -n * F * E$$

Where n is the number of electrons participating in the reaction, F is Faraday's constant (96,487 coulombs/g-mole electron), and E is the ideal potential of the cell.

The Gibbs free energy change is also given by the following state function:

$$\Delta G = \Delta H - T\Delta S$$

Where ΔH is the enthalpy change and ΔS is the entropy change. The total thermal energy available is ΔH. The available free energy is equal to the enthalpy change less the quantity TΔS which represents the unavailable energy resulting from the entropy change within the system.

The amount of heat that is produced by a fuel cell operating reversibly is TΔS. Reactions in fuel cells that have negative entropy change generate heat (such as hydrogen oxidation), while those with positive entropy change (such as direct solid carbon oxidation) may extract heat from their surroundings if the irreversible generation of heat is smaller than the reversible absorption of heat.

The Gibbs free energy change of reaction can be expressed by the equation:

$$\Delta G = \Delta G^0 + RTln\frac{\prod[reactant\ fugacity]}{\prod[product\ fugacity]}$$

ΔG° is the Gibbs free energy change of reaction at the standard state pressure (1 atm) and at temperature T.

The general form of the Nernst equation is:

$$E = E^0 + \frac{RT}{nF}ln\frac{\prod[reactant\ fugacity]}{\prod[product\ fugacity]}$$

The reversible potential of a fuel cell at temperature T, is calculated from ΔG° for the cell reaction at that temperature.

$$V_{rev} = \frac{\Delta G}{nF}$$

The Nernst potential, E, gives the ideal open circuit cell potential (OCV). This potential sets the upper limit or maximum performance achievable by a fuel cell, and provides a relationship between the ideal standard potential (E°) for the cell reaction and the ideal equilibrium potential (E) at other partial pressures of reactants and products [1].

## Normal performance

Useful amounts of work (electrical energy) are obtained from a fuel cell only when a reasonably current is drawn, but the actual potential is decreased from its equilibrium potential because of irreversible losses, which are divided in three groups as are represented in the figure 4:

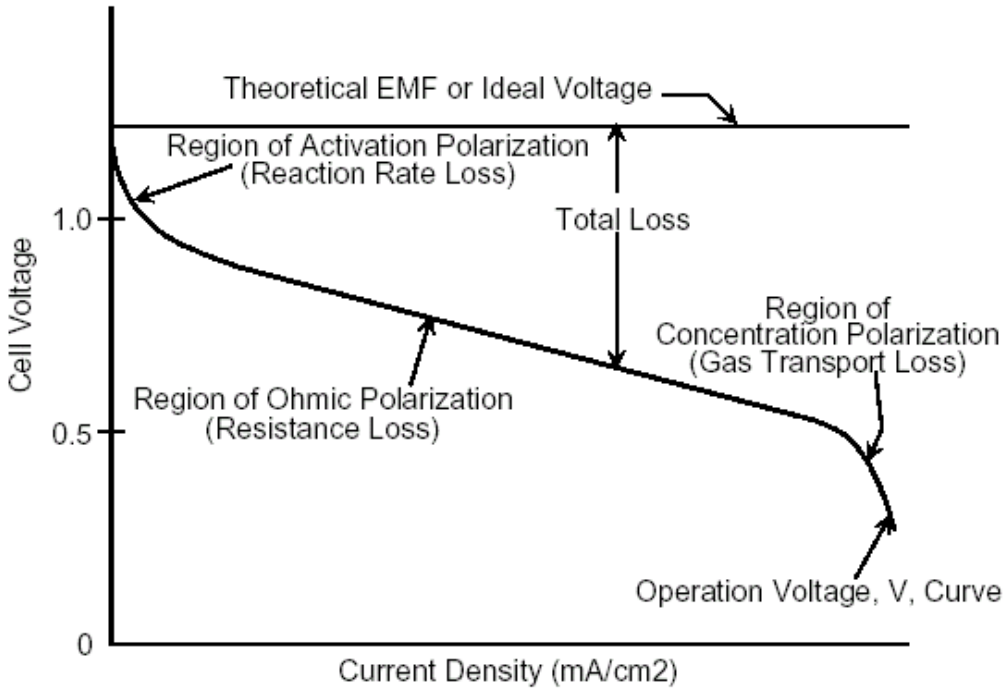


*Figure 4: Ideal and actual fuel cell voltage/current characteristic*

- Activation-related losses, which are directly related to the rates of electrochemical reactions. In the case of an electrochemical reaction ηact is described by the general form of the Tafel equation:

$$\eta_{act} = \frac{RT}{\alpha nF} ln \frac{i}{i_0}$$

Where α is the electron transfer coefficient of the reaction at the electrode being addressed, and io is the exchange current density.

- Ohmic losses, which occur because of resistance to the flow of ions in the electrolyte and resistance to flow of electrons through the electrode materials. Because both the electrolyte and fuel cell electrodes obey Ohm's law, the ohmic losses can be expressed by:

$$\eta_{ohm} = iR$$

Where i is the current flowing through the cell, and R is the total cell resistance, which includes electronic, ionic, and contact resistance

$$R = R_{electronic} + R_{ionic} + R_{contact}$$

The ohmic resistance normalized by the active cell area is the Area Specific Resistance (ASR). ASR has the units Ω*cm$^2$ and decreases with temperature.

$$ASR = \frac{\Delta V}{\Delta J}$$

- Concentration polarization, mass-transport-related losses, as reactants are consumed at the electrode by electrochemical reaction, there is a loss of potential due to the inability of the surrounding material to maintain the initial concentration of the bulk fluid. As a consequence, a concentration gradient is formed which drives the mass transport process. For gas-phase fuel cells, the rate of mass transport to an electrode surface in many cases can be described by Fick's first law of diffusion:

$$i = \frac{nFD(C_B - C_S)}{\delta}$$

D = diffusion coefficient of the reacting species.

$\delta$ = thickness of the diffusion layer.

$C_B$ = is its bulk concentration.

$C_Z$ = surface concentration.

Figure 5 shows a summary of the three kinds of losses there are in a fuel cell, although depending on the cell type, some are more noticeable than others [1] [2].

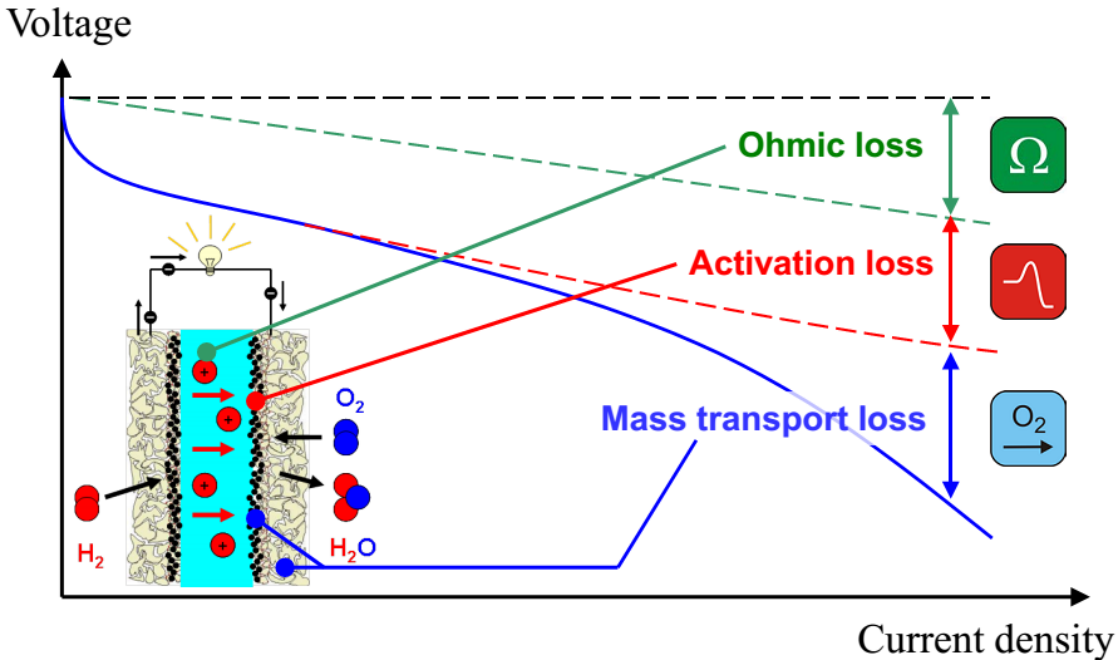


*Figure 5: Summary of the losses in the cell*

## Cell efficiency

The thermal efficiency of a fuel conversion device is defined as the amount of useful energy produced relative to the change in enthalpy, ΔH, between the product and feed streams.

$$\eta = \frac{Useful\ power}{entalphy\ variation}$$

Conventionally, chemical (fuel) energy is first converted to heat, which is then converted to mechanical energy, which can then be converted to electrical energy. For the thermal to mechanical conversion, a heat engine is conventionally used. Carnot showed that the maximum efficiency of such an engine is limited by the ratio of the absolute temperatures at which heat is rejected and absorbed, respectively.

Fuel cells convert chemical energy directly into electrical energy. In the ideal case of an electrochemical converter, such as a fuel cell, the change in Gibbs free energy, ΔG, of the reaction is available as useful electric energy at the temperature of the conversion. So cell efficiency is the ration between outlet power (electrical) and inlet power (fuel energy):

$$\eta = \frac{P_{out}}{P_{in}} = \frac{P_e}{LHV_{H_2} * H_2} = \frac{I * V}{n_{H_2} \Delta H}$$

The efficiency is divided in three parameters:

- The reversible efficiency, which is the ideal efficiency of a fuel cell (operating reversibly), it is a theoretical value:

$$\eta_{rev} = \frac{\Delta G_{rev}}{\Delta H_{rev}} = \frac{1 - T\Delta S_r}{\Delta H_r}$$

- The voltage efficiency, which makes reference to the similarity between the Vcell, and the $E_0$, It depends on the materials of the cell and on operative conditions (current density, utilization of fuel).

$$\eta_v = \frac{V}{E_0}$$

The cell voltage includes the contribution of the anode and cathode potentials and ohmic polarization:

$$V_{cell} = V_{cathode} - V_{anode} - iR$$

- The fuel utilization factor, which determines the $H_2$ consumed respect the $H_2$ introduced inside the stack. It depends on how well the geometrical design is and how well $H_2$ is distributed inside the stack.

$$U_f = \frac{H_{2\ in} - H_{2\ out}}{H_{2\ in}} = \frac{I}{n * F * n_{H_2}}$$

The overall efficiency equation can be modified to be expressed in these three terms, as in the following development [1] [2]:

$$\eta = \frac{IV}{n_{H_2}\Delta H} = \frac{IV}{n_{H_2}\Delta H} * \left(\frac{\Delta G * E_0 nF}{\Delta G * E_0 nF}\right) = \left(\frac{\Delta G}{\Delta H}\right)\left(\frac{V}{E_0}\right)\left(\frac{I}{n * F * n_{H_2}}\right)\frac{E_0 * n * F}{\Delta G}$$

$$\boldsymbol{\eta = \eta_{rev} * \eta_v * U_f}$$

### 1.1.5. Solid oxide fuel cell

SOFC is the most developed high temperature fuel cell. The stack utilised in the analysis of this thesis is a SOFC stack, so this section gives a more detailed explanation of this kind of fuel cell.

As it is known, there is no liquid electrolyte with its attendant material corrosion or electrolyte management problems. The high temperature of the SOFC, however, places stringent requirements on its materials. The development of suitable low cost materials and the low-cost fabrication of ceramic structures are presently the key technical challenges facing SOFCs. The cell is constructed with two porous electrodes that sandwich an electrolyte. Air flows along the cathode. When an oxygen molecule contacts the cathode/electrolyte interface, it acquires electrons from the cathode. The oxygen ions diffuse into the electrolyte material and migrate to the other side of the cell where they contact the anode. The oxygen ions encounter the fuel at the anode/electrolyte interface and react catalytically, giving off water, carbon dioxide, heat, and electrons. The electrons transport through the external circuit, providing electrical energy [1].

#### Cell and Stack Designs

Two types of cell designs are being pursued for SOFC: tubular cells and planar cells. The interest in tubular cells is unique to SOFC: all other types of fuel cells focus exclusively on planar designs. In SOFC, the benefit of a simple sealing arrangement potentially outweighs the disadvantages of low volumetric power density and long current path that are inherent in tubular cell geometries.

There are several kinds of tubular fuel designs, the conduction around the tube one (Siemens Westinghouse design of tubular SOFC) is by far the best-known and most developed, it is showed in figure 6. But there are also other types of tubular SOFCs that have different ways in which the cells are interconnected, as conduction along the tube or segmented in series.

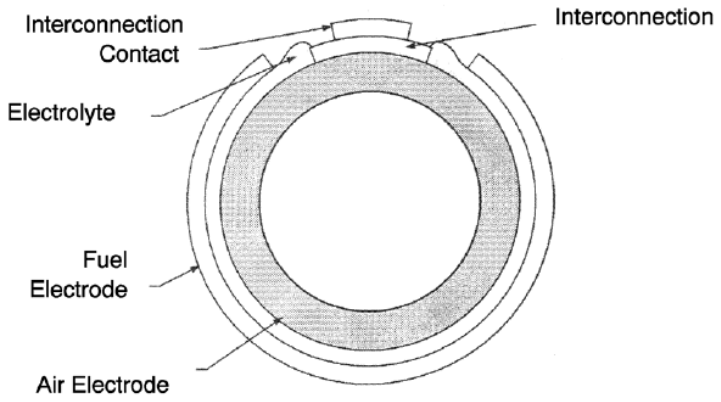


*Figure 6: Schematic cross-section of cylindrical Siemens Westinghouse SOFC tube*

Regarding the planar SOFC configuration, there are a variety of sub-types which are distinguished according to construction. Structural support for membrane/electrolyte assembly:

- Electrolyte-supported. This requires a relatively thick electrolyte (>100 but typically around 200 μm, with both electrodes at about 50 μm), which leads to high resistance, requiring high-temperature operation.
- Cathode-supported. This allows for a thinner electrolyte than electrolyte-supported cells, but mass transport limitations (high concentration polarization) and manufacturing challenges (it is difficult to achieve full density in a YSZ electrolyte without oversintering an LSM cathode) make this approach inferior to anode-supported thin-electrolyte cells.
- Anode-Supported. Advances in manufacturing techniques have allowed the production of anode-supported cells (supporting anode of 0.5 to 1 mm thick) with thin electrolytes. Electrolyte thicknesses for such cells typically range from around 3 to 15 μm (thermomechanically, the limit in thickness is about 20 to 30 μm (the cathode remains around 50 μm thick), given the difference in thermal expansion between the anode and the electrolyte). Such cells provide potential for very high power densities (up to 1.8 W/cm$^2$ under laboratory conditions, and about 600 to 800 mW/cm$^2$ under commercially-relevant conditions).
- Metal interconnect-supported. Metal-supported cells can minimize mass transfer resistance and the use of (expensive) ceramic materials. In such cells, the electrodes are typically 50 μm thick and the electrolyte around 5 to 15 μm. While the benefits are obvious, the challenges are to find a materials combination and manufacturing process that avoids corrosion and deformation of the metal and interfacial reactions during manufacturing as well as operation.

Interconnect material:

- Ceramic (lanthanum or yttrium chromite) suitable for high-temperature operation (900 to 1000°C). These materials, while chemically stable and compatible with the MEA from a chemical and thermal expansion perspective, are mechanically weak and costly.

- Cr-based or Ni-based superalloy for intermediate-high temperature operation (800 to 900°C). These materials are chemically stable at 900°C, but they require additional coatings to prevent Cr-poisoning of the electrodes. In addition, they are expensive and difficult to form.
- Ferritic steel (coated or uncoated) for intermediate temperature operation (650 to 800°C). While uncoated steels are chemically unstable, especially during thermal cycling, coated steels provide corrosion resistance as well as acceptable conductivity when new. However, thermal cycling performance still requires improvement.

Shape of the cell:

- Rectangular, with gases flowing in co-flow, counter-flow, or cross-flow.
- Circular, typically with gases flowing out from the centre in co-flow, and mixing and burning at the edge of the cells. Spiral flow arrangements and counter-flow arrangements have also been proposed.

Figure 7 shows a sample of recently-pursued planar SOFC approaches [1]:

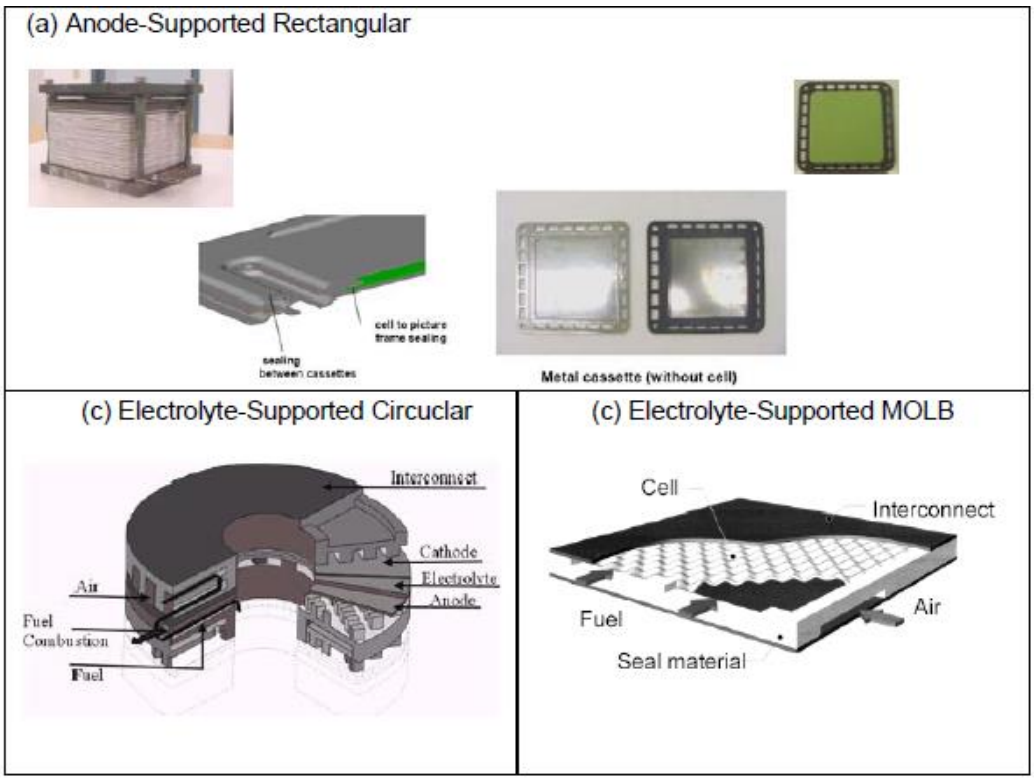


*Figure 7: Overview of Types of Planar SOFC: (a) Planar Anode-Supported SOFC with Metal Interconnects; (b) Electrolyte-Supported Planar SOFC Technology with Metal Interconnect; (c) Electrolyte-Supported Design with "egg-crate" electrolyte shape and ceramic interconnect*

## Single cell performance

The reduction of the operating SOFC temperature has been always a huge challenge. A significant advance in the development of intermediate temperature SOFCs has been the use of metallic "bipolar" interconnects in conjunction with thin electrolytes.

The utilization of the anode-supported approach with metallic interconnects leads to a lot of advantages:

- Sintering and Creep – Milder temperatures result in less sintering and creep of the stack materials. This helps maintain geometric stability and high surface area for reaction.
- Thermally Activated Processes – Thermally activated processes such as chromium vaporization, elemental inter-diffusion and migration, metallic corrosion, and ceramic aging become problematic at higher temperatures. The lower the operating temperature is maintained, the less damage these processes will cause to the fuel cell.
- Thermal Stress – Reduced width of the operating temperature band reduces thermal expansion and contraction stresses during cycling, thus maintaining geometric stability.
- Increase in Nernst potential.
- Heat Loss – Reduced heat loss from the more compact stack at lower operating temperature.
- Material Flexibility – The range of potential construction materials is somewhat greater at lower temperatures. In particular, certain metals can be incorporated in SOFC stack designs.
- Balance of Plant – The BOP costs may be less if lower cost materials can be used in the recuperators. In addition, the stack temperatures will be closer to typical reformer and sulphur removal reactor operating temperatures; this further reduces the load on the thermal management system. However, it must be remembered that the main factor driving the heat duty of the thermal management system is the amount of cooling air required for stable stack operation, which in turn depends on the internal reforming capability of the stack and on the acceptable temperature rise across the stack.
- Start-up time may be reduced. Lighter weight and high thermal conductivity of the metal interconnects may allow more rapid heat-up to operating temperature.

Some negative effects also result from reducing the operating temperature of the SOFC:

- A proven interconnect material for operating in the intermediate temperature range (650 to 800ºC) does not yet exist.
- Sulphur resistance decreases with temperature. However, recent work has shown that addition of certain materials provides adequate sulphur tolerance at lower temperatures [3].
- Lower temperatures generally require a planar configuration to minimize resistance losses. This is accomplished using ultra-thin electrode and electrolyte membranes. In turn, effective seals for the planar configuration are needed [1].

## System Considerations

System design depends strongly on fuel type, application, and required capacity, but the stack has several important impacts on the system design and configuration:

- The stack operating temperature range, degree of internal reforming, operating voltage, and fuel utilization determine the air cooling flow required, as well as level of recuperation required. This determines specifications for the blower or compressors and the thermal management system.
- The stack geometry and sealing arrangement typically determine stack pressure drop and maximum operating pressure, which can influence the system design especially in hybrid systems.
- The stack's sulphur tolerance determines the specifications of the desulfurization system.
- The degree of internal reforming that the stack can accept influences the choice and design of the reformer [1].

## Range of fuels

Solid oxide fuel cells allow conversion of a wide range of fuels, including various hydrocarbon fuels. The relatively high operating temperature allows for highly efficient conversion to power, internal reforming, and high quality by-product heat for cogeneration or for use in a bottoming cycle. Indeed, both simple-cycle and hybrid SOFC systems have demonstrated among the highest efficiencies of any power generation system, combined with minimal air pollutant emissions and low greenhouse gas emissions. These capabilities have made SOFC an attractive emerging technology for stationary power generation in the 2 kW to 100s MW capacity range.

The range of fuels that can be used in a SOFC is really extensive:

- Natural gas, which is the most common fuel, it is low cost, clean, abundant and readily available, with a supply infrastructure already in existence in many places. The predominant gas is methane, although there are also other hydrocarbons.
- Bottled gas, in small scale, (consisting of propane/butane), which can be internally reformed within the SOFC stack just like gas natural. But they have problems with carbon deposition which reduces the durability.
- Dimethyl ether (DME), which is an attractive fuel due to his facility to liquefy under practical conditions, making it easy to store and handle.
- Methanol, used for intermediate operating temperatures such as 500ºC, it is considered the most likely fuel, since methanol can be efficiently reformed at 300-600ºC and this reduction in the operation temperature is beneficious for the cell materials and for the cost.
- Gasoline and diesel, for internally reforming SOFCs, although there is a challenge in terms of avoiding coking on any of the active components of the cell.
- Coal gasification systems, although the sulphur content should be treated to avoid poisoning the anode.

- Biogas, an interesting possibility is the use of renewable fuels in SOFCs, biogas is a mixture of methane and carbon dioxide. It presents problems at low methane levels, but has the advantage that the methane can be reformed internally by the $CO_2$ in the biogas.

With all fuels, the elevated operating temperature of SOFCs makes them particularly suitable for combined heat and power applications (CHP) [4].

## Reforming possibilities

It seems clear that SOFCs have the ability to internally reform a range of practical hydrocarbon fuels within the stack, so it represents a significant advantage of SOFCs over low temperature fuel cells in terms of efficiency and cost. Three different modes are possible when a SOFC is fuelled with hydrocarbon fuels: external reforming, internal reforming, and direct utilization. In the first two cases the purpose is to completely convert the fuel into synthesis gas that is afterward electrochemically oxidized.

In typical SOFC, the reforming step is done after the desulphurization using an external unit (figure 8a). This type of design is known as external reforming SOFC, and is convenient for large-scale stationary systems with combined heat and power generation. For small-scale applications and particularly for portable systems, however, the complexity and size of the overall system can be reduced by eliminating the external reformer and annex units, and reforming the fuels inside the stack. This type of design is known as internal reforming and uses the waste heat generated by electrochemical oxidation and other non-reversible processes to offset the heat requirements of the reforming reactions.

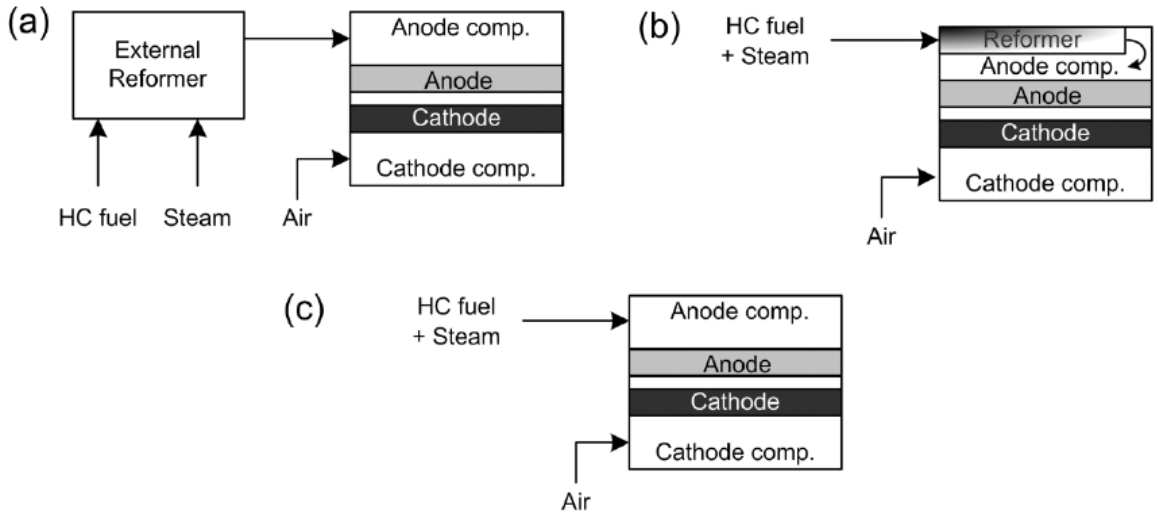


*Figure 8: Schematic of (a) external reforming SOFC, (b) indirect internal reforming SOFC, and (c) direct internal reforming SOFC*

There are some small differences between indirect and direct internal reforming that should be clarified. In *direct internal reforming (DIR)*, the fuel is reformed directly in the anode of the cell. It is the simplest and most cost-effective design for a SOFC system

and in principle provides the greatest system efficiency with least loss of energy. In this case, the anode has three roles; firstly as a hydrocarbon reforming catalyst; secondly as an electro-catalyst responsible for the electro chemical oxidation of $H_2$ and CO to water and $CO_2$ respectively; and finally as an electrically conducting electrode. In *indirect internal reforming (IIR),* a separate catalyst reforms the hydrocarbon fuel to synthesis gas, and it is integrated within the SOFC stack upstream of the anode. The heat from the exothermic fuel cell reaction is still utilised. The major advantage is that it is much easier to control from a thermodynamic standpoint, although it is less efficient and less simple than direct reforming [4] [5].

## Reactions

Reactions that take place in the fuel electrode of the cell depend on the kind of fuel which is introduced into the stack. The most common one is a mixture between hydrogen and carbon monoxide (synthesis gas), both components are electrochemically oxidised to carbon dioxide and water at the anode, with production of electrical power and high-grade heat.

$$H_2 + O = \rightarrow H_2O + 2e - \quad (hydrogen\ reaction)$$

$$CO + O = \rightarrow CO_2 + 2e - \quad (carbon\ monixide\ reaction)$$

$$CO + H_2O \rightarrow CO2 + H_2$$

$$H_2 + O = \rightarrow H_2O + 2e -$$

When the fuel is a hydrocarbon, it is catalytically converted (internally reformed), generally to hydrogen and carbon monoxide (synthesis gas) together with some carbon dioxide, within the cell stack, and the carbon monoxide and the hydrogen are then electrochemically oxidised as in the previous reactions. If the hydrocarbon fuelled is methane ($CH_4$), the reactions at the anode are:

$$CH_4 + 4O = \rightarrow 2H_2O + CO_2 + 8e - (total\ reaction)$$

$$CH_4 + H_2O \rightarrow CO + 3H_2$$

$$CO + H_2O \rightarrow CO_2 + H_2$$

$$4H_2 + 4O = \rightarrow 4H_2O + 8e -$$

If the hydrocarbon fuelled is ethylene ($C_2H_4$), the reactions at the anode are [4]:

$$C_2H_4 + 6O = \rightarrow 2H_2O + 2\,CO_2 + 12e - \ (total\ reaction)$$

$$C_2H_4 + 2H_2O \rightarrow 2CO + 4\,H_2$$

$$2CO + 2H_2O \rightarrow 2\,CO_2 + 2\,H_2$$

$$6H_2 + 6O = \rightarrow 6\,H_2O + 12e -$$

## Component for the reforming process

If the fuel introduced into the cell is not a mix between hydrogen and carbon monoxide, a component is needed to transform the initial fuel into synthesis gas (reforming process). There are many possibilities to reform hydrocarbons:

- Steam reforming, when the water gas shift (WGS) reaction occurs, whereby some of the CO is converted to $CO_2$, with production of one mole of hydrogen for every mole of CO converted. $CH_4$ and hydrocarbons also react with steam.

$$CH_4 + H_2O \rightarrow CO + 3H_2$$

$$CO + H_2O \rightarrow CO_2 + H_2$$

$$C_nH_{2n+2} + nH_2O \rightarrow nCO + (2n+1)H_2$$

The first reaction is strongly endothermic (consumes heat, $\Delta H^o r$= 249,9 kJ/mol), the second reaction is lightly endothermic ($\Delta H^o r$= 2,83 kJ/mol). Then, the $H_2$ and CO are then electrochemically oxidised to $H_2O$ and $CO_2$ at the anode by oxide ions electrochemically pumped through the solid electrolyte. An excess of steam is typically required to prevent carbon deposition by promoting the WGS reaction and reducing the partial pressure of CO.

- Dry reforming or $CO_2$ reforming, the carbon dioxide formed by the water gas shift reaction and by electrochemical oxidation of carbon monoxide, present in the exit gas leaving the anode, can be recirculated in the fuel supply at the cell inlet. It is well known that $CO_2$ can act as an oxidant for hydrocarbons in the presence of a suitable catalyst.

$$CH_4 + CO_2 \rightarrow 2CO + 2H_2$$
$$C_nH_{2n+2} + nCO_2 \rightarrow 2nCO + (n+1)H_2$$

The reaction is endothermic ($\Delta H^o r$= 247,1 kJ/mol). An excess of $CO_2$ can promote carbon deposition but, on the other hand, $CO_2$ is much easier to handle than steam.

- Partial oxidation (POX), oxygen or simply air in many cases is used as the oxidant rather than steam.

$$CH_4 + \frac{1}{2}O_2 \rightarrow CO + 2H_2$$
$$C_nH_{2n+2} + n/2O_2 \rightarrow nCO + (n+1)H_2$$

The reaction is exothermic ($\Delta H^o r$= -71,8 kJ/mol). It is suitable for small-scale portable applications where system simplicity and rapid start-up rather than system efficiency are crucial factors. The problem is that if an excess of oxygen is used, there is a tendency for complete oxidation (combustion) to $CO_2$ and $H_2O$.

$$CH_4 + 2O_2 \rightarrow CO_2 + 2H_2O$$
$$C_nH_{2n+2} + \frac{3n+1}{2}O_2 \rightarrow nCO_2 + (n+1)H_2O$$

The reaction is strongly exothermic ($\Delta H^o r$= -1411 kJ/mol).

- Auto-thermal reforming, when it is integrated steam reforming and partial oxidation. Both air and water (and partly $CO_2$) react with the fuel. Auto-thermal reforming requires a simpler design than steam reforming; it has higher system efficiency than partial oxidation, and can be used to take an SOFC from zero

power to operation at full load. As one reaction is endothermic and the other one is exothermic, there is a thermal equilibrium.

- Direct electro-catalytic oxidation, SOFCs can operate directly oxidising the hydrocarbon fuel on the anode using the oxide ions which have passed through the solid electrolyte from the cathode.

$$CH_4 + O^= \rightarrow CO + 2H_2 + 2e^-$$
$$C_nH_{2n+2} + nO^= \rightarrow nCO + (n+1)H_2 + 2ne^-$$

The hydrocarbons can also be fully oxidised to $CO_2$ and water, or undergo a mixture of partial and total oxidation.

$$CH_4 + 4O^= \rightarrow CO_2 + 2H_2O + 8e^-$$
$$C_nH_{2n+2} + (3n+1)O^= \rightarrow nCO_2 + (n+1)H_2O + 2(3n+1)e^-$$

The major problem with direct electro-catalytic oxidation of the hydrocarbon fuel at the anode is the market tendency towards carbon deposition via hydrocarbon decomposition [4] [5].

## Carbon deposition and sulphur tolerance and removal

Nickel in particular is well known for its propensity to promote hydrocarbon pyrolysis and the build-up of carbon. This carbon deposition can occur on the reformer catalyst and anode in the SOFC due to different reactions:

$$2CO \rightarrow C + CO_2$$

$$CH_4 \rightarrow C + 2H_2$$

$$CO + H_2 \rightarrow C + H_2O$$

The first reaction is called Boudouard reaction and it is more likely to happen than the other two, although it depends on the fuel composition and the operating temperature.

The build-up of carbon, also known as coking, is a critical problem to be avoided, or at least minimised, since over time this this can lead to a loss on reforming activity and blocking of active sites on the reforming catalyst and the anode, and a loss in cell performance and poor durability. It is well know that higher hydrocarbons are more reactive and show a much greater propensity towards carbon deposition than methane. Coke formation occurs by cracking the hydrocarbons to the correspondent alkene, followed by subsequent formation of a carbonaceous overlayer, which undergoes further dehydrogenation to from coke.

Regarding the sulphur tolerance, although the elevated temperature of SOFCs, the nickel anode, and any internal reforming catalyst, show some tolerance to sulphur, generality the majority of the sulphur is removed from the natural gas prior entering the SOFC to prevent poisoning of the anode and the reformer catalyst. At low concentrations of sulphur-containing compounds, the absorption of sulphur on nickel is reversible, and thus low concentrations of sulphur in the feed gas can be tolerated, especially at higher operating temperatures, since the tolerance of the anode and reforming catalyst to

sulphur progressively increases with temperature. Any absorbed sulphur can be removed, and the activity restored to the original activity, by switching to a sulphur free fuel feed or by a short exposure to steam. However, at higher sulphur concentrations, irreversible sulfurization of the catalyst or anode can occur [4].

## 1.2. Electrolysis

The electrolysis process is just the opposite of the fuel cell one. In this case, electric energy is transformed into chemical energy; hydrogen is produced splitting the elements of water in an electrolyser. Fuel cell and electrolyser is the same device operating under different conditions, so an energy storage system can be developed using this technology.

The basic equipment common to all the electrolysis technologies is the electrochemical cell, constituted basically by two electrodes and an electrolyte. At the electrodes electrochemical reactions take place, while the delivered ions are transferred through the electrolyte layer and electrons along external conductors, (the same as a fuel cell). Electrochemical reactions, the type of ions conducted by the electrolyte, materials and working temperatures depend on the specific electrolysis technology; however, the overall reaction of water electrolysis is the same for all the technologies:

$$H_2O + energy \rightarrow H_2 + \frac{1}{2}O_2$$

In the electrolysis process, water is split in its elements $H_2$ and $O_2$, using heat and work according to the previous equation. Regarding the operation temperature, there are two kinds of electrolyzers:

- Low temperature electrolyzers (LTE), such as proton exchange membrane electrolyzer (PEME) (40-80ºC), which has a solid electrolyte and alkaline electrolyzer (80-90ºC), which has a liquid electrolyte.
- High temperature electrolyzers (HTE), such as solid oxide electrolyzer cell (SOEC), whose electrolyte is solid and works at 700-900ºC.

The theoretical energy required to electrolyze one mole of water is equal to its enthalpy of formation (ΔH). According to the second law of thermodynamics, the energy required by the reaction can be supplied as thermal energy (TΔS) and electrical energy (ΔG). This reaction is endothermic and the total energy required by the reaction is:

$$\Delta H = \Delta G + T\Delta S$$

Where ΔH (J/mol) and ΔG (J/mol) are the enthalpy and Gibbs free energy changes of the reaction respectively, T (K) is the temperature and ΔS (J/mol/K) is the entropy change. ΔG represents the minimum electric energy required for the electrolysis process and TΔS is the thermal energy demand.

Energy is supplied only as electricity, in the low temperature electrolysis, and as electricity and heat, in the high temperature electrolysis. Figure 9 shows the required energy of the reaction as a function of the temperature.

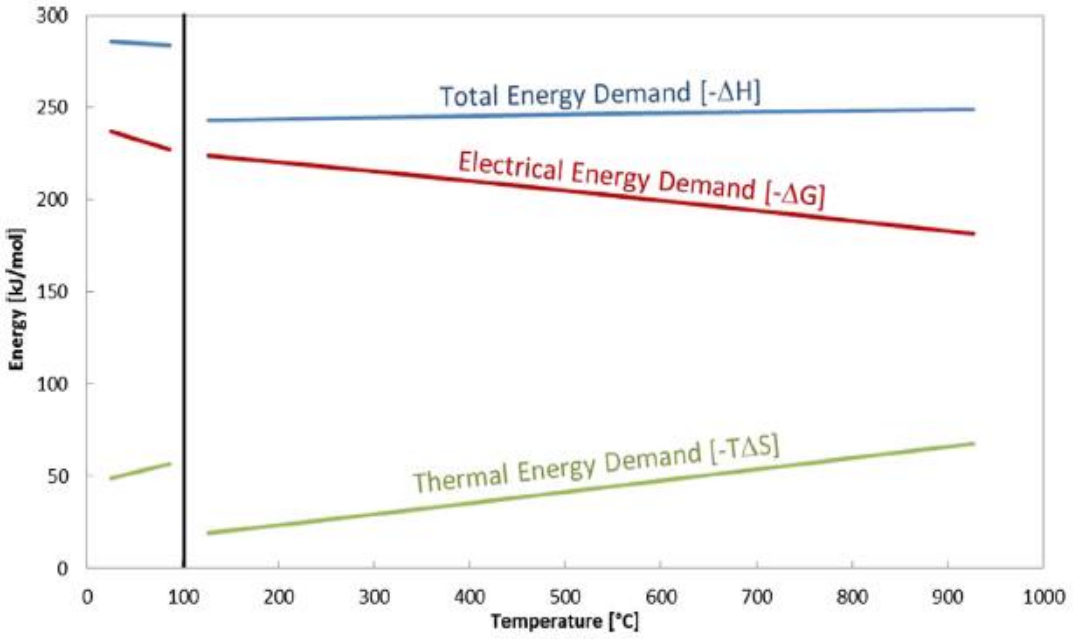


*Figure 9: Energy required by electrolysis process as a function of temperature*

The minimum (electric) energy required by the electrolysis reaction (ΔG), decreases with increasing temperature; indeed it represents the 93% of the total energy required by the reaction at 100ºC, and only the 76% at 800ºC. Therefore, strictly from a thermodynamic point of view, an SOEC intrinsically requires less electric power than a PEME cell because it works at higher temperature.

As shown in figure 9, the total energy ΔH slightly increases with the temperature but the thermal to electrical ratio increases more quickly with the temperature. This means that less electrical energy is needed when increasing the operating temperature to convert the same amount of water into hydrogen [6] [7].

### 1.2.1. Low temperature electrolysers

The Proton Exchange Membrane electrolyzer (PEME) is more developed than the alkaline electrolyzer. This subsection gives an overview of the PEME, but the alkaline electrolyzer would be quite similar.

#### Theoretical background of PEME

The PEME process is similar to the PEMFC process, but the operation principles are opposite. A basic schematic of a PEME is shown in figure 10, where the principle of operation of a single PEME cell is represented. The PEME cell consists primarily of a PEM as an electrolytic conductor. The anode and cathode are fixed together and are known as the membrane electrode assembly (MEA). In the PEME, water molecules and ionic particles are transferred across the membrane from the anode to the cathode, where it is decomposed into oxygen, protons and electrons. In the reaction process, electrical energy is supplied to the system and transformed into chemical energy. The electrons exit the cell through an external circuit. The electrons and protons recombine at the cathode to

release hydrogen gas. The chemical reactions at the anode and cathode sides of a PEME are respectively [6]:

$$H_2O \rightarrow \frac{1}{2}O_2(g) + 2H^+ + 2e^= \qquad (fuel\ electrode, anode)$$

$$2H^+ + 2e^= \rightarrow H_2(g) \qquad (air\ electrode, cathode)$$

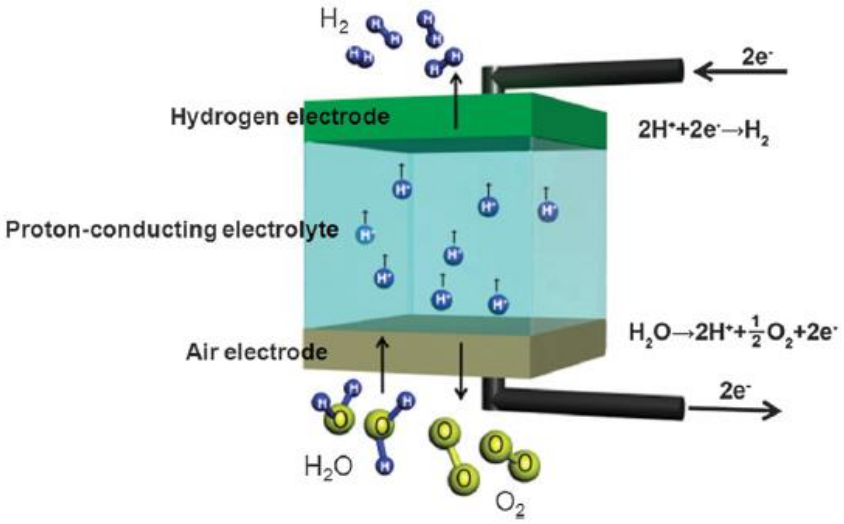


*Figure 10: Schematic diagram of PEME* **[8]**

## Thermodynamic model of PEME

The reversible potential or open circuit voltage at the cell can be derived from Gibbs free energy:

$$V_{rev} = \frac{\Delta G}{nF}$$

Where G is the Gibbs free energy, Vrev is the reversible voltage, n is the number of the electrons and F=96485C/mol is the Faraday's constant.

When PEME operates, the input voltage is applied to the electrodes and several voltage drops appear due to fundamental overpotential associated with the PEME. These overpotentials are characterized by reversible potential (Vrev), activation overpotential (ηact), and ohmic overpotential (ηohm). Therefore, the operating or cell voltage of a PEME is the summation of all the overpotential models as shown by:

$$V_{cell} = V_{rev} + \eta_{act} + \eta_{ohm}$$

Activation overpotential represents the overpotential to initiate the proton transfer and the electrochemical kinetic behaviour in the PEME, it can be written as:

$$\eta_{act,a} = \frac{RT}{\alpha_a zF}\ln\left(\frac{i_a}{i_{0,a}}\right) \qquad \eta_{act,c} = \frac{RT}{\alpha_c zF}\ln\left(\frac{i_c}{i_{0,c}}\right)$$

Where R is the universal gas constant, R=8.314 J/K/mol, z is the stoichiometric coefficient which refers to the number of electrons transferred in the global semi

reactions (defined by Faraday's law). The value of the stoichiometric coefficient in water electrolysis is 2. αa and αc is the charge transfer coefficients, their values are 0,5 on the symmetry reactions.

Ohmic overpotential is the resistance caused against the flow of electrons and electronic resistance of the PEME. The ohmic overpotential contributes significant losses to the PEME. This ohmic overpotential depends on the type of PEM, and electrode material. It can be expressed as a function of ionic an electronic resistance:

$$\eta_{ohm} = (R_{ion} + R_{ele})i_0$$

Figure 11 shows numerical simulations of loss characterization in a PEME:

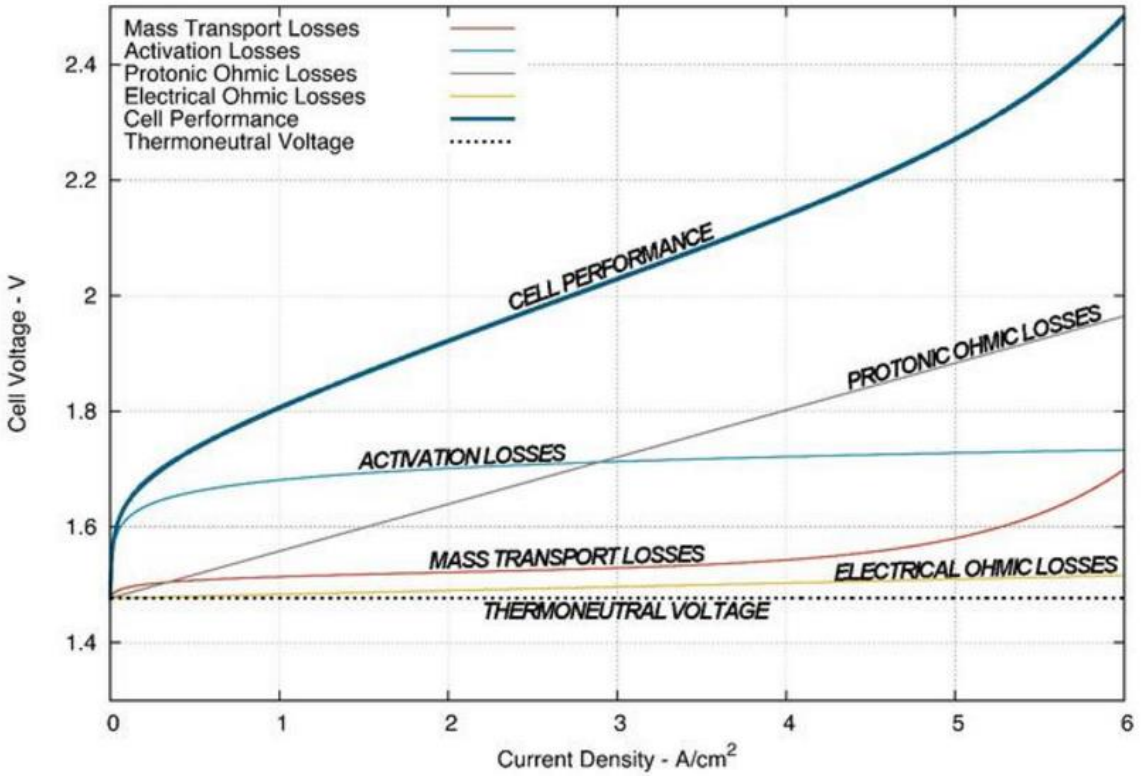


*Figure 11: Loss characterization of overpotentials in PEME*

It is observed in the graph how different types of losses make the voltage increases respect current density. Activation losses make an impact at the beginning while ohmic losses are linear. PEME efficiency is not very high due to the impossibility of working at the thermo-neutral potential, as can be noticed looking at the graph [9] [6].

### 1.2.2. High temperature electrolysers

The solid oxide electrolyzer cell (SOEC) is the only one high temperature electrolyser.

#### Theoretical background of SOEC

The SOEC process is similar to the SOFC process, but the operating principles are opposite. A basic schematic of a SOEC is shown in figure 12, where the principle of

operation of a single SOEC cell is represented. The electrochemical reactions that take place in an SOEC are:

$$H_2O + 2e^- \rightarrow H_2(g) + O^= \qquad (fuel\ electrode, cathode)$$

$$O^= \rightarrow \frac{1}{2}O_2(g) + 2e^- \qquad (air\ electrode, anode)$$

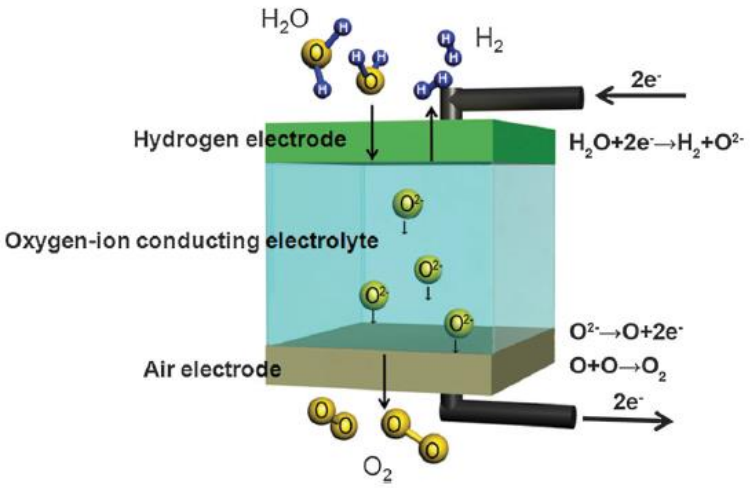


*Figure 12: Schematic diagram of SOEC* **[8]**

Although only water and energy are needed in the reaction, the input should be a mix between $H_2O$ and $H_2$, because hydrogen is necessary to prevent the cell of degradation [7].

## Thermodynamic model of SOEC

As the behaviour of the SOEC is quite similar to the behaviour of the SOFC but in reverse mode, the performance is better understood if both of them are explained and graphed together. The thermo-neutral potential corresponds to the potential at which the heat generated by the Joule effect into the cell is equal to the heat demand of the electrolysis reaction:

$$V_{th} = \frac{\Delta H}{nF}$$

Where $\Delta H$ is calculated at the working temperature, n is the number of electrons involved in the reaction and F is the Faraday constant. If the SOEC works at 800°C this potential is about 1.285 V. Similarly to SOFC, the reversible potential can be defined as:

$$E_0 = \frac{\Delta G}{nF}$$

Where $\Delta G$ is calculated at the working temperature and defines the minimum potential required by the electrolysis.

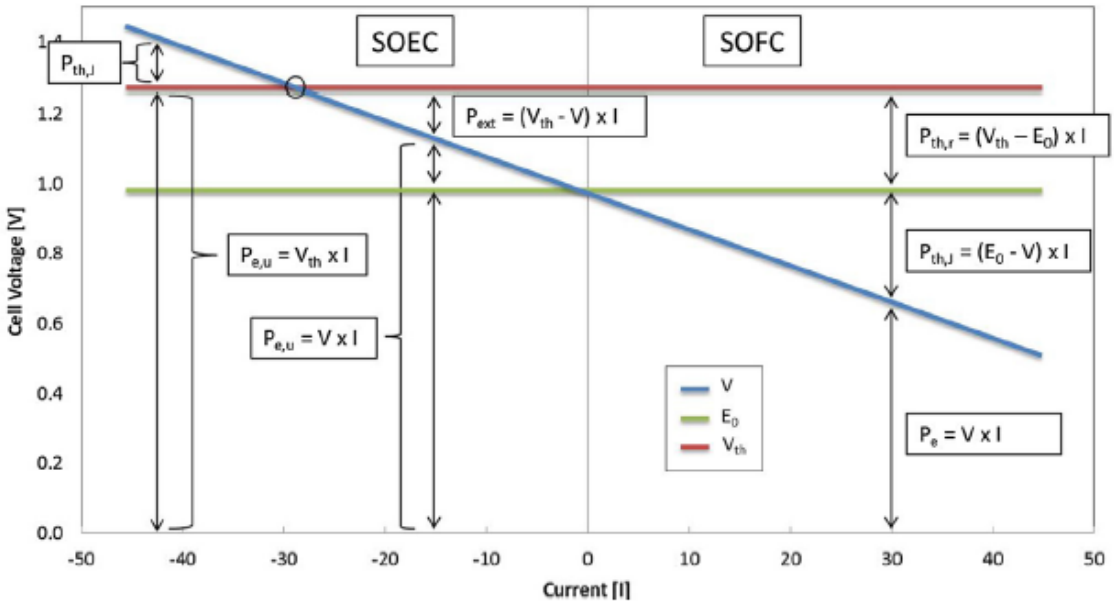


*Figure 13: Definition of electrical and thermal power involved in solid oxide fuel cell and electrolysis mode operation*

The reversible potential level, (green line), the thermos-neutral potential level (red line) and a hypothetical potential behaviour along a generic cell polarization (blue line) are shown in figure 13, either for SOEC or SOFC operation. The blue line is built on an experimental polarization performed with gas inlet composition of 50% of water and 50% of hydrogen.

From these three voltage curves it is possible to quantify, for each applied current, the electrical and thermal power involved in the reaction. With reference to SOFC operation, the electrical power produced ($P_e$) and the thermal power caused by the irreversibilities as Joule effect ($P_{th,J}$) and as chemical reaction ($P_{th,r}$) can be identified. When operating the SOFC as a SOEC, two zones can be identified, over and under the thermo-neutral potential, shown in figure 13 by red line. The electrical power fed to the system to decompose the water ($P_e$) can be defined as useful power ($P_{e,u}$) until the cell's voltage is equal to the thermo-neutral potential. Indeed, in the range of voltage between OCV and thermo-neutral potential, the share of thermal power produced by Joule effect caused by irreversibilities is used to counterbalance the thermal power required by the reaction. Meanwhile above that potential, part of electrical power fed to the system is lost as Joule heat. Thus for cell's potential lower than thermo-neutral voltage, the electrical power supplied is not enough to complete the reaction and an additional thermal power ($P_{ext}$) is required from an external source to complete the reaction and prevent cell cooling. Instead at the thermo-neutral voltage and over, all the electrical power is used to complete the reaction. At thermo-neutral voltage the Joule heat is fully used, while at higher potential a part of the generated Joule heat is wasted.

If the objective is working at high efficiency, the current (electric power) has to be regulated to work in the thermo-neutral point, since in that point, the heat generated by Joule effect is exactly the heat needed to complete the electrolysis reaction. However, it is

sometimes more interesting to introduce more power to produce more hydrogen, even knowing that it is not the maximum efficiency as there are heat losses by Joule effect.

The behaviour of thermal and electrical power, calculated as indicated in figure 13, is plotted in figure 14.

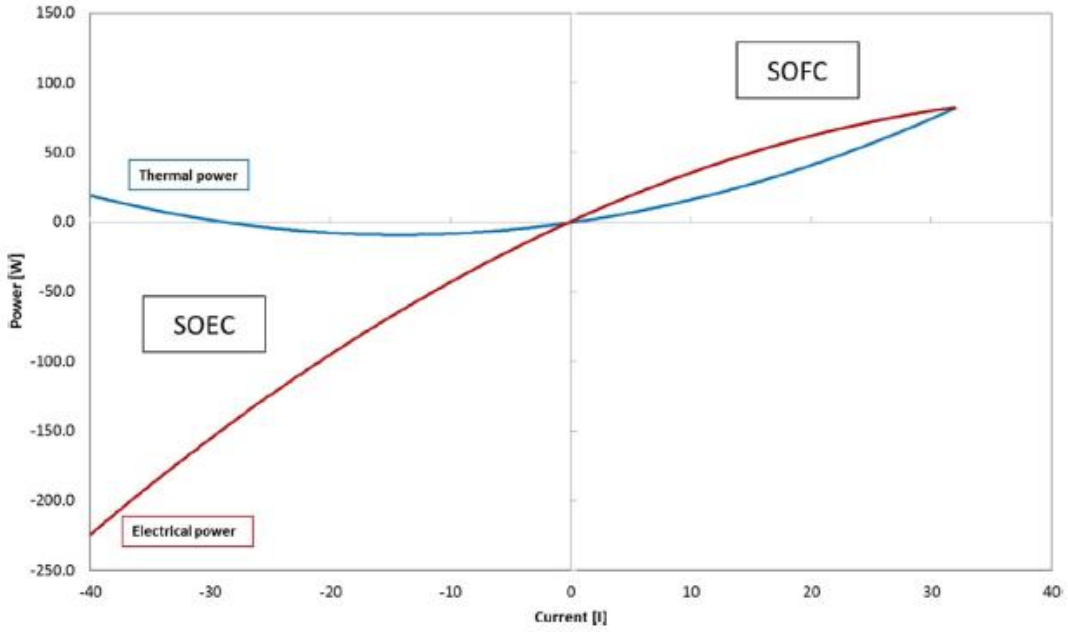


*Figure 14: Thermal and electrical power behaviour along SOFC - SOEC curve*

While in SOFCs the thermal power produced grows up, in SOEC the thermal power used by the reaction has a maximum in the range I=0(OCV) - $I_{th}$ (thermo-neutral potential); for higher (negative) currents, more heat than required is produced by the SOEC, which produces an increase of cell temperature. Whereas the electrical power passes from positive, in SOFC condition, to negative, in SOEC condition, with a parabolic behaviour as a consequence of the irreversibilities [7] [10].

## Efficiency of SOEC

There are three different formulations of efficiency. For a generic electrolyzer as for the SOEC, thermal efficiency (or Faraday efficiency) is defined as:

$$\eta_{th} = \frac{\Delta H}{\Delta G}$$

Which represents, at a given temperature, the maximum electrical efficiency of the process and it is also known as Faraday efficiency. This formulation of efficiency does not take into account the heat contribution therefore its value can be higher than unity. This equation can also be written in terms of input and output power as:

$$\eta_{th} = \frac{P_{out}}{P_{in}} = \frac{LHV_{H_2} * H_2}{P_e}$$

Where LHV is the low heating value of $H_2$, $H_2$ is the hydrogen flow produced by the cell and Pe is the electric power input.

Another definition of efficiency takes into account the heat required by the SOEC reaction without considering the energy demand for the water's evaporation. Based on input and output power involved into the SOEC the efficiency is:

$$\eta_{SOEC} = \frac{P_{out}}{P_{in}} = \frac{LHV_{H_2} * H_2}{P_e + P_{ext}}$$

Finally, taking into account also the energy needed to evaporate the water, neglecting the thermal losses; it is possible to define the "system" efficiency:

$$\eta_{sys} = \frac{P_{out}}{P_{in}} = \frac{LHV_{H_2} * H_2}{P_e + P_{ext} + P_{vap,H_2O}}$$

The last definition considers the thermal power of the water vaporization. All the efficiency definitions do not consider how the electrical and thermal energy are produced and how much their efficiencies of production are.

In figure 15 the efficiencies are plotted as a function of reactant utilization. As fuel utilization in fuel cell represents the amount of fuel used for a certain collected current ($U_f = \frac{I}{n*F*H2}$), into the electrolyzers the reactant utilization corresponds to the amount of water converted into hydrogen by the applied current ($RU = \frac{I}{n*F*H2O}$).

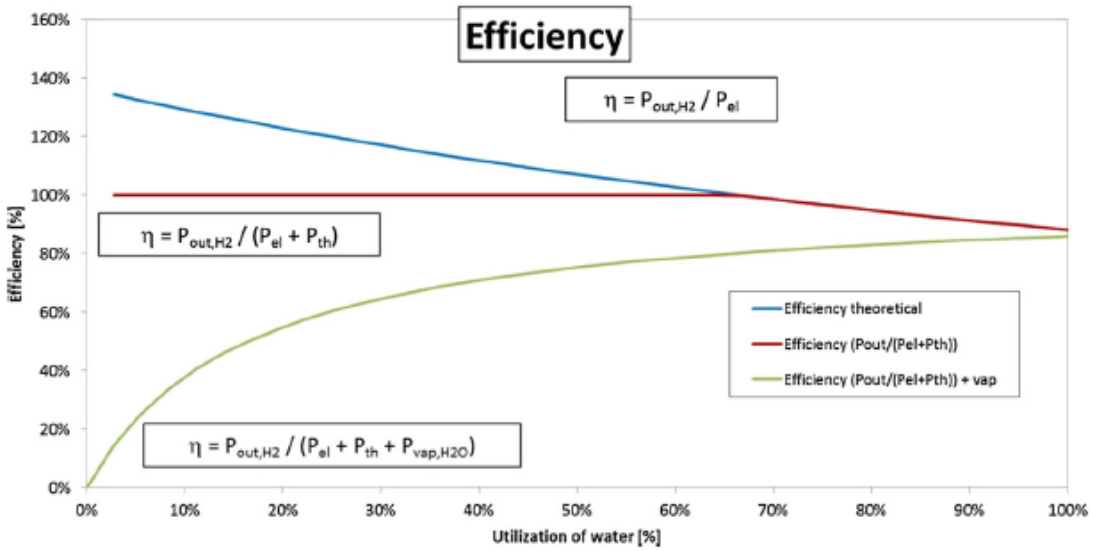


*Figure 15: Efficiencies as a function of utilization of water*

On figure 15 three curves of efficiency are displayed obtained by applying the equations to a generic linear polarization curve. Figure 15 shows that the efficiency of the SOEC (red line), considered as a black box, is constantly 100% up to the thermo-neutral potential; after that value it decreases, joining the thermal efficiency curve (blue line). This behaviour is due to the loss of the electrical power by Joule heat. The curve of the system efficiency (green line) shows that the vaporization of water, keeping constant the

amount of inlet water, strongly reduces the efficiency of the system at low water utilization. While, at high water utilization, part of the amount of energy needed to evaporate the water is supplied by the irreversibilities, the system efficiency moves to the SOEC efficiency value [10] [7].

### 1.2.3. Comparison among electrolysers

The main advantages and disadvantages of the three kinds of electrolysers are represented in the following table [11]:

*Table 3: Comparative among electrolysers characteristics*

| | Advantages | Disadvantages |
|---|---|---|
| **Alkaline electrolyser** | Well established technology<br>Non noble catalysts<br>Long-term stability<br>Relative low cost | Low current densities<br>Crossover of gases (degree of purity)<br>Low partial load range<br>Low dynamics<br>Low operational pressures<br>Corrosive liquid electrolyte |
| **Proton exchange membrane electrolyser (PEME)** | High current density<br>High voltage efficiency<br>Good partial load range<br>Rapid system response<br>Compact system design<br>High purity | High cost of components<br>Acidic corrosive environment<br>Possibly low durability<br>Commercialization<br>Stacks below MW range |
| **Solid oxide electrolyser cell (SOEC)** | Efficiency up 100% (thermo-neutral)<br>Efficiency<100% w/hot steam<br>Non noble catalysts<br>High pressure operation | Laboratory state<br>Bulky system design<br>Durability (brittle ceramics)<br>No dependable cost information |

The main difference among the three kinds of electrolysers can be represented in a graph, as shown in figure 16. The area where the systems can operate in terms of voltage and current density is represented.

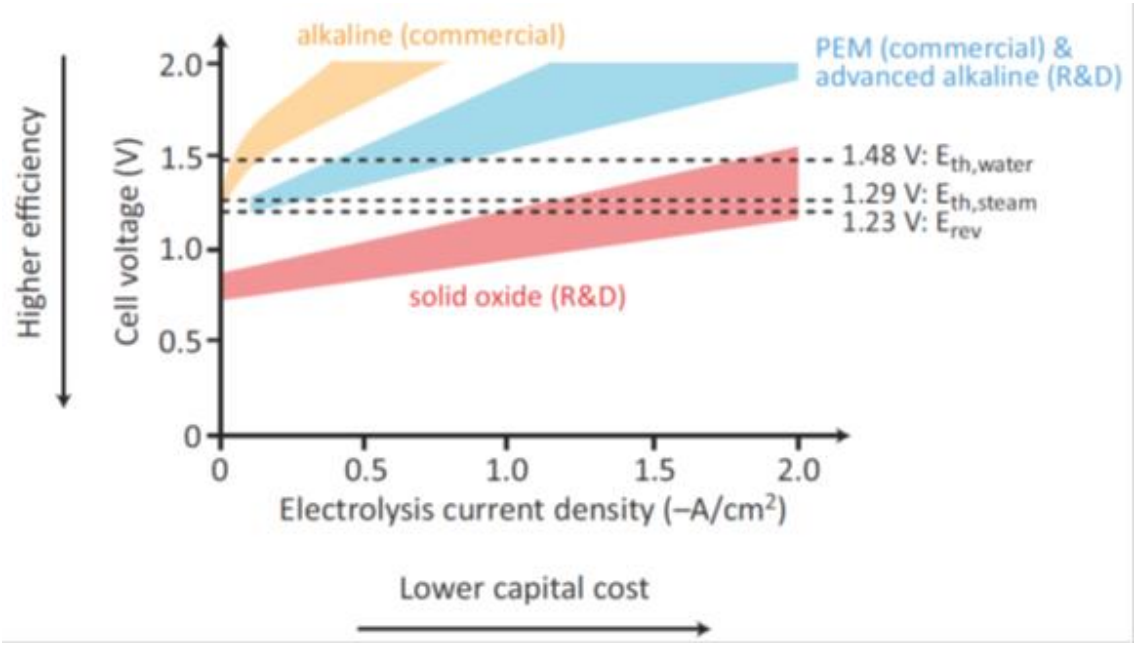


*Figure 16: Comparative polarization curves of electrolysers*

It is observable that the solid oxide electrolyser has lower OCV and ASR, so less electric power has to be applied to the stack. Moreover, SOEC is the only one capable of working at the thermo-neutral potential, where the efficiency is 100%. It means that in terms of efficiency, high temperature electrolysers have better performance than low temperature electrolysers [12].

## 1.3. Energy storage: reSOC

As electric energy is not storable in big amount, it has to be consumed at the same time it is generated. Trying to take advantage of the renewable sources, it is really important to develop efficient storage systems nowadays. The concept of developing a hydrogen economy based on renewable energy sources (RES) to overcome global environmental pollution issues and fossil fuels dependence has already attracted great interest in recent years.

Energy storage facilities are generally categorized as either energy management applications, which have a high energy-to-power capacity ratio, or power management applications, which have a low energy-to- power capacity ratio. Energy management applications require long-duration, high efficiency, and low cost energy storage. Alternatively, power management applications require fast dynamics and high reliability. Various energy storage technologies are represented in figure 17:

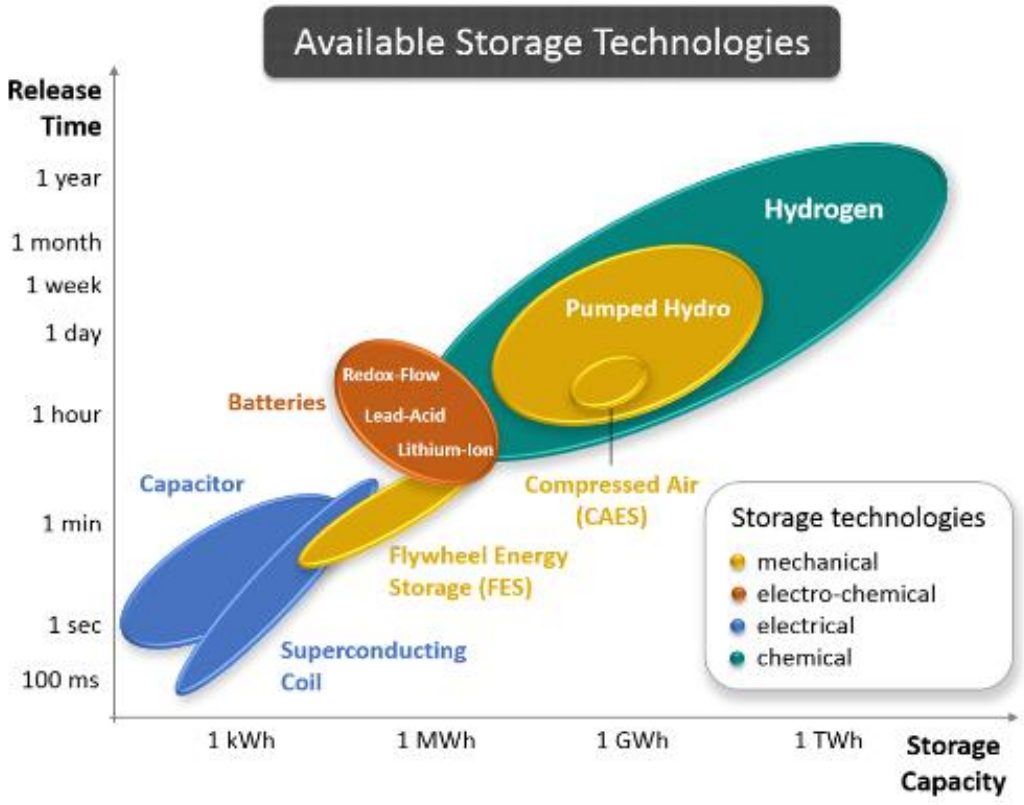


*Figure 17: Different energy storage technologies* **[13]**

Technologies that are currently advancing toward meeting the technical requirements for energy management applications include compressed air energy storage (CAES), pumped hydro storage (PHS), conventional batteries (lead-acid, nickel-cadmium), advanced batteries (lithium ion, sodium beta alumina, redox flow batteries), and energy management flywheels. However, these technologies face unique development challenges such that the requirements for highly efficient, durable, and cost-effective energy store systems have not been met yet.

Among the most studied energy storage systems, only pumped hydro and chemical storage have demonstrated to provide long-term storage and an easily controllable discharge according to the energy demand. Pumped hydro is an effective way but it can only be realized in specific locations where there are at least two basins available at different heights. However, chemical storage by producing hydrogen is not site specific and can operate with high efficiency.

An important concept in terms of chemical energy storage is reversible solid oxide cell (reSOC), hydrogen is produced from electric energy (SOEC mode) and electric energy is produced from hydrogen (SOFC mode) in the same device. This presumes an important strength in terms of efficiency and cost. The system, when working as a SOFC, it has the advantages explained in previous sections, efficiency is not limited by the Carnot theorem, lower pollutant emissions (there is no combustion and formation of NOx), fuel flexibility, etc. Moreover, it has the possibility to work as an electrolyser to generate hydrogen when there is an overage of electric energy. It is really useful when renewables

energies such as wind or photovoltaic energy are producing electric energy. A general scheme of this energy stororge system is represented in the figure 18.

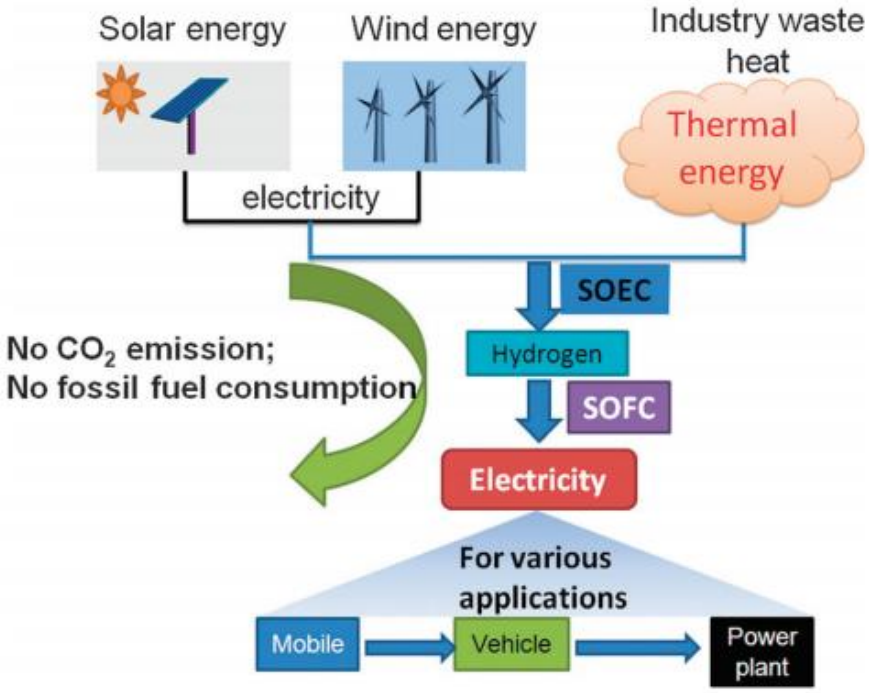


*Figure 18: Concept diagram of applications of a sustainable energy system based on SOEC/SOFC technology* **[8]**

A ReSOC energy storage system is well suited for energy management applications because such a system can operate over a wide range of energy-to-power ratios by sizing the energy and power ratings independently and is expected to have high energy storage efficiency and energy capacity suitable for storage duration on the order of hours to days. Moreover, a ReSOC is theoretically able to be both an energy management application and a power management application due to the fast electrochemical dynamics. Realizing the potential of ReSOCs for electrical energy storage requires research and development at both the cell and system levels [14].

### 1.3.1. Theoretical background of reSOC

A reversible solid oxide cell (reSOC) is physically the same as solid oxide fuel cells but can operate in both current directions. High temperatures (500-1000°C) are required for efficient ReSOC operation to allow mobility of oxygen ions in the solid electrolyte. Depending on the cell polarity, the ReSOC can operate either as a fuel cell (SOFC mode) to electrochemically oxidize fuel species and generate electricity, or as an electrolysis cell (SOEC mode) to electrochemically reduce reactant species while consuming electrical energy. The two modes of operation are depicted in figure 19. The PEN (positive/electrolyte/ negative), is a laminated ceramic and metal structure composed of a porous fuel electrode (anode in SOFC mode, cathode in SOEC mode), a thin solid electrolyte, and a porous oxygen electrode (cathode in SOFC mode, anode in SOEC mode).

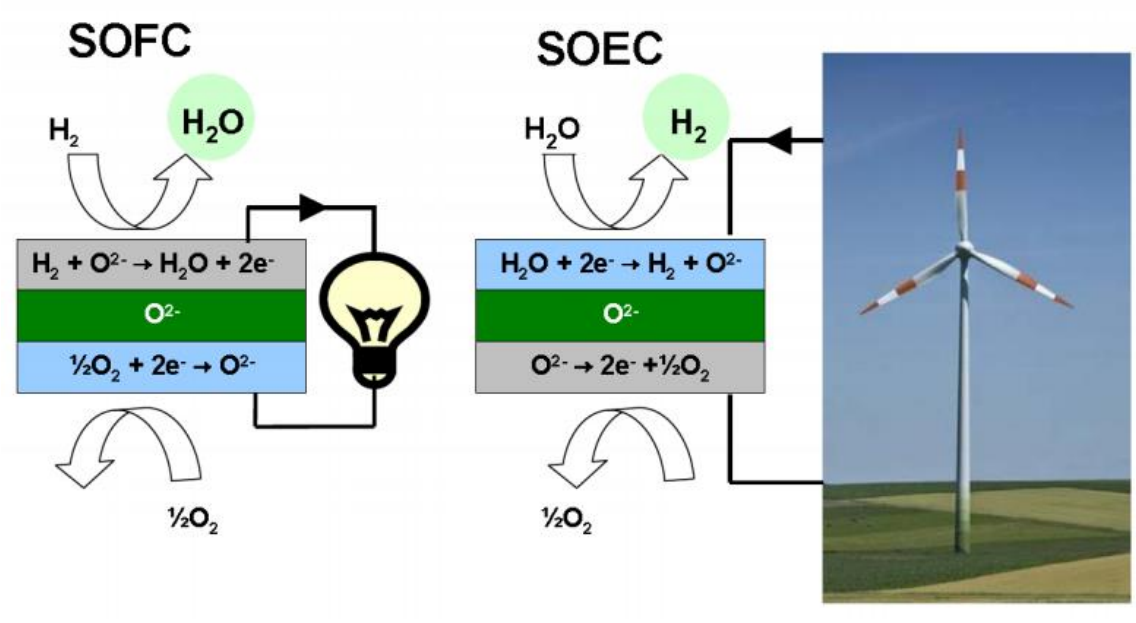


*Figure 19: Schematic diagram of ReSOC* [15]

During operation, reactant species flow through the fuel channel adjacent to the fuel electrode. In SOFC mode, these reactant species can include hydrogen, syngas ($H_2$ + CO), natural gas (reformed or not), or reformate from other gaseous, liquid, or solid fuels. In SOEC mode the reactant species are $H_2O$ and/or $CO_2$. If steam is the lone reactant, the process is typically referred to as electrolysis, while co-electrolysis refers to simultaneous reduction of $H_2O$ and $CO_2$ to produce syngas. The oxygen electrode requires an oxygen supply during SOFC mode operation to act as a reactant in the electrochemical conversion. The oxygen is typically supplied as either air or oxygen. In SOEC operation, oxygen is produced at the air electrode and an efficiency improvement is achieved blowing air, or a different sweep gas, through the channel to improve transport of the produced oxygen away from the reaction site. A single ReSOC typically operates between 0.5 and 2.0 V and cell stacking is required to achieve useful voltage output from the device. Cell stacking introduces the need for electronically conductive interconnect materials and sealing to prevent gas-crossover or leaking from the stack. For high temperature devices, cell stacking is further complicated because of the potentially varying thermal expansion behaviour of the various materials used to construct the ReSOC stack.

The electrochemical oxidation reactions occurring during SOFC operation are exothermic such that excess cooling airflow is typically provided to the stack to remove excess heat. Internal reforming reactions can also act as a thermal energy sink. Alternatively, the reduction reactions in SOEC mode are endothermic and maintaining the cell operating temperature requires additional heat, typically either from an external source or by operating the cell less efficiently such that waste-heat generation overcomes the thermal energy deficit. The difference in thermal behaviour in each operating mode presents a significant challenge in system design of an integrated ReSOC system. Another important challenge to face is the cell performance degradation. In fact the cell

has to work in both oxidizing and reducing environments, and it is important to develop electrode materials which are stable in both conditions [14] [7].

### 1.3.2. Thermal management strategy of reSOC

SOFC and SOEC operations have different behaviours with reference to the heat consumed or produced depending on the operating point among other factors. So the thermal management is an important challenge to be studied, as well as the cell life or the operating mode change.

As shown before, ReSOC stack, when working in SOFC mode, even in ideal conditions, cannot transform all the energy of the fuel in work and a part of it becomes thermal energy (the $T\Delta S$ term). Another heat source is represented by the irreversibilities.

In SOEC mode, an ideal cell requires heat to perform electrolysis. Part of this thermal energy is produced by the irreversibilities. If the cell operates under the thermo-neutral voltage, the heat generated by the irreversibilities is not enough and the cell will need more thermal energy, the stack is cooling down due to heat is absorbed to complete the electrolysis reaction. On the contrary, if the cell voltage is higher than the thermo-neutral voltage, the cell will produce more heat than needed, so the stack is heating up because of the heat produced by irreversibilities. SOEC efficiency can be fixed at 100% if the stack works in the thermo-neutral potential.

A huge challenge is to develop a system which optimises the thermal behaviour of a stack which is run as a SOFC or as a SOEC depending on the necessities. The goal of the system is to store the heat losses ($T\Delta S$) produced by the SOFC operation, and use it in SOEC operation. A theoretical example of the benefits of the addition of heat in SOEC operation is represented in the following graph:

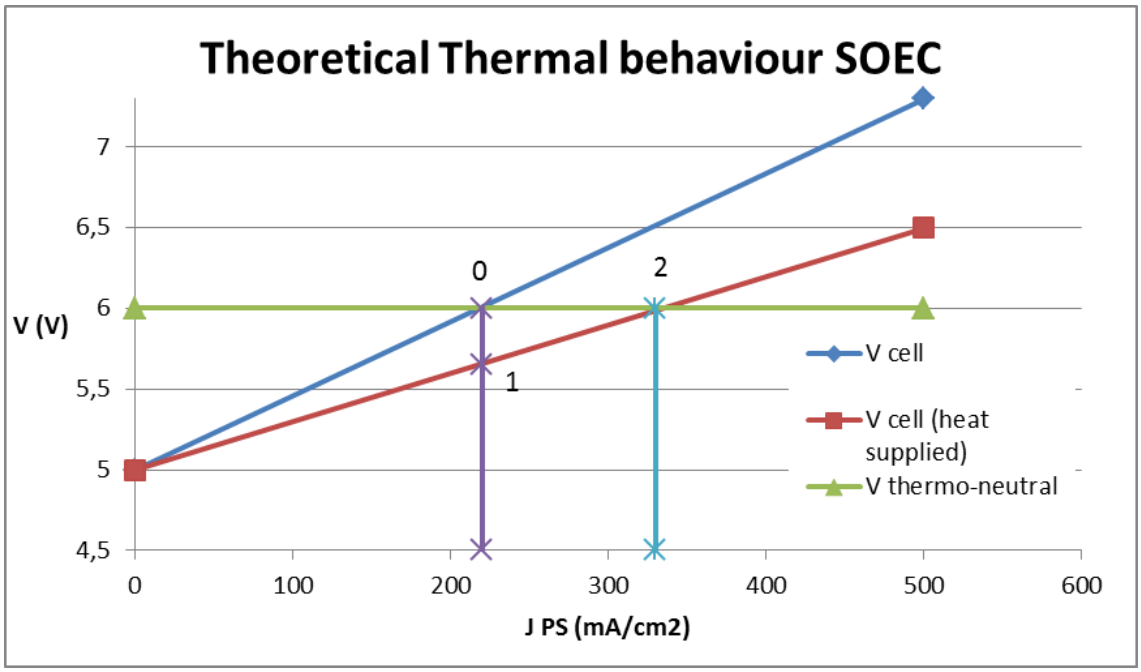


*Figure 20: SOEC Theoretical thermal behaviour*

If no heat is applied to the SOEC, the operating point can be fixed at the thermo-neutral potential to achieve an efficiency of 100% (point 0 in the graph). However, if some heat is supplied, the stack temperature increases and it leads to a better performance of the stack, represented as a drop voltage (cell voltage straight moves down from the blue line to the red one). This new polarization curve leads to two different possibilities: if the operating point (J) does not change (passing from point 0 to point 1), the hydrogen produced is the same while efficiency is higher than 100% because less electric power is needed. If the operating point (J) goes to the new thermo-neutral point (passing from point 0 to point 2), hydrogen produced increases while efficiency is kept at 100% as in the starting point.

To get this ideal thermal performance, some alternatives to store heat have been proposed in literature reviews: using chemicals (high temperature hydrogen, high temperature steam…), using physicals (ceramic materials, phase change materials, high temperature pipes…), or using specific chemical reactions. In the system which is tested to do this thesis, a furnace is utilised to simulate the thermal behaviour explained before, keeping constant the temperature as much as possible.

For a stand-alone energy storage system it is important that the stack is operated to be net exothermic so that reactant preheating can be satisfied by stack tail-gases that have increased in temperature as they flow through the stack. Thus, a particular challenge is the endothermic electrolysis reactions which must be overcome with a heat supply. Operating at overpotential high enough to achieve a net exothermic process is prohibitively inefficient for most energy storage applications. Various strategies have been proposed to try to accumulate part of the heat produce in SOFC mode to use it in SOEC mode to enhance the roundtrip efficiency of the system that will be discussed in the next subsection [14].

### 1.3.3. Roundtrip efficiency of reSOC

The most important parameter that has to be evaluated when discussing about electrical energy storage systems is the roundtrip efficiency. This parameter indicates the fraction of electricity which can be recovered of the electricity used to charge and discharge the device including all parasitic power loads from components, such as compressors, power produced from turbines, and energy entering the system in the form of fuel or process streams.

$$\eta_{rountrip} = \frac{E_{el,out} - W_{aux,SOFC}}{E_{el,in} + W_{aux,SOEC}}$$

$E_{el,out}$ is the output energy, $W_{aux,SOFC}$ and $W_{aux,SOEC}$ are the auxiliary system energy consumption during respectively SOFC and SOEC mode. When considering only the stack, the roundtrip efficiency can be expressed as follows:

$$\eta_{rountrip,stack} = \frac{V_{SOFC,cell}}{V_{SOEC,cell}}$$

Two things have to be clarified about system and stack roundtrip efficiency: the given definitions do not take into account system thermal energy variation. For this reason to apply the formula shown before, system final temperature has to be equal to system initial temperature. The definition of stack roundtrip efficiency can be higher than one, because does not take into account the thermal energy that has to be provided to perform electrolysis. This means that if reactant reaction change from SOFC to SOEC mode, and the thermal energy required by the cell is higher than the thermal energy produced during SOFC mode, the overall efficiency will be lower than one, but the electric stack roundtrip efficiency will be higher than unity.

The roundtrip stack efficiency is useful for understanding system performance by quantifying the efficiency impact of the ReSOC stack and the other components independently. Operating at the high overpotential required to generate net heat in a steam-hydrogen electrolyser is prohibitively inefficient for an energy storage application. More specifically, the overpotential require to reach the thermo-neutral voltage is approximately 240 mV for steam electrolysis at 800°C and 1 atm. Supposing that in SOFC mode there is the same OCV and the same overpotental (in this case cell potential will be lower than OCV), the roundtrip stack efficiency is limited to 63%. This simple consideration underlines the importance of a thermal management strategy [14].

# 2. Test rig

The main goal of the study is to operate a short SOFC stack as a reversible fuel cell, producing electrical energy from hydrogen (SOFC mode), and hydrogen from water and electric energy (SOEC mode).

A scheme of the physical connections of the system is represented in the following figure:

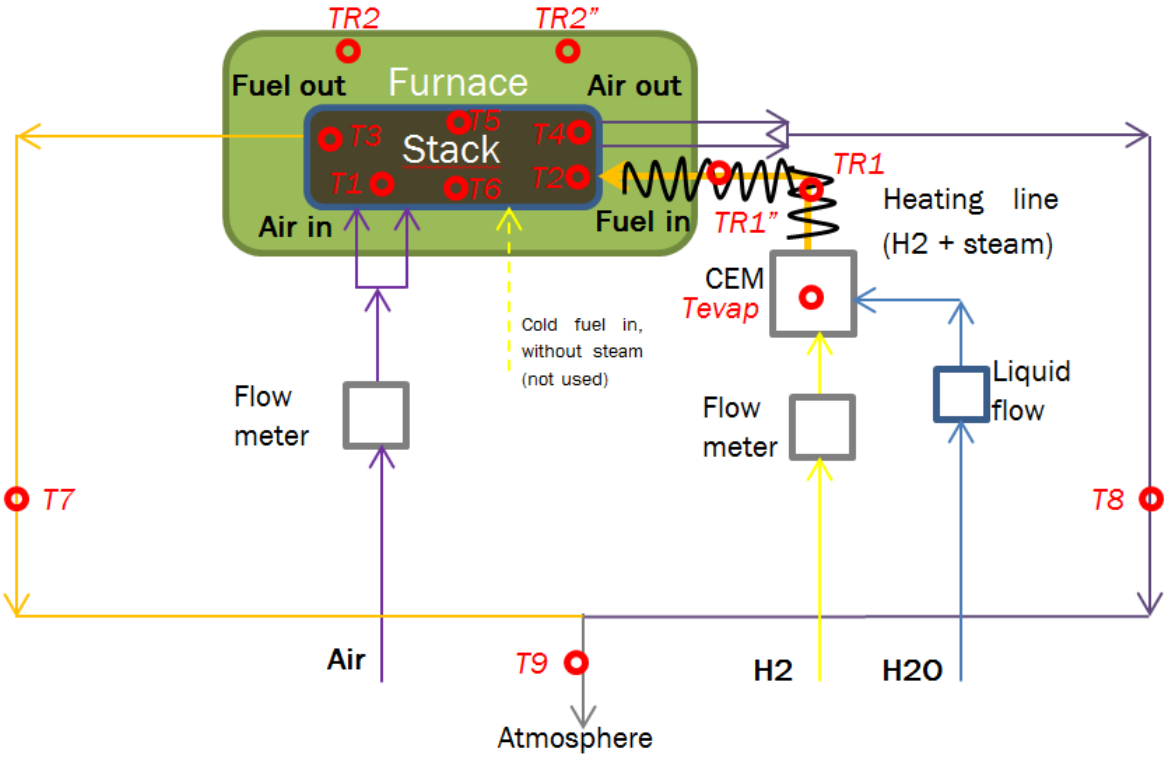


*Figure 21: Scheme of test rig physical connections*

The stack is the main component of the system; it is covered by a furnace to add heat when it is necessary. The gas inlets and outlets are also represented with the control and measure elements. The thermocouples are also represented with red circles. All these components are explained in detail in the following subsections.

A picture taken to the system is showed in the figure below:

*Figure 22: Test rig physical shape*

# 2.1. Stack

Stack is the main element of the system in which the reactions take place. It is composed of six single cell connected in series, each one has the three principal elements, fuel electrode, air electrode and electrolyte. They also have a seal and the air and fuel distributor. Their functions have been explained in the introduction.

Each cell has voltage from 0,7 V to 1,2 V in SOFC operation, so the total voltage of the stack is from 4,2 V to 7,2 V. However, in the SOEC operation voltage will be higher due to irreversibilities makes voltage to increases with current. The current of all cells is the same (they are in series). The active area is 80 $cm^2$ and the maximum current density is 1 A/ $cm^2$, so the maximum current is 80 A. However, it will not pass from 40 A due to the water limit, as will be explained in the test plan. The technical specifications of the short stack are reported in the following table:

*Table 4: Stack specifications*

| Characteristic | Measurement unit | |
|---|---|---|
| Cell number | | 6 |
| Nominal power | W | 150 |
| Minimum cell voltage | V | 0,7 |
| Nominal cell voltage | V | 0,75 - 0,8 (SOFC mode) |
| Nominal operation temperature | °C | 750 |
| Maximum operating temperature | °C | 800 |
| Operating pressure | | Atmospheric |
| Fuel | | Hydrogen, syngas or reformate |
| Oxidant | | Air |
| Input temperature air/fuel | °C | 600 - 750 |

The stack is provided by the company "SOLID power", they provides anode-supported, thin-film electrolyte, solid oxide fuel cells produced in its pilot production line in Trento. The cells are composed of an electrolyte (YSZ) sandwiched between two electrodes, a porous perovskite cathode and the anode support structure. A ceria barrier layer separates the cathode form the electrolyte. Good mechanical stability is provided by the relatively dense anode structure; the thin anode hardly shows any gas diffusion limitations. The cells are produced by anode and electrolyte co-casting and co-sintering followed by screen-printing of the cathode layer [16].

A real picture of the stack in the structure can be seen in figure 23.

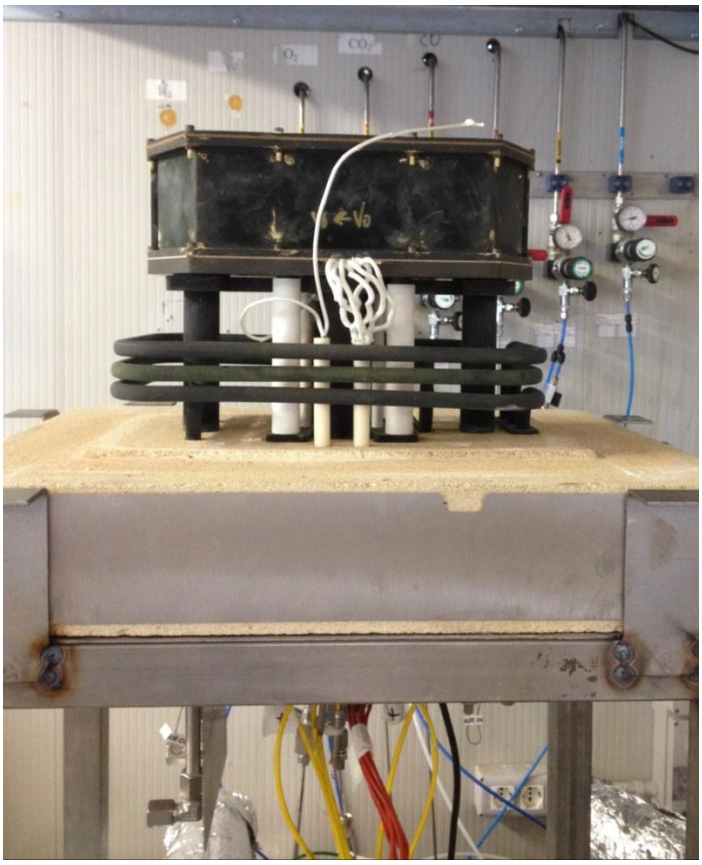

*Figure 23: Stack in the test rig structure*

On the low part of the stack, there are several pipes and cables with different goals:

- Two air input pipes.
- Two air outputs pipes.
- One fuel input pipe, suitable when introducing hydrogen with no steam (start -up).
- One fuel output pipe.
- Four springs which provide mechanical load and are also used to drain current to the electrical circuit.
- One menus connection, which is the other electrical terminal.
- Four pipes to measure pressure, which will be not used in the study and covered during the stack operation.
- Six thermocouples to measure the temperature of the air in, fuel in, air out, fuel out, top of the stack and bottom of the stack, (yellow cables).
- Seven voltage meters to measure the voltage between two cells (differential potentials), (red cables).

*Figure 24: Stack bottom*

On one side of the stack there is another fuel input that is connected to the gas heated line (see description above). This inlet is suitable when introducing steam and hydrogen, so it will be used when making the tests.

## 2.2. Electrical circuit

With reference to the electric connections of the system, the main elements connected to the stack are the electronic load and the power supply. When operating the stack SOFC, the electronic load is working to consume the power generated by the stack. And when operating the stack as SOEC, the power supply is working to apply the necessary power to the stack allowing the electrolysis reaction. A scheme of the electrical circuit is represented in the following figure:

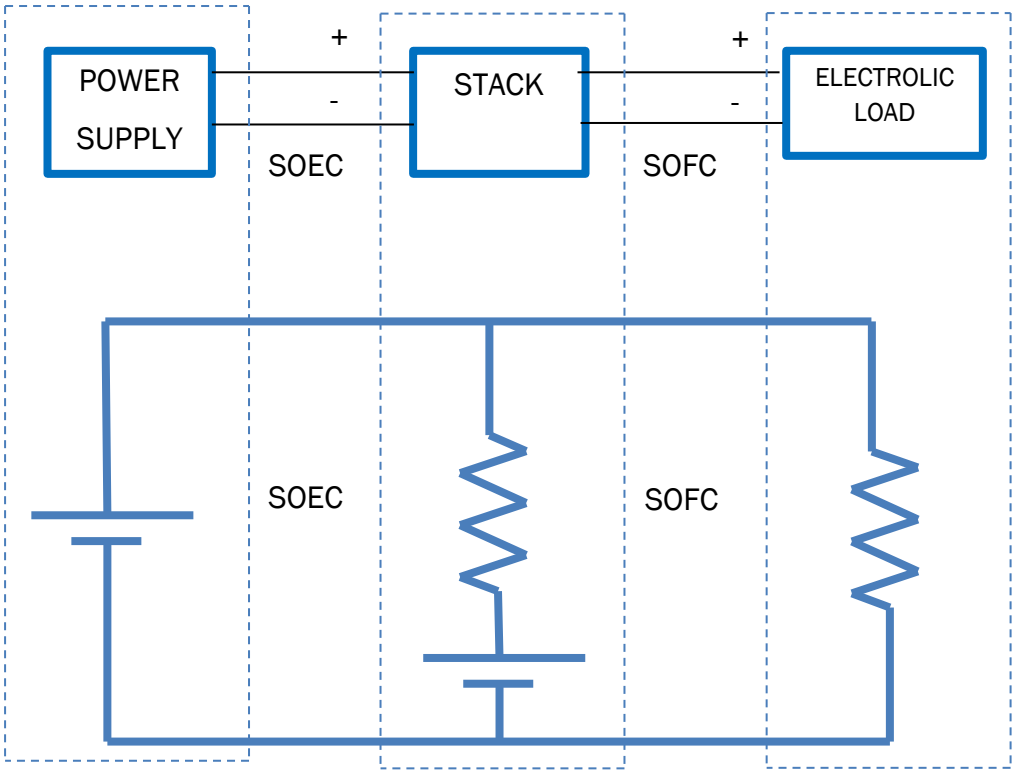


*Figure 25: Test rig electrical circuit*

The electrical connections do not vary to pass from one operating mode to the other one, but while the power supply is working in SOEC, the electronic load is off; and just the opposite SOFC.

The electronic load is in charge to consume electronically the electric energy generated by the fuel cell. It also measures the electric parameters and manages the performance of the stack operating on the current value.

*Figure 26: Test rig electronic load*

The model is BK PRECISION 8510 600 W Programmable DC Electronic Load, the maximum power is 600 W, the current can go from 0 A to 120 A and the voltage can also go from 0 V to 120 V, but the maximum voltage at the maximum current cannot be achieved. The characteristic curves of this model are represented in the following figure:

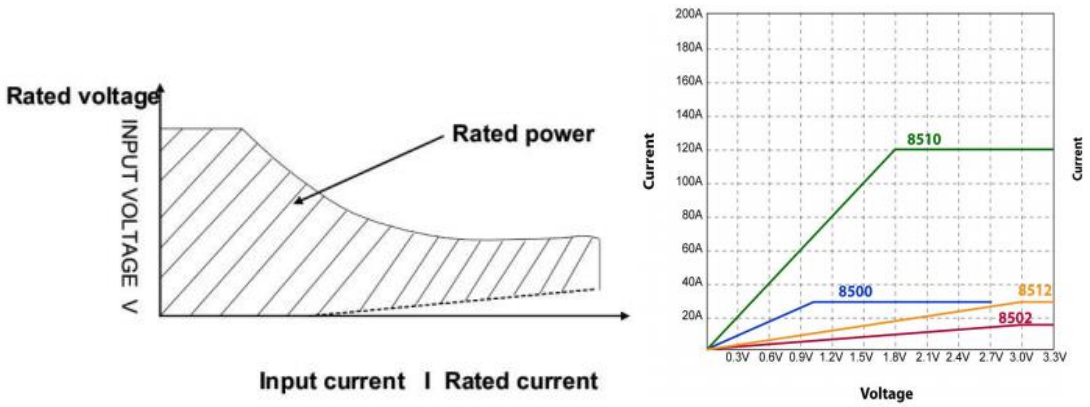


*Figure 27: Electronic load specifications*

The performance of the load is showed in the green line, as the system will work up to 40A, there is no problem with the current voltage [17].

The power supply model is in charge to apply power to the stack in SOEC operation.


*Figure 28: Test rig power supply*

The model is N5763A System DC Power supply, and the parameters are 1500 W of power, 120 A of current and 12,5 V of voltage. In this element, it is possible apply the maximum current at the maximum voltage [18].

With reference to the power measurement, there are seven voltage cables to measure the differential voltages of the six cells of the stack. These cables exit from the bottom of the stack and go to the acquisition data system. The current cables let up to 50 A of current, but in the essays the maximum current will be limited to 40 A. The voltage cables (red) and the current ones (black) can be seen in the following picture taken in the test rig:

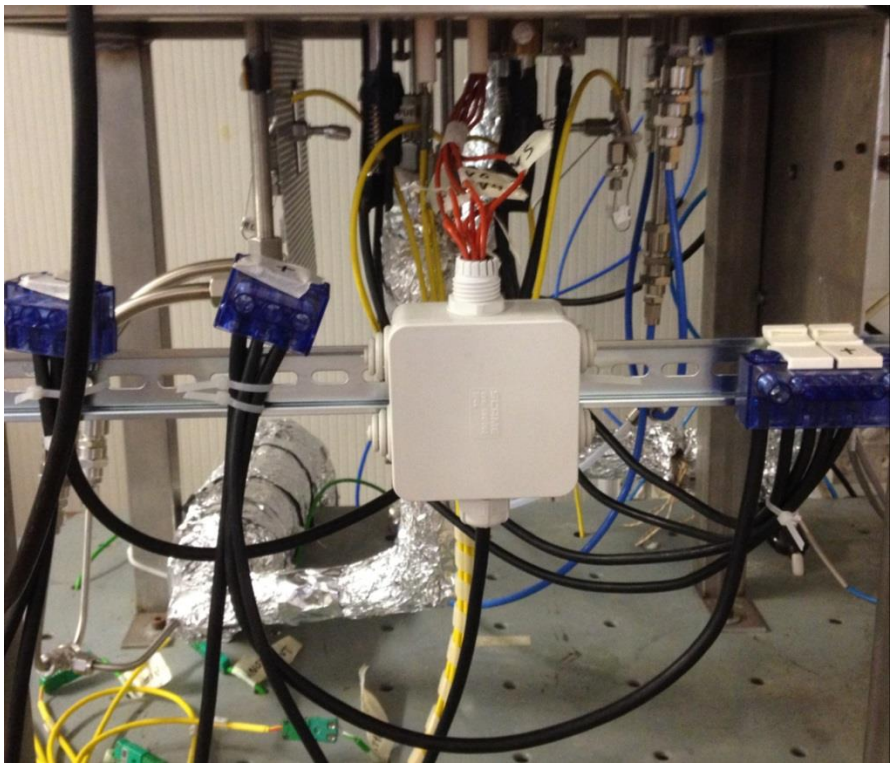

*Figure 29: Test rig voltage and current cables*

The voltage cables coming from the stack connect to the voltage cables of the acquisition data system in a white box to keep it as clean as possible. Regarding the current cables, there are four + cables which start from the bottom of the stack and join in a blue connector. Then, there is a blue connector for the + cables of the three elements (stack, power supply and electronic load), and another one for the – cables.

## 2.3. Gas Inputs and outputs

The input to the stack is a mix of $H_2O$ and $H_2$ in the fuel inlet and air in the air inlet in both operation modes. As it is shown in the physical scheme of the system (figure 21), there are two air inlets, two air outlets, one cold fuel inlet, one hot fuel inlet and one fuel outlet. Before the gas entrance into the stack; components are measured and controlled.

Hydrogen enters into the system through a pipe and goes directly to a flow meter controller, where it is measured and controlled, then it goes to a gas collector (although in this research there is no other gases). After that, $H_2$ goes inside a controlled evaporator mixer when it is mixed with the $H_2O$ and the flowmix is heated, then, the mixture is introduced into the stack fuel inlet by a heating line, which increases the temperature to prevent water from condensation.

Water comes from a bottle where it goes out due to the pressure applied by nitrogen, it pass through a liquid flow where it is measured and controlled, after that it enters in the controlled evaporator mixer and it is mixed with the $H_2$. To avoid condensation, the temperature has to be higher than 100ºC from the controlled evaporator mixer.

Ambient air is comprised outside the test rig in a compressor and it goes inside the system through a pipe, the flow passes through a flow meter controller similar to the hydrogen one, where it is also measured and controlled before the entrance in the air electrode.

There are two output lines, the fuel output, which is a mix between hydrogen and steam (the amount of each compound depends on the operation mode), and the air output, whose composition of oxygen will also depend on the operation mode. Both outputs are already vented in the atmosphere.

The specific elements which take part in this process are:

- Hydrogen and air entrance: the test rig is connected to six inputs pipes where different compounds are supplied (air, nitrogen $N_2$, hydrogen $H_2$, carbon monoxide CO, methane $CH_4$ and carbon dioxide $CO_2$), in this research only hydrogen and air are used. The gases enter in the test rig via metal pipe from external bottles.


*Figure 30: Test rig input gases*

- Flow meter controllers: instruments to control and measure the amount of each gas which will go inside the stack, there is one flow meter controller for each gas except hydrogen, whose flow is divided in two flow meters. The amount of gas is measured inside and an electronic system allows the control of the flow.
  The two hydrogen flow meters have a range of 60 and 600 Nl/h. The air flow meter has a range of 1000 Nl/h.

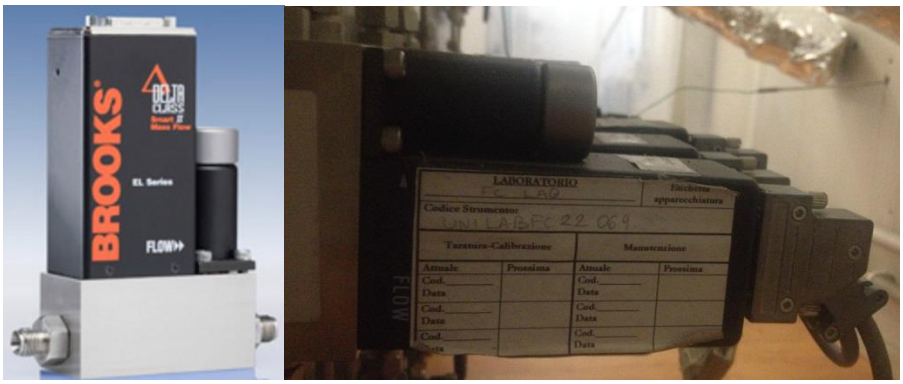


*Figure 31: Test rig flow meters*

- Water entrance, the water is bi-distilled and comes from a container (bottle); it starts to flow when some pressure is applied to the bottle by an inert gas, which in this case in nitrogen. It flows as a liquid until the entrance into the controlled evaporator mixer, when it changes to steam due to the high temperature.


*Figure 32: Test rig water bottle*

- Liquid flow and controlled evaporated mixer: these two elements work together, they measure and control the water, that is consequently mixed with the hydrogen flow while the temperature of the gas mixture increases. Liquid water at room temperature from the container is measured by a liquid mass flow meter before entering into the controlled evaporator mixer, the amount of liquid is limited at 120 g/h.
  The required flow rate is controlled to the set point value by a control valve (C) forming an integral part of the patented liquid flow and carrier gas mixing valve (M). The then formed mixture is subsequently led into the evaporator to achieve total evaporation (E). This explains the abbreviation of CEM: Control - Evaporation - Mixing, the 3 basic functions of the Liquid Delivery System [19].

The mixture between steam and hydrogen exits the CEM from the bottom in a thermal isolated pipe to avoid steam condensation.

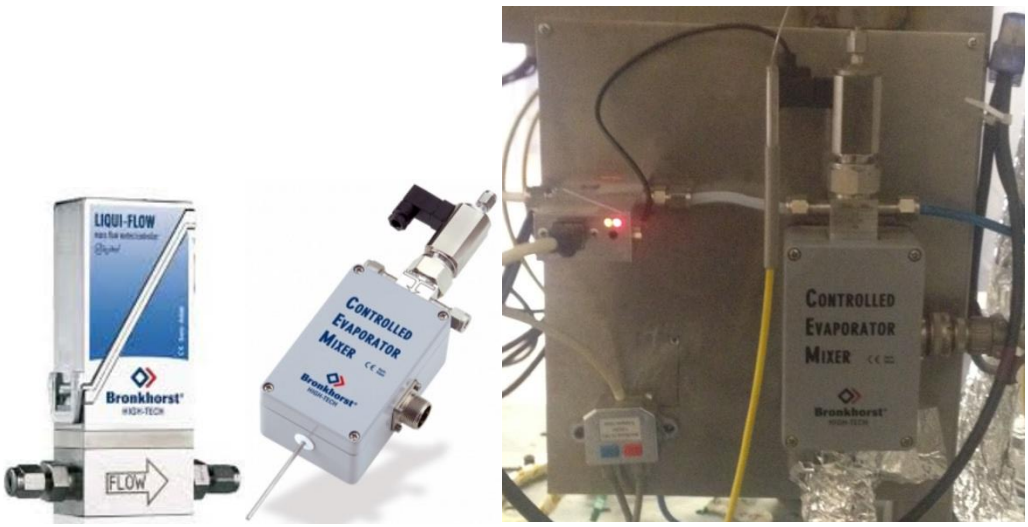


*Figure 33: Test rig liquid flow and controlled evapotaror mixer (CEM)*

- Heating line: the pipe that connects the CEM output with the stack fuel input has a system to increase the temperature of the gas to prevent the steam condensation. The main objective is to conduct and heat the fuel to achieve an optimum temperature of the flow in the entrance of the stack. This pipe is also isolated (as it is showed in the second picture) to reduce heat losses as much as possible.

*Figure 34: Test rig heating line fuel input*

- Output gas lines: there are two isolated pipes where the fuel and air outputs are leaded to the exterior. In this part, it is also important to prevent the steam

condensation, because this phenomenon would suppose a prejudicial increase in the stack pressure.

*Figure 35: Test rig output pipes*

# 2.4. Thermal Control system

With reference to the temperature, there are three principal elements:

- Thermocouples, which measure temperature in different points, as represented in the physical scheme (figure 21). There are two kinds of them, one type is directly connected to the temperature control system and is able to read and send the temperature value to the specific thermal controller, and the other type of thermocouple is only able to read the temperature of a specific part of the test rig. The thermocouples numeration is in the following table:

*Table 5: Summary of thermocouples in the test rig*

| Control thermocouples | Reading thermocouples |
|---|---|
| **Tevap** Controlled evaporator mixer | **T1** Air inlet (stack) |
| | **T2** Fuel inlet (stack) |
| **TR1, TR1"** Heating line thermoregulatory | **T3** Air outlet (stack) |
| | **T4** Fuel outlet (stack) |
| | **T5** Top (stack) |
| | **T6** Bottom (stack) |
| **TR2, TR2"** Furnace thermoregulatory | **T7** Fuel outlet (pipe) |
| | **T8** Air outlet (pipe) |
| | **T9** Atmosphere |

- Furnace, which covers the stack and applies heat through some resistances to keep constant the temperature. An electronic controlled furnace is necessary to

maintain the operating temperature, because the process can be endothermic or exothermic depending on the parameters.

*Figure 36: Test rig furnace*

- Thermal controller, which receives temperature from two thermocouples and varies the current in resistances of the furnace to apply more or less heat. One thermocouple is only to be safe while the other one send the value to compare with the reference.

*Figure 37: Test rig thermal controller*

## 2.5. Communication system

An electronic system is needed to control the process in real time and communicate with the elements of the test rig with a computer. This system is formed by an Ethernet-switch, data acquisition system, junction box, etc.

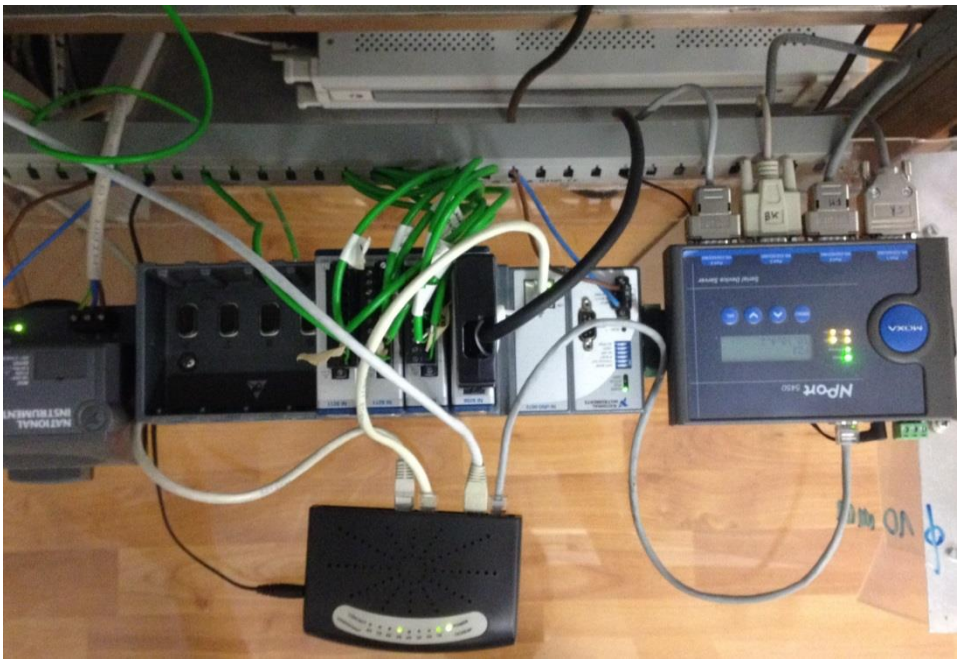

*Figure 38: Test rig data acquisition system*

# 3. Test plan

The main goal of this test is to evaluate the operation of a SOFC stack as a fuel cell and as an electrolizer. The objective is to achieve an efficient way to store energy as hydrogen when there is an energy excess, and to produce electrical energy in the fuel cell when power is needed. To operate this system, there are several parameters which can be modified to achieve high efficiency, long cell life, good relation voltage-intensity, etc. Those parameters have to be modified in different tests to compare the results and obtain useful conclusions for the design and operation of the system.

Concretely, there are three parameters in the test rig which can be varied to make modifications in the global process. First of all, temperature, this will be 750ºC in all tests, typical SOFC temperature. Then the current, which is limited by the electrolysis process, since the maximum water measurement is 120 g/h and that makes a limit of 50 A, but the maximum current in each essay will be limited at 40 A to work safely. And the gas flow, which will be always a mix between water and hydrogen in different proportions in the fuel electrode and air in the air electrode.

There are some electrochemical, thermodynamic and electrical constants which are important to take into account before starting making the tests. They are summarized in the following table:

*Table 6: Electrochemical and thermodynamic constant*

| Symbol | Value | Explanation |
|---|---|---|
| Vm | 22,41 Nl/mol | Molar volume $H_2$, $H_2O$ and air (pure gases) |
| P | 0,0899 Kg/m3 | Hydrogen density |
| LHV ($H_2$) | 119,96 MJ/Kg | Lower heating value $H_2$ |
| LHV ($H_2$) | 240420 J/mol | Lower heating value $H_2$ |
| F | 96485,33 C/mol | Faraday constant |

It is also important to know that each of the six cells of the stack has a surface of 80 $cm^2$, so the total stack surface is 480 $cm^2$.

The fuel electrode input both as SOFC and SOEC has to be a mix between $H_2O$ and $H_2$ to prevent the cell from degradation, but the percentages should not be the same. In SOFC operation, the major compound is hydrogen, which is consumed to produce electric energy, and in SOEC operation, the major compound is $H_2O$, which is divided into $H_2$ and $O_2$ consuming power. To be able to calculate the amount of each compound which is consumed in each operation mode, there is a term to calculate the $H_2$ consumed in the stack as SOFC, and another one to obtain the $H_2O$ consumed as SOEC, both are called fuel rates (they were briefly explained in a previous section).

In SOFC operation, the fuel rate is named utilization of fuel:

$$Uf = \frac{H_{2\,in} - H_{2\,out}}{H_{2\,in}} = \frac{c \cdot I}{2 \cdot F \cdot H_2}$$

In SOEC operation, the fuel rate is named reactant utilization:

$$RU = \frac{H_2O_{in} - H_2O_{out}}{H_2O_{in}} = \frac{c \cdot I}{2 \cdot F \cdot H_2O}$$

These two values can also be fixed to obtain the amount of $H_2$ and $H_2O$, as in the following equations:

$$H_2 = \frac{c \cdot I}{2 \cdot F \cdot Uf}$$

$$H_2O = \frac{c \cdot I}{2 \cdot F \cdot RU}$$

Taking into account that the only input to the fuel electrode is a mix between $H_2$ and $H_2O$ in both cases, and dividing the fuel rates between them, it seems clear that there are two equations and four unknowns, so two of them should be fixed to obtain the other two:

$$H_2O_{con} + H_{2_{con}} = 1$$

$$\frac{Uf}{RU} = \frac{H_2O_{con}}{H_{2_{con}}}$$

With reference to the input to the air electrode, the amount of air is calculated fixing the oxygen rate (utilization of oxygen):

$$Uox = \frac{O_{2\,in} - O_{2\,out}}{O_{2\,in}} = \frac{c \cdot I}{4 \cdot F \cdot O_2} = \frac{c \cdot I}{4 \cdot F \cdot 0{,}21 \cdot Air}$$

$$Air = \frac{c \cdot I}{4 \cdot F \cdot 0{,}21 \cdot Uox}$$

Looking at the fuel and oxygen rate equations, these depend on the current, so a specific current value should be chosen to fix an initial rate, and that is the start point to obtain the other fuel rate values. The operating point of the system is thought to be 500 mA/cm$^2$ of current density, which equals to a 40 A, so the first rates are fixed at this current and they are named Uf@500, RU@500 and Uox@500.

The values of the fuel rates Uf@500 and RU@500 are the same only if $H_2$ and $H_2O$ have the same percentage, 50-50%. The following data are an example of test design using the same Uf@500 and RU@500 of 0.8. So in this case, the amount of $H_2O$ and $H_2$ has to be exactly the same.

$$H_2 = \frac{c \cdot I}{2 \cdot F \cdot Uf} = \frac{6C * 40A}{2 * 96485{,}33 \frac{C}{mol} * 0{,}8A * s} = 0{,}00155 \frac{mol}{s} = 125{,}42\ Nl/h$$

$$H_2O = \frac{c \cdot I}{2 \cdot F \cdot RU} = \frac{6C * 40A}{2 * 96485{,}33 \frac{C}{mol} * 0{,}8A * s} = 0{,}00155 \frac{mol}{s} = 100{,}74\ g/h$$

Normally, the amount of hydrogen is expressed in Nl/h and the amount of water in g/h due to the measurement systems, so in the example, the final values are different but not the molar values.

With reference to the tests planned, two parameters are modified:

- Gas flow: the amount of $H_2$ and $H_2O$ in the fuel inlet and the amount of air in the air inlet are a critic factor to modify, obtaining different results with different values.
- Current: whose value is changing continuously to pass from 0 A to the operating point, 40 A.

The analysis is divided in two essays. Essay one makes reference to the obtaining of the polarization curve of each operating mode under different gas compositions, five tests for each operating mode are planned. Essay two makes reference to the operation with fuel rates constant (constant utilization test) but with a fuel composition of 50-50% with low current levels (safe area), one test has been done with the most favourable gas composition.

All these tests are carried out after the start-up process and the polarization reference of the system.

## 3.1. Start-up and polarization reference

The start-up of the system is the process whose goal is to lead the stack from the ambient temperature to the operation temperature, which in this case is 750ºC. The start-up takes twelve hours, because the considered temperature ramp rate increases one degree per minute. As there is not any thermocouple inside the stack, the assumed reference temperature to the stack is the cathode outlet temperature. When the cathode output thermocouple gets 750ºC, the system is ready to be tested. During the start-up process, water is not used; the fuel is a mix between hydrogen (103 Nl/h) and nitrogen (69 Nl/h) in constant amounts. During this phase gas flow goes inside the stack through the pipe below him, the cold fuel input. The air introduced into the stack through the air input is also constant, and it is 1000 Nl/h approximately. Neither the power supply nor the electronic loads are working during the start-up, so the stack is operating at open circuit (0 A current).

After the start-up, a polarization reference is done to certificate the correct performance of the system. It is a standard procedure which verifies correct behaviour of the stack. The input flows are just the same as the start-up process. However, electronic load is connected to obtain the SOFC polarization curve, so current load goes from 0 to 40 A. As in the start-up process, there is no water, so the fuel entrance is done through the cold line; evaporator is not working during this test.

## 3.2. Polarization curve tests

The first essay is the most typical one; the objective is to obtain the polarization curve (V-J or V-I) of the stack at both operating modes. The stack operated as SOFC and SOEC independently; there will be five tests in each operating mode with different relation $H_2$ - $H_2O$, although one is common to both. In all tests, the current density will go up to 500 mA/cm$^2$ (40 A), which is the estimated working point of the stack. However, the parameter that determines the maximum current is the voltage, which cannot be less than 0,7V in SOFC operation. In each test, there is a different relation between $H_2$ and $H_2O$, which is constant. The fuel rates (Uf in SOFC and RU in SOEC) and the oxygen rate (Uox) at 500 mA/cm$^2$ are fixed to 0,7 and 0,3 respectively. To obtain the polarization curves, the flows are calculated at 500 mA/cm$^2$ and kept constant, while fuel and oxygen utilization rates increase with current. Power and efficiency obtained are thought to have large variations.

The following table lists all the tests made in this essay, half of them correspond to SOFC operation and the rest to SOEC operation, always with different proportions of hydrogen and water.

*Table 7: Summary polarization curve tests*

| Test number | | $H_2$ (%) | $H_2O$ (%) | Uf@500 | RU@500 | Uox@500 | $H_2$ (Nl/l) | $H_2O$ (g/h) | Air (Nl/h) |
|---|---|---|---|---|---|---|---|---|---|
| 1 | SOFC | 0,9 | 0,1 | 0,7 | 6,3 | 0,3 | 143,34 | 12,79 | 796,33 |
| 2 | | 0,8 | 0,2 | 0,7 | 2,8 | 0,3 | 143,34 | 28,78 | 796,33 |
| 3 | | 0,7 | 0,3 | 0,7 | 1,63 | 0,3 | 143,34 | 49,34 | 796,33 |
| 4 | | 0,6 | 0,4 | 0,7 | 1,05 | 0,3 | 143,34 | 76,75 | 796,33 |
| 5 | SOFC-SOEC | 0,5 | 0,5 | 0,7 | 0,7 | 0,3 | 143,34 | 115,13 | 796,33 |
| 6 | SOEC | 0,4 | 0,6 | 1,05 | 0,7 | 0,3 | 95,56 | 115,13 | 796,33 |
| 7 | | 0,3 | 0,7 | 1,63 | 0,7 | 0,3 | 61,43 | 115,13 | 796,33 |
| 8 | | 0,2 | 0,8 | 2,8 | 0,7 | 0,3 | 35,83 | 115,13 | 796,33 |
| 9 | | 0,1 | 0,9 | 6,3 | 0,7 | 0,3 | 15,93 | 115,13 | 796,33 |

The values of RU@500 in SOFC and the values of Uf@500 in SOEC are calculated with the equations explained at the beginning of this section. It seems clear that in SOFC tests, $H_2$ flow is always the same while $H_2O$ flow increases from one test to the following. In SOEC the situation is just the opposite, the $H_2O$ flow keeps constant and the $H_2$ flow varies to each test.

The following table shows, as example, the inputs to run test number five 5, whose data are equal for SOEC and SOFC due to the 50-50% relation between hydrogen and water. In all tests, each step is about 1 A and last one minute.

*Table 8: Inputs polarization curves test number five*

| J (mA/ $cm^2$ ) | I (A) | $H_2$ (mol/s) | $H_2$ (Nl/h) | Uf | RU | $H_2O$ mol/s) | $H_2O$ (g/h) | Uox | Air (mol/ s) | Air (Nl/h) | Total fuel flow (mol/s) |
|---|---|---|---|---|---|---|---|---|---|---|---|
| 0 | 0 | 0,0018 | 143,3 | 0,00 | 0,0 | 0,0018 | 115,13 | 0,00 | 0,01 | 796,3 | 0,0036 |
| 12,5 | 1 | 0,0018 | 143, | 0,02 | 0,02 | 0,0018 | 115,13 | 0,01 | 0,01 | 796,3 | 0,0036 |
| 25 | 2 | 0,0018 | 143,3 | 0,04 | 0,04 | 0,0018 | 115,13 | 0,02 | 0,01 | 796,3 | 0,0036 |
| 37,5 | 3 | 0,0018 | 143,3 | 0,05 | 0,05 | 0,0018 | 115,13 | 0,02 | 0,01 | 796,3 | 0,0036 |
| ... | ... | ... | ... | ... | ... | ... | ... | ... | ... | ... | .. |
| 500 | 40 | 0,0018 | 143,3 | 0,7 | 0,7 | 0,0018 | 115,13 | 0,3 | 0,01 | 796,3 | 0,0036 |

In this test, the dates are the same in SOFC and SOEC because the relation between H2 and H2O is 50-50%. The test plan of this essay is better understood looking at the following graphs:

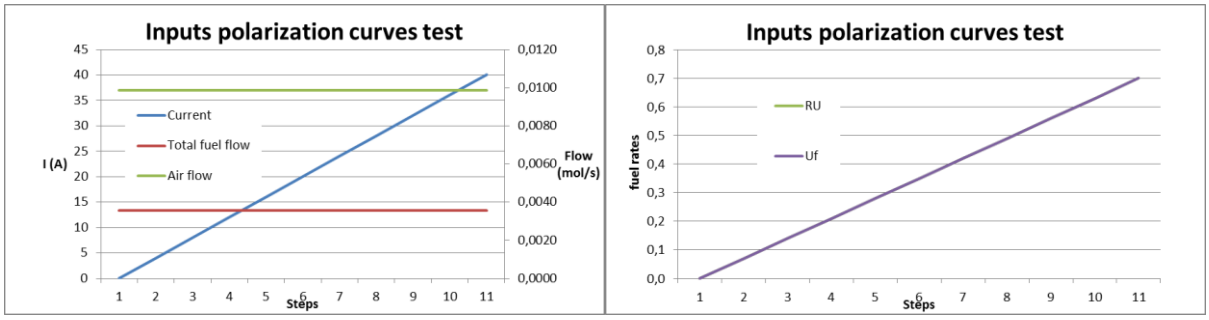


*Figure 39: Inputs polarization curve test five*

The current is increasing from 0 A up to 40 A. The total flow keeps constant all test and the fuel rates are equal, they go from 0 to 0,7, which is the fixed as the minimum value of voltage.

# 3.3. Constant utilization test

In this essay, both SOEC and SOFC in the same procedure, so the current values go from 40 A to 0 A in SOEC operation, and then it goes up to 40 A in SOFC operation. The operating temperature is also 750ºC. The percentage of hydrogen and water is different from SOEC (10% $H_2$ and 90% $H_2O$) to SOFC (90% $H_2$ and 10% $H_2O$), except at low current values, where the relation is 50-50%.

The main difference with reference to the polarization curves is that flows are not constant while the utilization of fuel and the reaction utilization are constant every step. This is how the stack is run except at low current values (from 0 to 12 A), it is called safe area. There, the flows are fixed to avoid a high risk of reoxidation of the stack, which is really dangerous for the cells. Such risk is useless because the cell is not operated for power production but it is only passing from one operation to the other (high efficiency is not needed).

In SOEC operation, the relation chosen between $H_2$ and $H_2O$ is supposed to be similar to real operative conditions. RU@500 is fixed at 0,7 and the Uf@500 is calculated with the equations explained before. Both utilization rates are constant until the safe area, while the $H_2$ and $H_2O$ flows are calculated in each point. The amount of air is constant at 286,68 Nl/h, because the current does not depend on the oxygen; oxygen is produced so only a small flow of air is needed to avoid a concentration of oxygen of 100%. From 0 to 150 mA/cm$^2$ (safe area), the fuel flow is constant and the relation between hydrogen and water is 50-50%, so total fuel flow is constant while the utilization rates change.

In SOFC operation, the relation between hydrogen and water is just the opposite of SOEC. Uf@500 is fixed at 0,7, Uox is fixed at 0,25 and the RU@500 is calculated. Utilization rates are constant until the safe area, while the flows are calculated in each point. The SOFC safe area is in the same current range as the SOEC one and the numerical values are the same.

A summary of the operational parameters chosen to this test is represented in the following table:

*Table 9: Summary of constant utilization test*

| SOEC | | | SOFC | | | Safe area | | Air |
|---|---|---|---|---|---|---|---|---|
| $H_2$ (%) | $H_2O$ (%) | RU@500 | $H_2$ (%) | $H_2O$ (%) | Uf@500 | $H_2$ (%) | $H_2O$ (%) | Uox@500 |
| 0,1 | 0,9 | 0,7 | 0,9 | 0,1 | 0,7 | 0,5 | 0,,5 | 0,25 |

The following table shows inputs to run the test. In this case, each step has taken one hour and each step is 8 A different from the previous one. Each operating step was increased in terms of time to achieve thermal stability.

*Table 10: Inputs constant utilization test*

| J (mA/cm$^2$) | I (A) | $H_2$ (mol/s) | $H_2$ (Nl/h) | Uf | RU | $H_2O$ (mol/s) | $H_2O$ (g/h) | Uox | Air (mol/s) | Air (Nl/h) | Total Fuel flow (mol/s) |
|---|---|---|---|---|---|---|---|---|---|---|---|
| **500** | 40 | 0,0002 | 15,93 | 6,3 | 0,7 | 0,0018 | 115,13 | 1,0 | 0,0036 | 286,68 | 0,0020 |
| **400** | 32 | 0,0002 | 12,74 | 6,3 | 0,7 | 0,0014 | 92,11 | 0,67 | 0,0036 | 286,68 | 0,0016 |
| **300** | 24 | 0,0001 | 9,56 | 6,3 | 0,7 | 0,0011 | 69,08 | 0,5 | 0,0036 | 286,68 | 0,0012 |
| **200** | 16 | 0,0001 | 6,37 | 6,3 | 0,7 | 0,0007 | 46,05 | 0,33 | 0,003 | 286,68 | 0,0008 |
| **100** | 8 | 0,0005 | 43,00 | 0,5 | 0,5 | 0,0005 | 34,54 | 0,17 | 0,0036 | 286,68 | 0,001 |
| **0** | 0 | 0,0005 | 43,00 | 0,0 | 0,0 | 0,0005 | 34,54 | 0,0 | 0,0036 | 286,68 | 0,001 |
| **100** | 8 | 0,0005 | 43,00 | 05 | 0,5 | 0,0005 | 34,54 | 0,17 | 0,0036 | 286,68 | 0,001 |
| **200** | 16 | 0,0007 | 57,34 | 0,7 | 6,3 | 0,0001 | 5,12 | 0,25 | 0,0047 | 382,24 | 0,0008 |
| **300** | 24 | 0,0011 | 86,00 | 0,7 | 6,3 | 0,0001 | 7,68 | 0,25 | 0,0071 | 573,36 | 0,0012 |
| **400** | 32 | 0,0014 | 114,7 | 0,7 | 6,3 | 0,0002 | 10,23 | 0,25 | 0,0095 | 764,48 | 0,0016 |
| **500** | 40 | 0,0018 | 143,3 | 0,7 | 6,3 | 0,0002 | 12,79 | 0,25 | 0,0118 | 955,60 | 0,0020 |

The first part corresponds to the SOEC operation, the last one corresponds to the SOFC operation and the part in the middle is the safe area. The way in which inputs are to change during the test can be better understood looking at the following graphs:

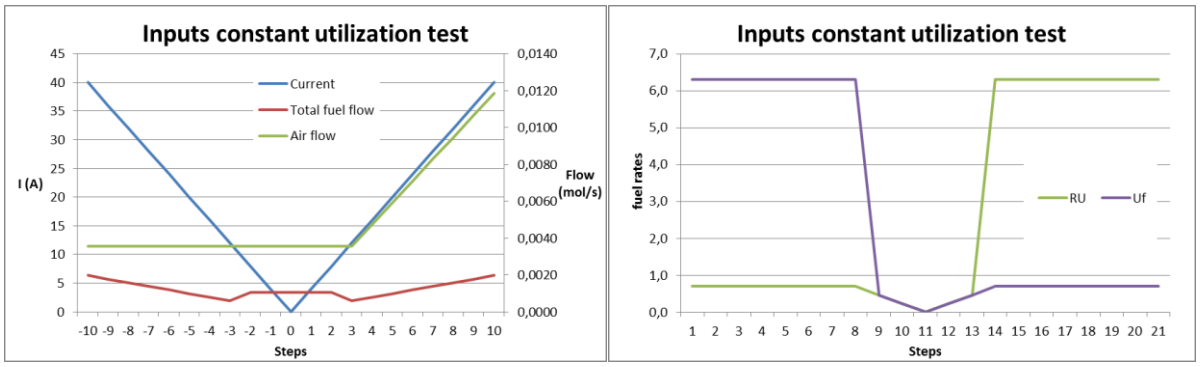


*Figure 40: Inputs constant utilization test*

The first half of each graph corresponds to the SOEC operation and the other to the SOFC operation. Current is decreasing from 40A up to 0A and then it goes again to 40A. On both sides of the graph, Uf and RU are constant, while total fuel flow varies as it depends on current. In the middle of the graph (safe area), total fuel flow is constant while Uf and RU go up to 0 due to the dependence to current.

The gas composition in the fuel inlet can be represented in the following graph:

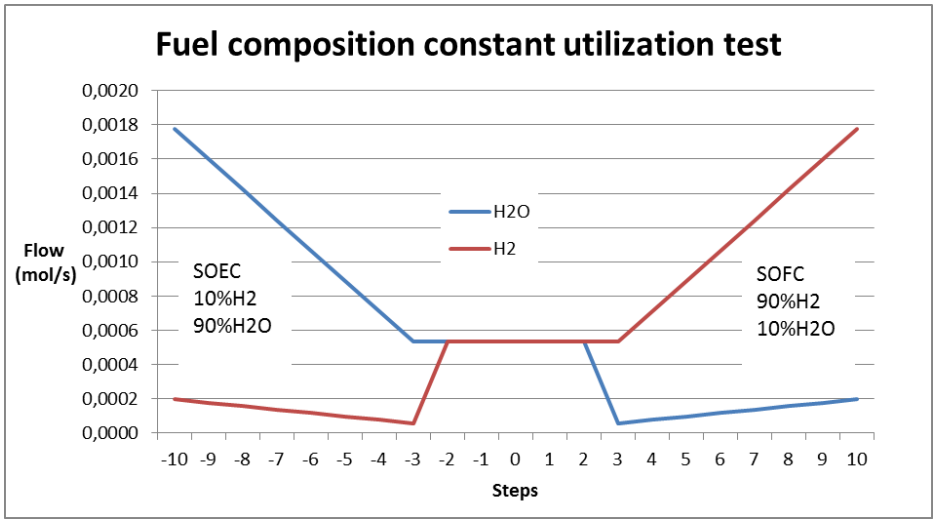


*Figure 41: Fuel composition of constant utilization test*

Both sides of the graph show a variation of the $H_2$ and $H_2O$ flows in SOEC and SOFC with constant proportions, 10-90% in SOEC and 90-10% in SOFC. In the safe area, both flows are equal, 50-50%. There are two composition percentage changes in both limits of the safe area.

# 4. Results and analysis

## 4.1. Start-up and polarization reference results

As it has been explained before, the start-up is the process to achieve the high temperature needed to run the stack in any of both operating modes. Flows are constant, no water is utilized and the stack is not connected to the circuit (open circuit, 0 A). Current is zero while voltage is zero until a specific temperature, as it is showed in the following graph:

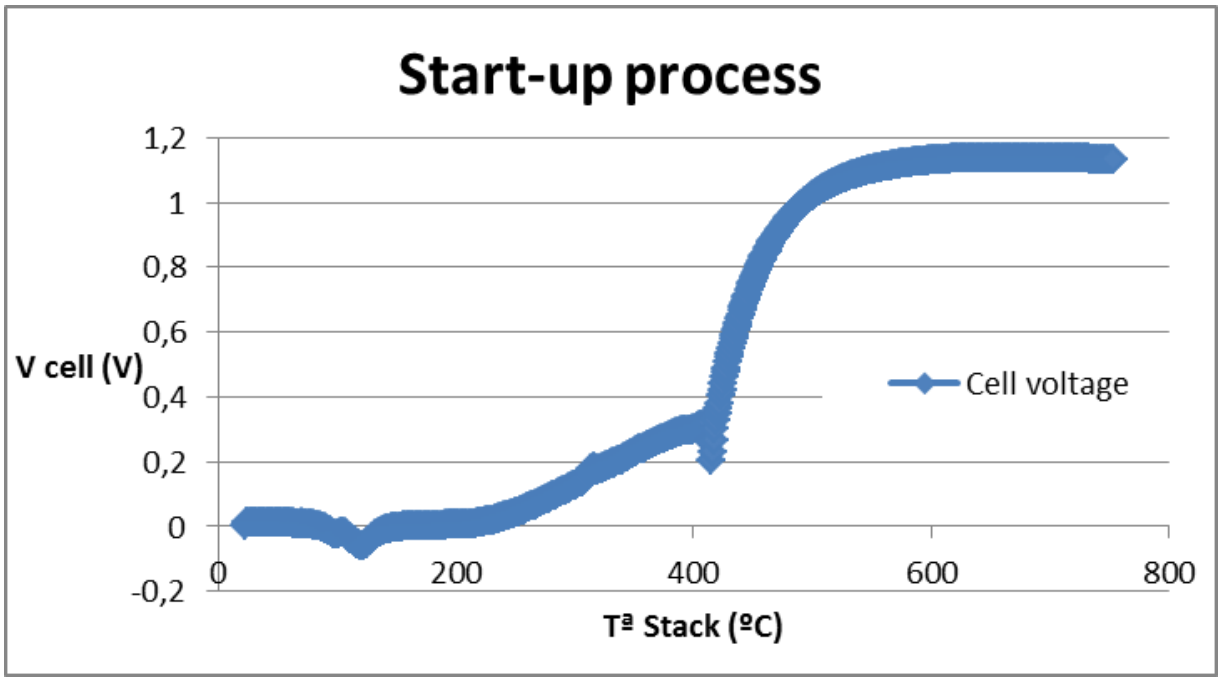


*Figure 42: Cell voltage – Stack temperature start- up process*

The average voltage of the cells is represented as function of the stack temperature (Tª cathode out). After c.a. -400ºC the cells have a potential which increase with temperature until it gets stable.

Regarding the polarization reference, the SOFC polarization curve is represented in the following graph:

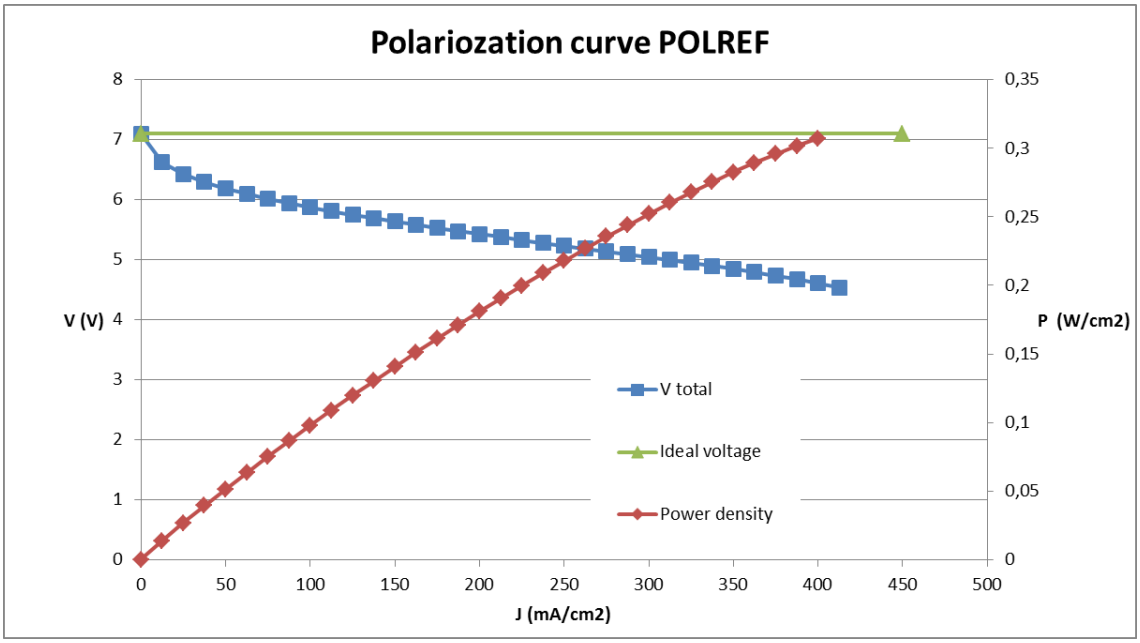


*Figure 43: SOFC polarization reference curve*

Looking at the voltage curve, the shape is just the same as the theoretical fuel cell curve explained in the introduction. The voltage is not the ideal voltage due to irreversibilities that can be summarised in three losses groups explained previously. The first turn at low current density represents the activation losses, then the following part is a straight with low pending which makes reference to the ohmic losses, and the last part of the line seems to start another small turn which is the mass transport losses.

# 4.2. Polarization curve tests results

The first essay is the calculation of polarization curves at different compositions, as it was explained in the test plan. The first four tests are SOFC, the number five is a SOFC/SOEC test, and the next four are SOEC.

First of all, a typical SOFC and SOEC operation are individually analysed in detail. Then, there are comparisons of the SOFC and SOEC tests. And by last, SOFC and SOEC with the same composition are analysed together.

## SOFC operation

The polarization curve of SOFC operation with a composition of 90% $H_2$ and 10% $H_2O$ (test one) is showed in the following graph:

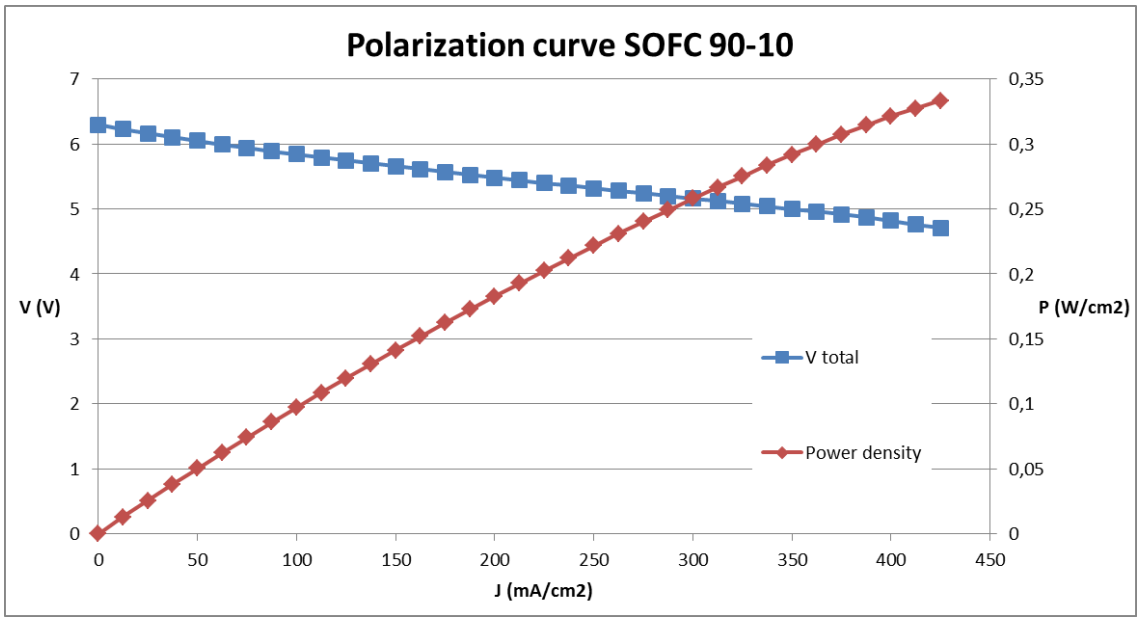


*Figure 44: SOFC polarization curve test one*

The voltage of the stack is the addition of the voltage of each cell. The shape of the curves is quite similar as the theoretical ones; voltage decreases with current due to irreversibilities. However, the shape is different, more linear, because of the addition of steam. The maximum current density is not 500 mA/cm$^2$ as cell voltage is limited to 0,7 V. The power density reaches a maximum value of 0,33 W/cm$^2$, which corresponds to a value of 160 W (maximum SOFC power).

Figure 45 shows the voltage of each cell individually.

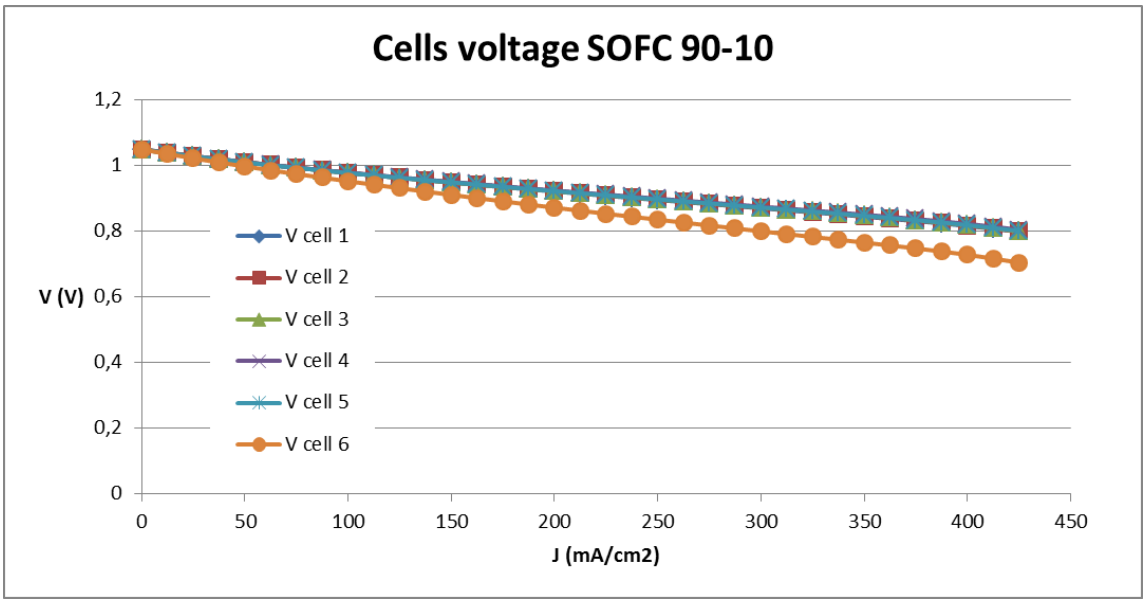


*Figure 45: SOFC cells voltage polarization curve test one*

It is clearly observable the voltage limitation (0,7 V) is reached by cell 6. Five cells have exactly the same behaviour while the last one has behaved worse than the others making a limitation on the stack. The reasons of the problem are unknown.

Regarding the thermal behaviour, the most important temperature to be focused on is the stack temperature, as there is not any thermocouple inside the stack, the air output temperature is considered as reference. The variation of this temperature with current density is showed the following graph:

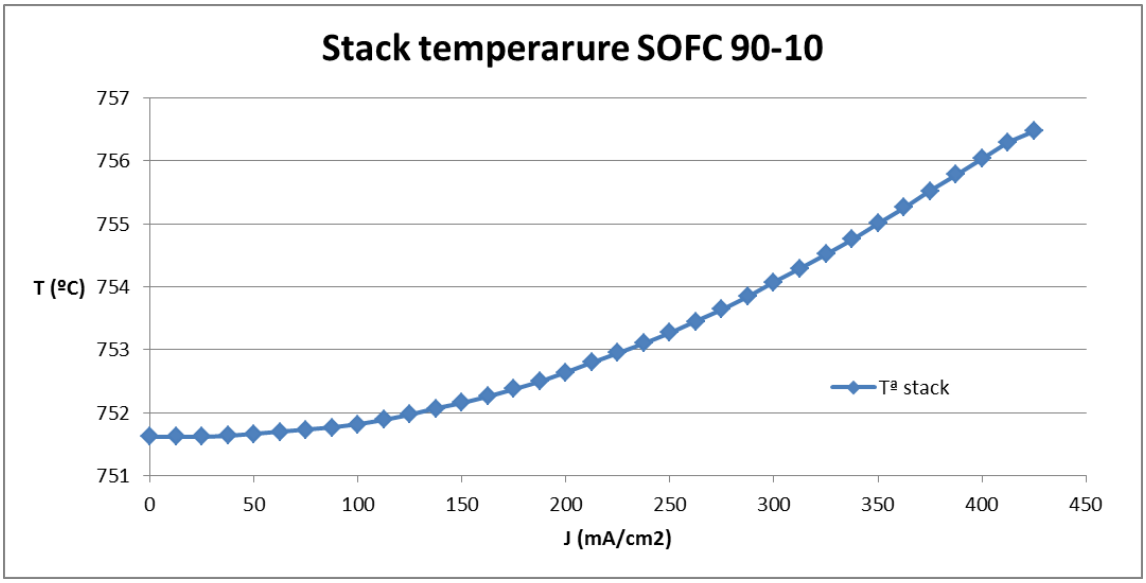


*Figure 46: SOFC thermal behaviour polarization curve test one*

There is an increase of temperature with current: this phenomenon is expected because the SOFC reaction is exothermic and the stack is heating up during operation.

Regarding the system efficiency, as it is SOFC operation, the power output is the stack electric power and the power input is the power correspondent to the amount of hydrogen which is introduced, because the hydrogen in the outlet is not recovered. The efficiency increases linearly with current, so the maximum efficiency corresponds to the maximum current possible.

$$\eta_{SOFC} = \frac{P_{out}}{P_{in}} = \frac{P_e}{LHV_{H_2} * H_{2,in}} = \frac{34 * 4{,}7}{240420\ J/mol * 0{,}0018 mol/s} = 0{,}3692$$

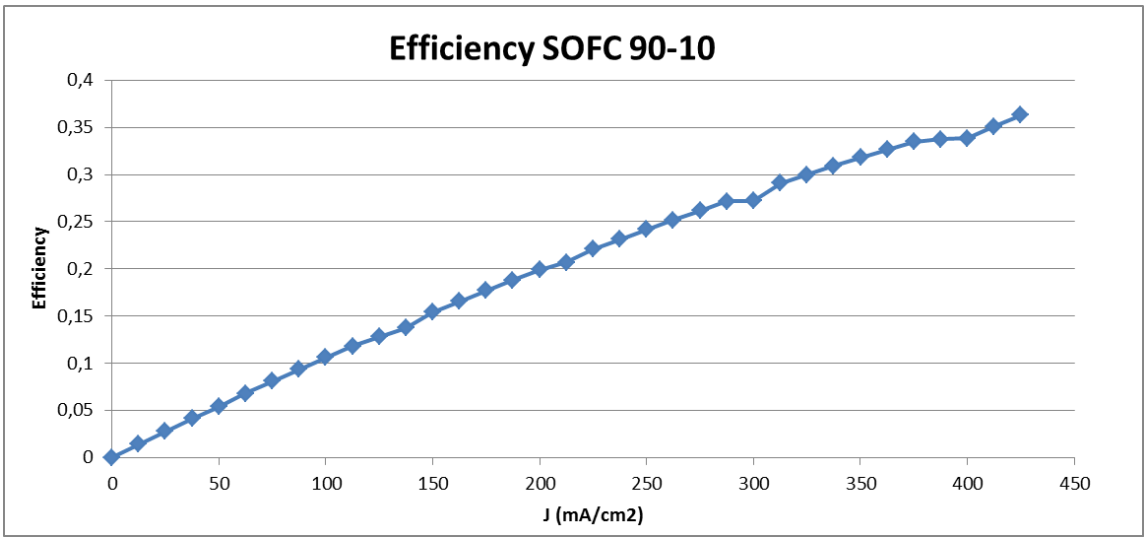


*Figure 47: SOFC stack efficiency polarization curve test one*

In polarization tests, more current level is achieved, more efficient the system is.

## SOEC operation

The following case is the most interesting of SOEC operation because the amount of $H_2$ is the minimum of all tests (10%). The polarization curve of the SOEC operation with a composition of 10% $H_2$ and 90% $H_2O$ is showed in the following graph:

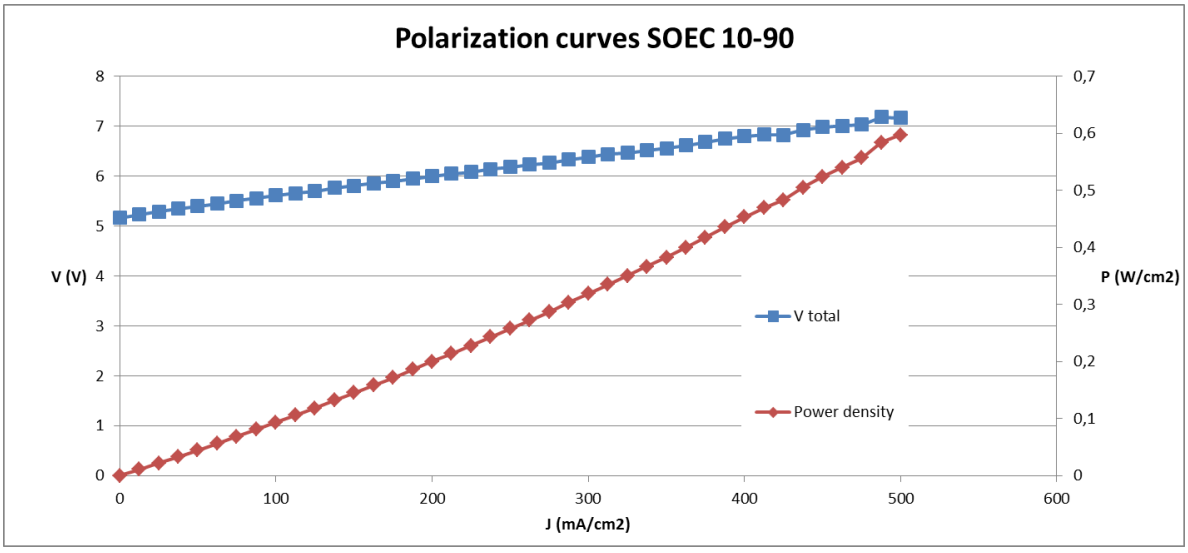


*Figure 48: SOEC polarization curve test nine*

The system operation is in accordance with the theoretical behaviour of a high temperature electrolizer. The voltage increase with the current due to the overpotentials explained in the introduction. The maximum current density is 500 mA/cm$^2$. The power density in this case is applied to the system by the power supply, and the maximum value is 3,6 W/cm$^2$, 287 W.

Figure 49 shows the voltage of each cell individually.

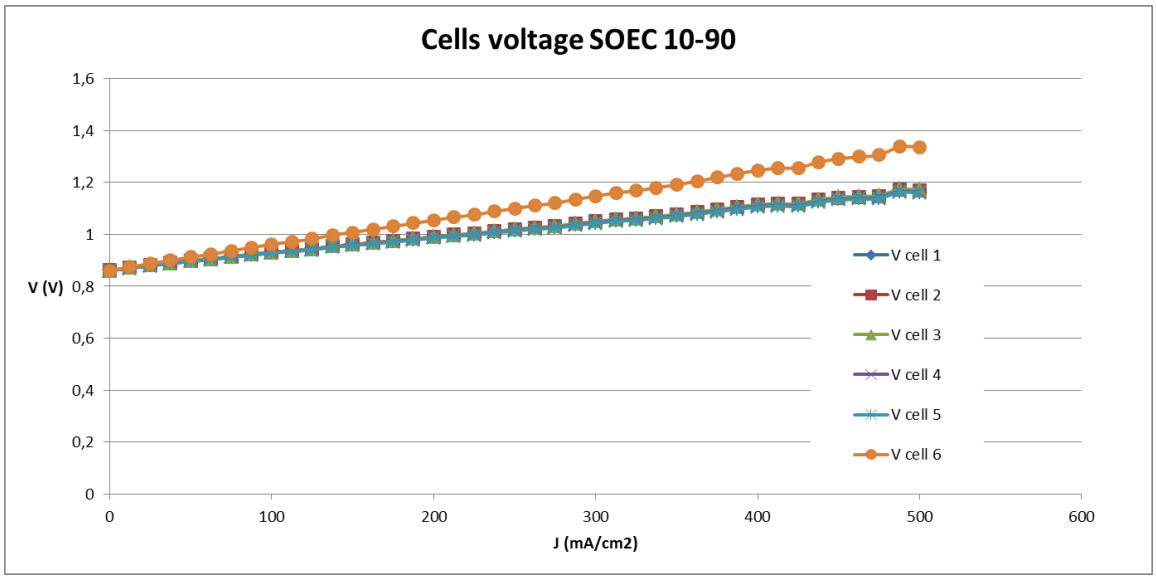


*Figure 49: SOEC cells voltage polarization curve test nine*

Looking at the cells individually, it is clearly observable how the voltage grows up linearly, just in the same way as SOFC operation but increasing instead of decreasing. This is due to the necessity to apply more power to the system to counter the losses, which are higher at higher current levels. As in the other tests, there is a cell whose behaviour is worse than the others.

The thermal behaviour is represented in figure 50.

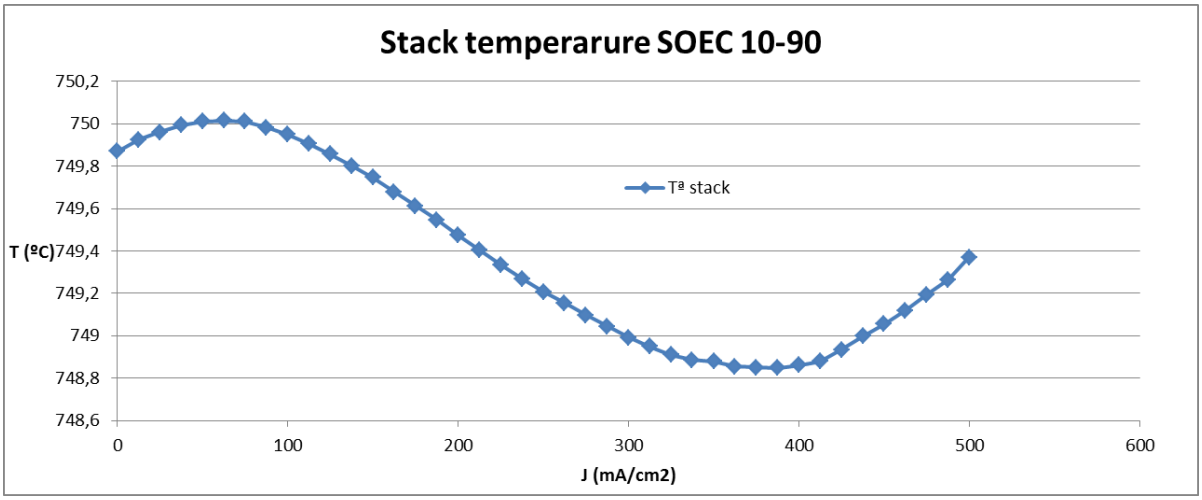


*Figure 50: SOEC thermal behaviour polarization curve test nine*

The temperature shows ups and downs around the operating temperature. At the beginning, there is a decrease in temperature due to the stack is absorbing heat to complete the electrolysis reaction. Then, it changes because from the thermo-neutral potential the stack produces more heat than needed, so the stack is heating up. The furnace of the system is the responsible of achieve a constant operation temperature.

With reference to the SOEC efficiency, as it has been explained in the introduction, the power input is the electric power applied to the stack and the power output is the

power correspondent to the amount of $H_2$ produced. As the outlet flows are not measured, it is more difficult to obtain the efficiency. But the amount of $H_2$ produced can be obtained taking into account the electrolysis reaction (one hydrogen mole is produced each two electrons).

$$H_{2,produced} = \frac{c * I}{2 * F}$$

There are two numerical ways of calculating the efficiency:

$$Efficiency_1 = \frac{H_{2,produced} * LHV}{P_e}$$

$$Efficiency_2 = \frac{H_{2,out} * LHV}{P_e + H_{2,in} * LHV}$$

Efficiency one makes reference to the chemical reaction efficiency, it considers that the hydrogen introduced is recirculated and introduced again inside the stack. On the contrary, efficiency two considers hydrogen as an energy flow which enters and exists in the stack, so hydrogen input and output are two energy terms which appear into the equation.

Both equations have different results at low currents, but they are more or less the same near the thermo-neutral potential, when the efficiency is supposed to be 1, because the heat generated and produced are equal. Thermo-neutral is a theoretical value which can be calculated.

$$Efficiency = 1 = \frac{\frac{I}{2 * F} * LHV}{I * V_{th}} \qquad \boldsymbol{V_{th}} = \frac{LHV}{2 * F} = \frac{240420 J/mol}{2 * 96485{,}33 C/mol} = \boldsymbol{1{,}24 V}$$

Efficiencies, a cell voltage and the thermo-neutral potential are represented in figure 51.

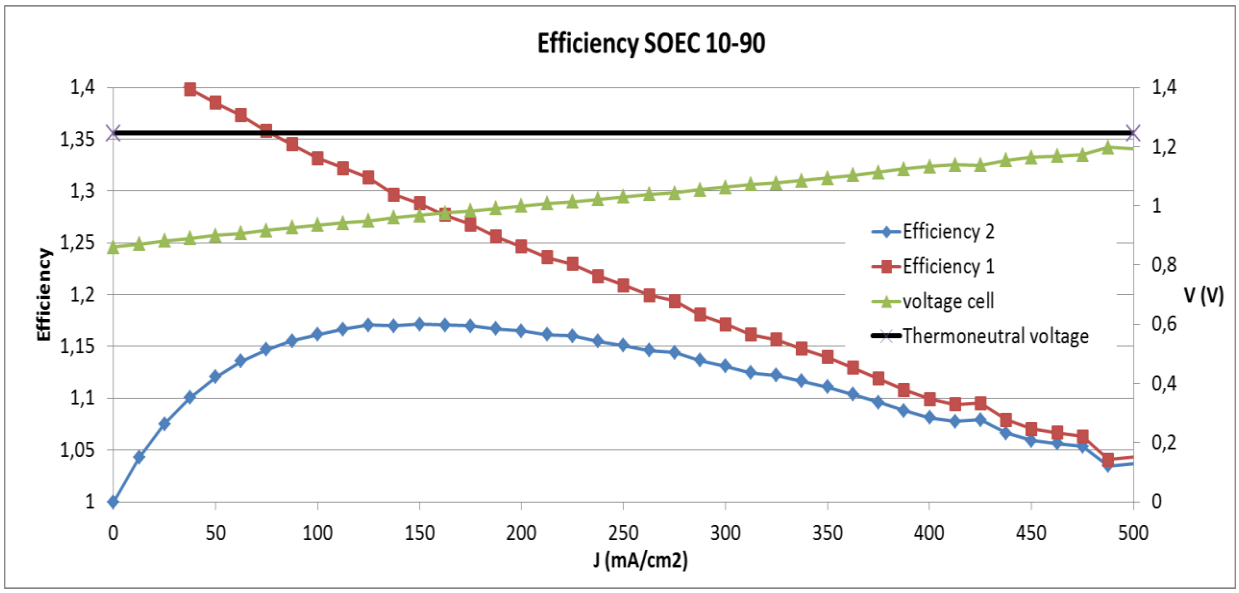


*Figure 51: SOEC stack efficiency polarization curve test nine*

The first conclusion that can be obtained looking at this graph is that the thermo-neutral potential is achieved at 500 mA/cm$^2$. That is very good news because it means that in the point estimated as the stack working point, the efficiency is 100%. Before that point, efficiency is higher than 1 because heat is absorbed to complete the reaction and is not considered in the efficiency equations.

Efficiencies can be also represented with reference to the hydrogen produced in Nl/h:

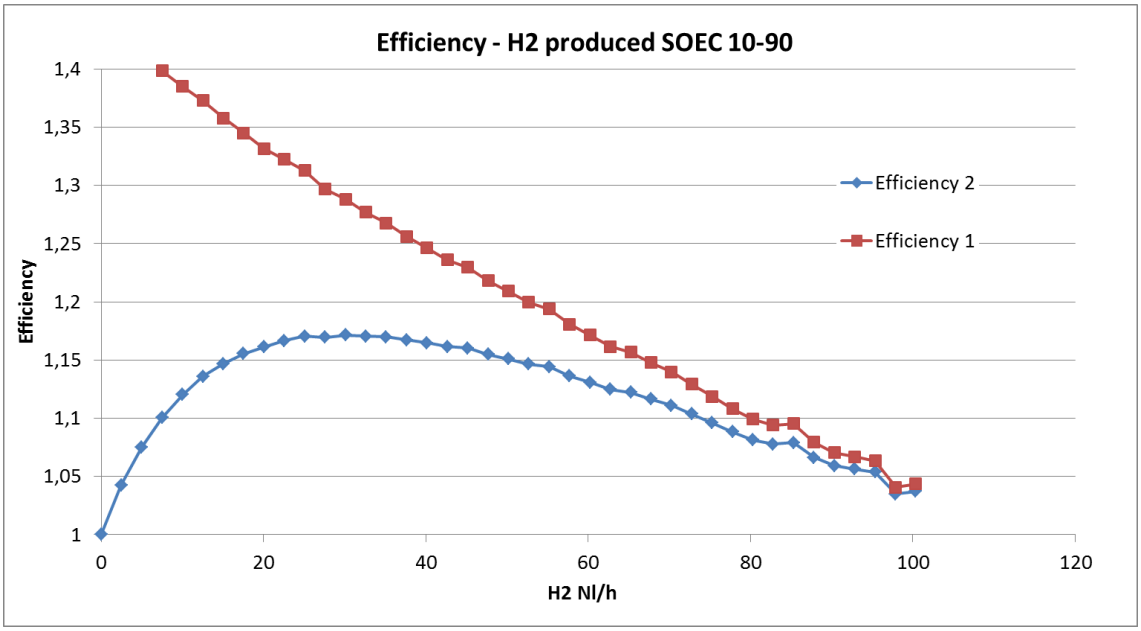


*Figure 52: SOEC efficiency - hydrogen produced polarization curve test nine*

100 Nl/h of hydrogen at 100% efficiency is produced if working at 500 mA/cm$^2$ (operating point). It gives the size of the system. However, it would be possible to apply

more power into the stack to produce more hydrogen with less efficiency (heat excess). It is a trade-off between the energy price and the operational costs.

## SOFC comparison

It is possible to represent the polarization curves of all SOFC tests in the same graph to compare the performance of the stack as a SOFC with different fuel composition, as it is seen in figure 53.

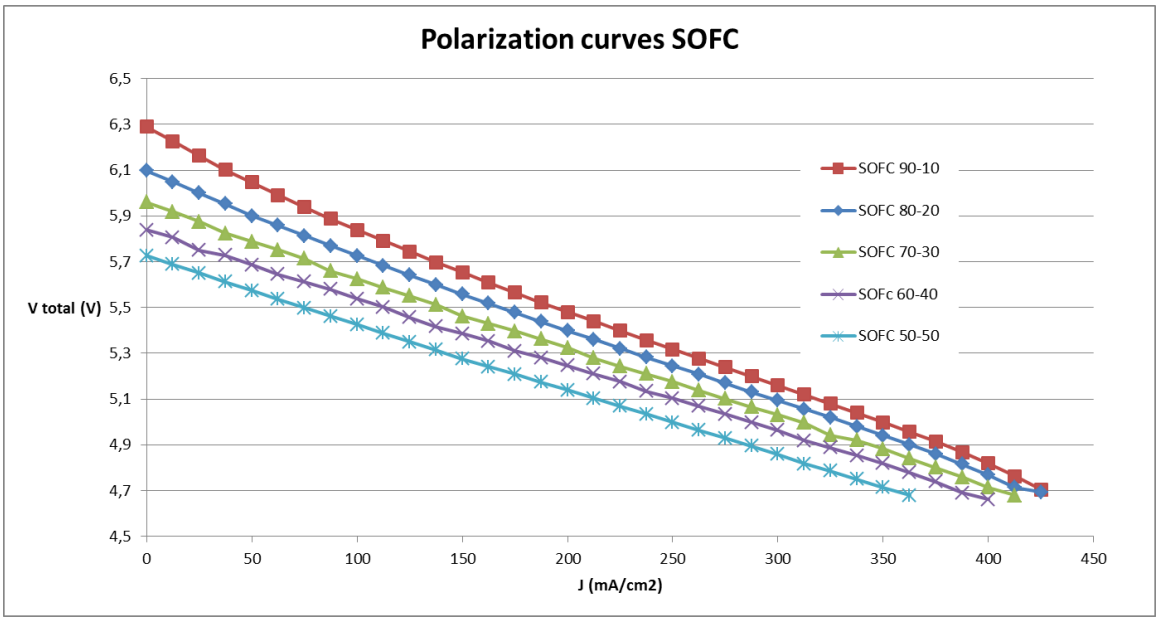


*Figure 53: SOFC comparison polarization curve tests*

It is clear that the performance in SOFC is equal in all tests; all curves are straight and decrease due to irreversibilities. However, there are some differences between them; the OCV is higher with less steam concentration and it lets to achieve higher current level because of the voltage limit. The pending (ASR) is more or less the same in all cases because it depends on the temperature which is constant is all tests.

If figure 54, polarization reference curve is introduced into the same graph:

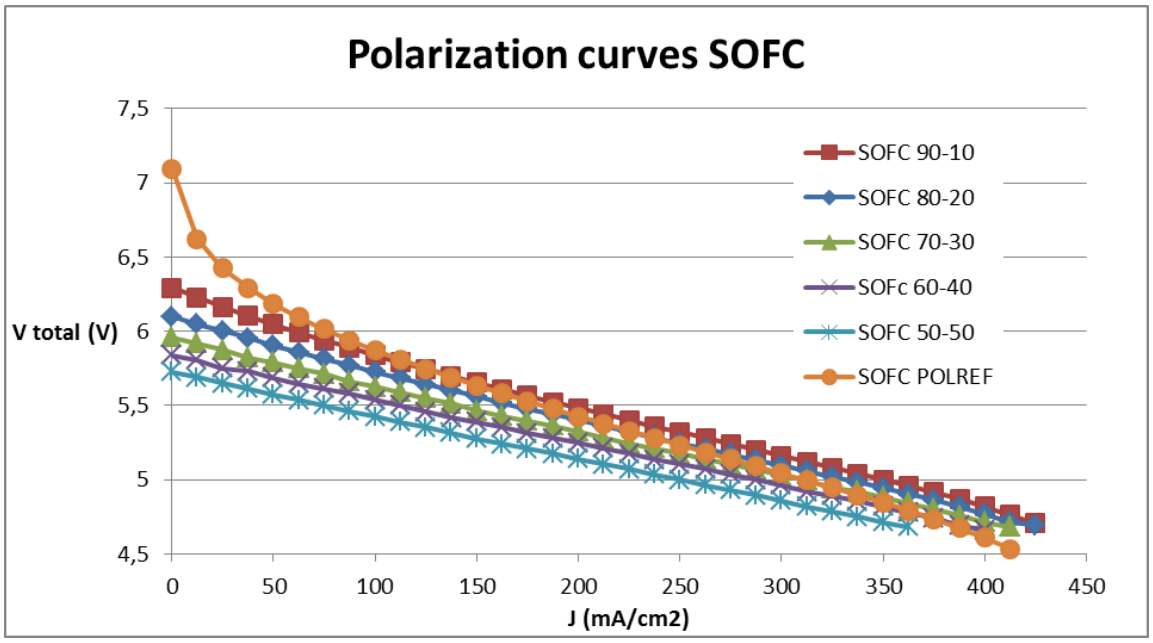


*Figure 54: SOFC comparison polarization curve test and polarization reference*

It clearly observable that polarization reference curve is much more similar to the theoretical fuel cell curve. In the other curves, the OCV is lower and the curve is straight. This difference is due to the addition of steam with hydrogen inside the stack; water has an important role in the activation area of the stack operation, and that is why SOFC polarization curves have this particular shape.

Figure 55 shows a comparative analysis among the stack temperature of all SOFC tests.

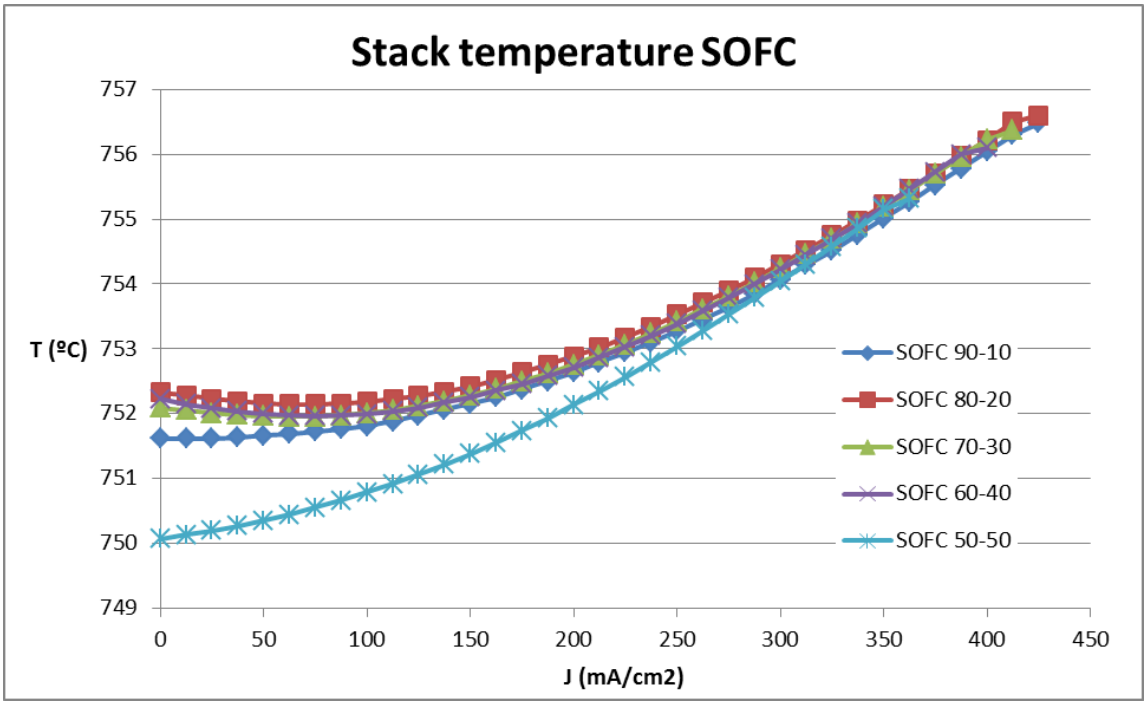


*Figure 55: SOFC thermal behaviour polarization curve tests*

Thermal behaviour is the same in all test, so the stack temperature does not depend on the composition, it depends mainly on the current. The SOFC 50-50 has a different shape because it was done after a SOEC test, and the time to stabilise the system was not enough to start the test from the same point to the other tests. However, the temperature performance is the same as the others.

If the efficiencies are compared, the following graph is obtained:

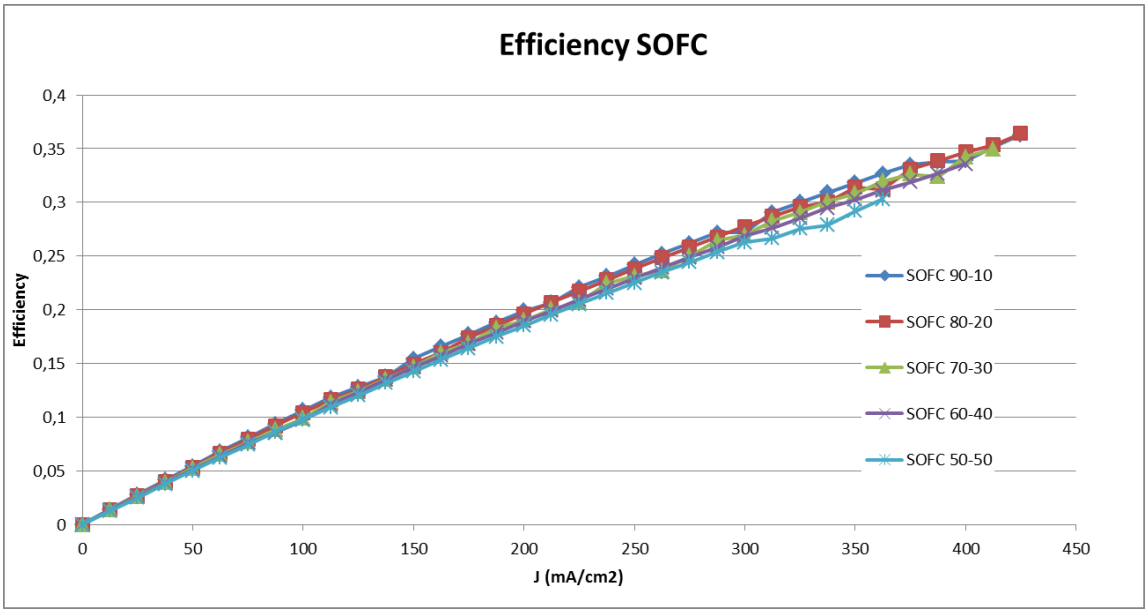


*Figure 56: SOFC efficiencies polarization curve tests*

The fuel composition has not influence in the shape of the efficiency curve. But it limits the maximum current the stack can operate, so in an indirect way, it conditions the maximum efficiency that can be achieved. The test with less steam is able to reach higher current level, so more efficiency is achieved.

The numerical values of the ARS, the OCV, maximum power achieved and maximum efficiency has been calculated and they are showed in the following table:

*Table 11: SOFC test numerical values*

| Test | Stack ASR ($\Omega*cm^2$) | Av. Cell ASR ($\Omega*cm^2$) | Stack OCV (V) | Av. Cell OCV (V) | Power (W) | Efficiency |
|---|---|---|---|---|---|---|
| 1) SOFC 90-10 | 3,53 | 0,589 | 6,29 | 1,05 | 159,81 | 0,37 |
| 2) SOFC 80-20 | 3,24 | 0,539 | 6,098 | 1,02 | 159,59 | 0,36 |
| 3) SOFC 70-30 | 3,05 | 0,508 | 5,96 | 0,99 | 154,49 | 0,35 |
| 4) SOFC 60-40 | 2,91 | 0,485 | 5,839 | 0,97 | 149,15 | 0,34 |
| 5) SOFC 50-50 | 2,87 | 0,478 | 5,726 | 0,95 | 134,67 | 0,30 |

Looking at the ASR results, they are quite similar because there is not dependence to composition. On the contrary, the OCV depends on the composition and it is higher at low steam inputs. Regarding the power, it is higher in the first test because the OCV is

higher and higher current is achieved. The efficiency shows how the first test is the most efficient because the power is higher while hydrogen input does not vary.

Stack OCV and ASR can be represented in a graph:

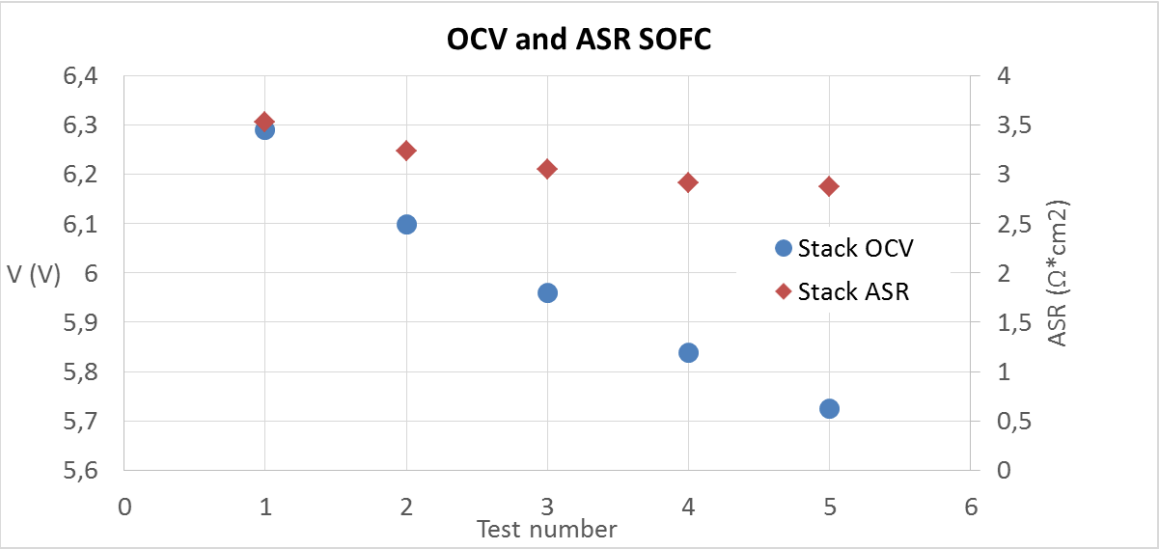


*Figure 57: SOFC OCV and ASR polarization curve tests*

It is clearly observable how OCV is higher in the first test (SOFC 90-10), and it decrease with the steam addition in the stack. With reference to the ASR, there are not many variations due to the operation temperature does not change among tests, although there is a slight decrease with composition.

The conclusion of this essay is that less $H_2O$ in the fuel inlet leads to better performances. But it is always necessary to introduce a low amount of steam with the hydrogen to protect the cells.

## SOEC comparison

If the polarization curves of all SOEC tests are represented in a graph, it is possible to compare the performances. All curves are represented in figure 58.

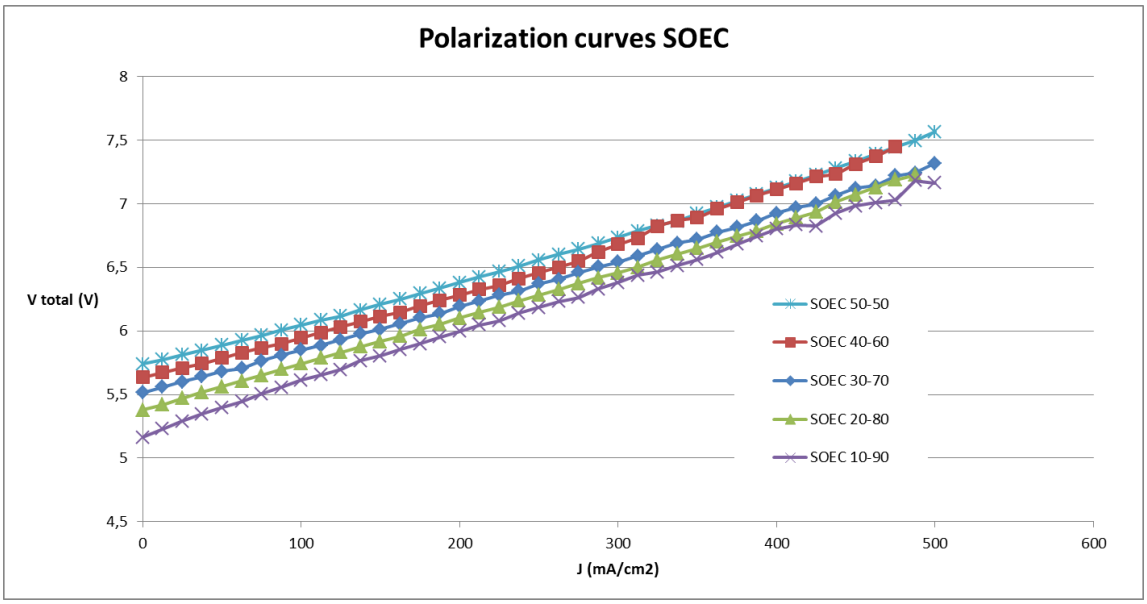


*Figure 58: SOEC comparison polarization curve tests*

All curves have the same shape, voltage increases due to the irreversibilities. However, the OVC is not the same; it is higher when the amount of $H_2$ is higher. In SOEC operation, high OCV values are not convenient as the power supply is applying power to the system. The system has better performance when less is the amount of $H_2$ in the fuel inlet of the stack. However, it is always necessary some $H_2$ mixed with water in the inlet to prevent the fuel cell from degradation, as it has been explained before.

Figure 59 shows a comparative analysis among the stack temperature of all SOEC tests.

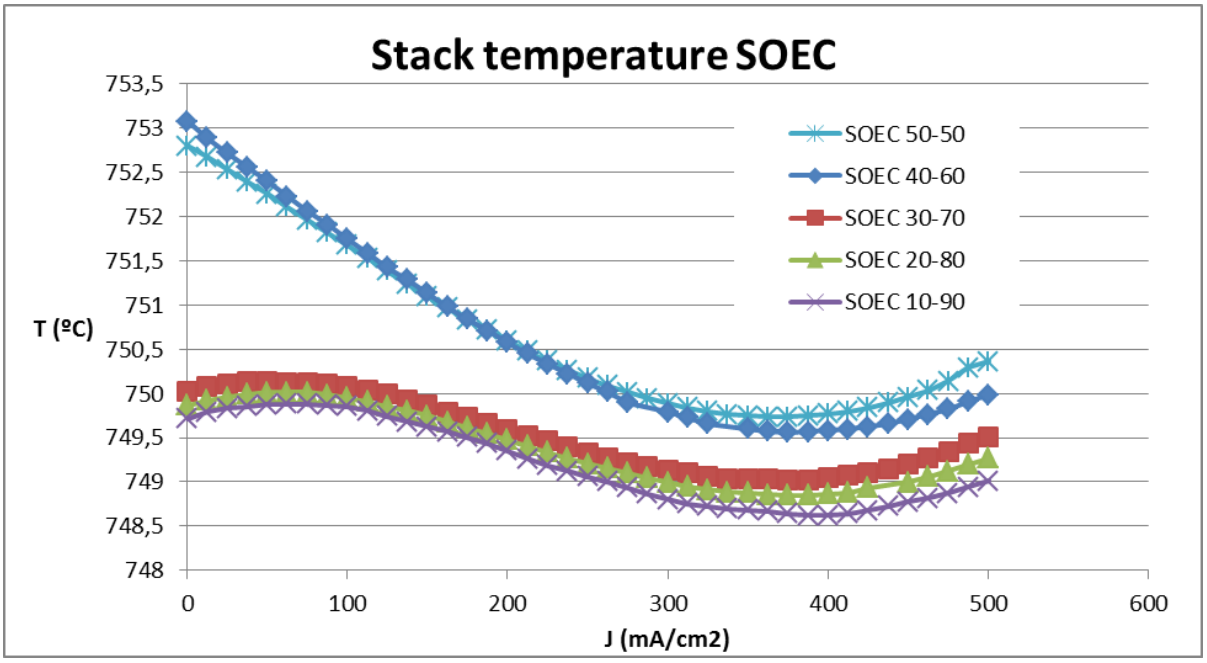


*Figure 59: SOEC thermal behaviour polarization curve tests*

As in SOFC, all test show the same behaviour regarding the stack temperature, which is explained in the SOEC operation. The two different curves are from the tests which have been done after SOFC tests without enough time to stabilise the temperature, so that is the reason for the different start. However, the shape is the same as the others.

It is also interesting to represent the stack temperature variation in some consecutive SOEC tests.

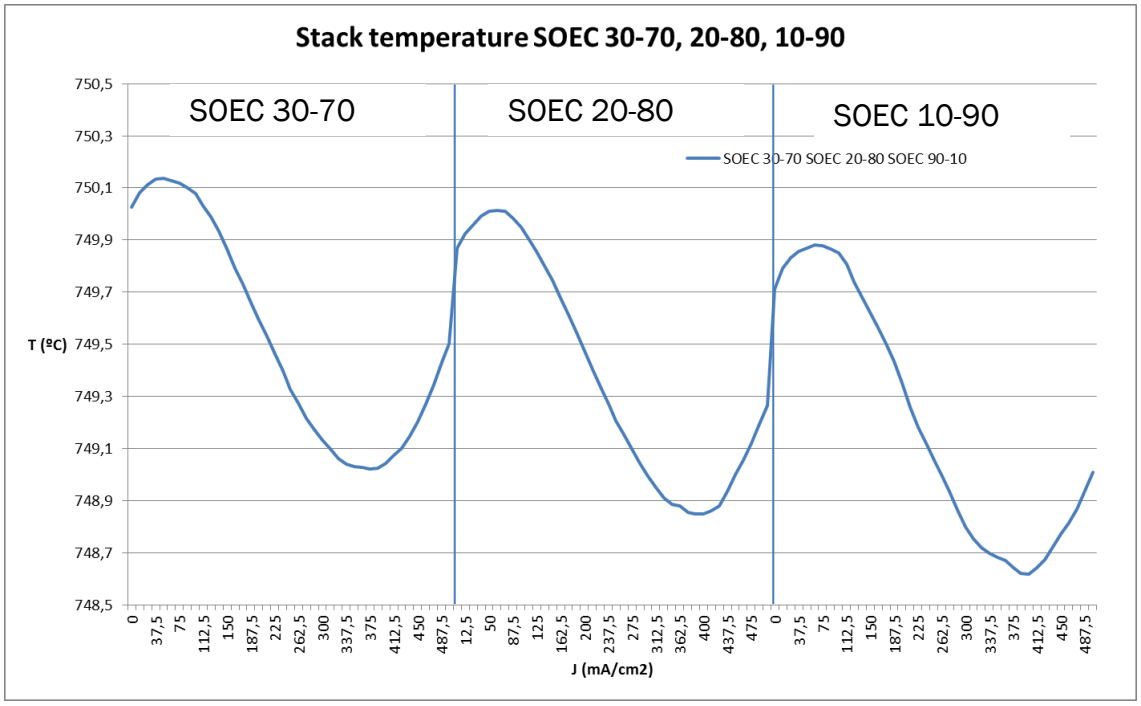


*Figure 60: SOEC thermal behaviour of three consecutive polarization curve tests*

It is clearly observable how stack temperature increases at the beginning of each test due to the thermal inertial of the previous test. After some time, temperature decreases because the stack is absorbing heat to complete the reaction. Finally, the thermal behaviour changes near the thermo-neutral potential. It can be also noticed that there is a reduction in the average temperature.

Regarding the efficiency, a comparison has been made taking as reference both efficiencies in different graph, whose equations are written previously.

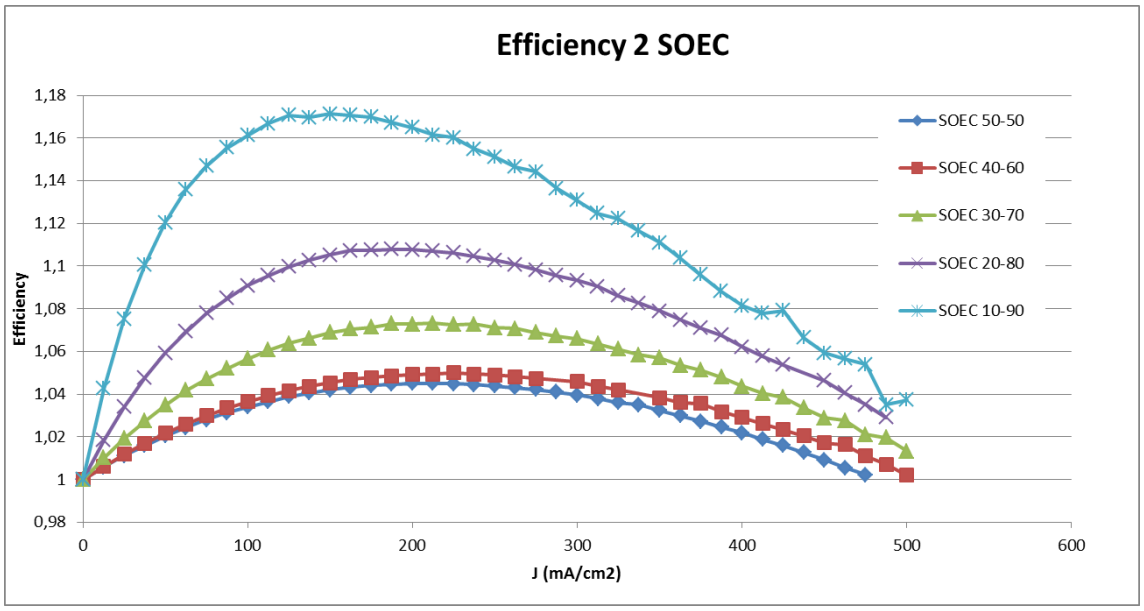


*Figure 61: SOEC efficiency 2 polarization curve test*

The end of all curves is similar; efficiency is around 100% in the thermo-neutral. However, when the amount of hydrogen is lower, efficiency is higher because the hydrogen input is a term which appears in the equation, so SOEC 10-90 leads to a higher efficiency.

Representing efficiency one in a graph:

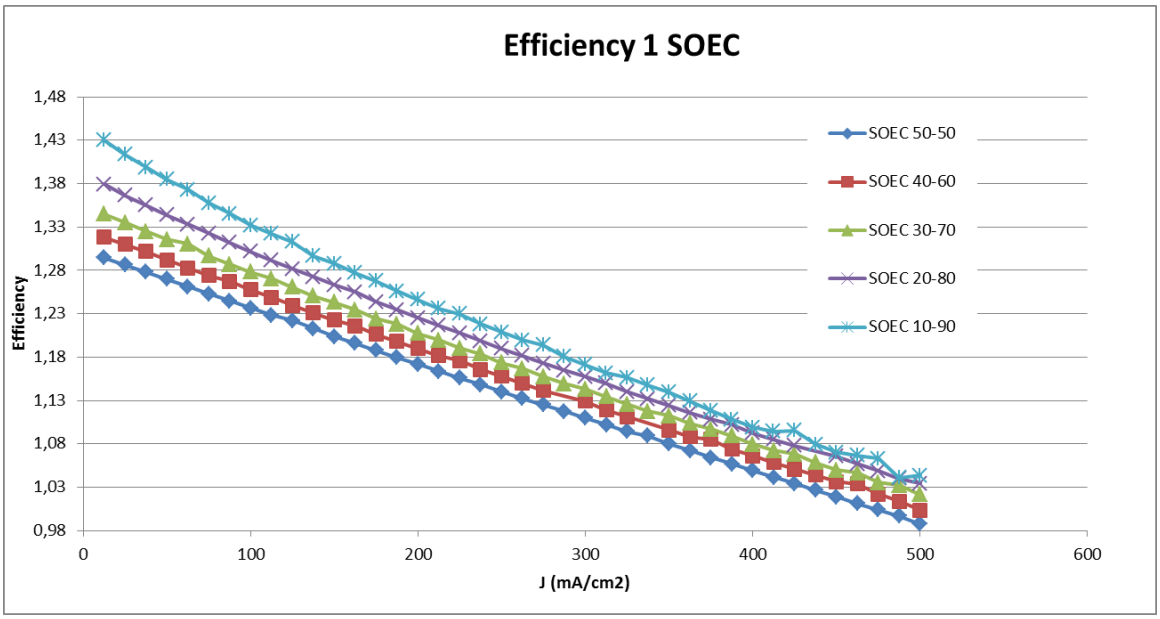


*Figure 62: SOEC efficiency 1 polarization curve test*

With this efficiency equation, there is not such difference among tests because the amount of hydrogen in the inlet is not taken into account. However, it is totally demonstrated that the best SOEC performance is when the amount of hydrogen is lower. Although the amount of hydrogen produced is the same in all cases, the electric power applied to the stack is not the same, and it makes the difference.

As in SOFC comparison, the ASR, the OCV and the maximum power have been calculated and they are showed in the following table:

*Table 12: SOEC test numerical values*

| Test | Stack ASR ($\Omega*cm^2$) | Av. Cell ASR ($\Omega*cm^2$) | Stack OCV (V) | Av. Cell OCV (V) | Power (W) |
|---|---|---|---|---|---|
| 6) SOEC 50-50 | 3,614 | 0,602 | 5,739 | 0,594 | 307,731 |
| 7) SOEC 40-60 | 3,562 | 0,594 | 5,634 | 0,939 | 297,95 |
| 8) SOEC 30-70 | 3,572 | 0,595 | 5,515 | 0,919 | 292,82 |
| 9) SOEC 20-80 | 3,67 | 0,612 | 5,379 | 0,896 | 289,16 |
| 10)SOEC 10-90 | 3,936 | 0,656 | 5,162 | 0,860 | 286,61 |

Looking at the ASR results, the numerical values are quite similar, so the overpotentials don not depend on the composition. The OCV increase when increasing the amount of hydrogen, this means that less power is needed at low hydrogen concentration. This is confirmed looking at the power, which is higher in the 50-50% composition. Efficiency is not calculated because is almost the same in all cases. As it has been explained in SEOC operation, it is 100% in the thermo-neutral potential and from that point; it is reduced due to extra heat produced.

Stack OCV and ASR can be represented in a graph:

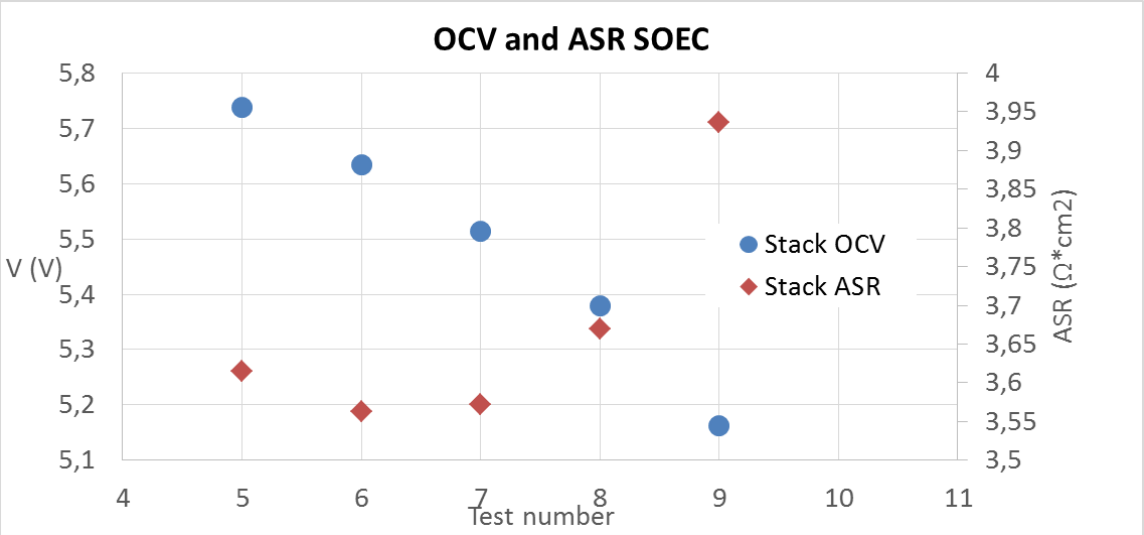


*Figure 63: SOEC OCV and ASR polarization curve tests*

Looking at the OCV points, OCV decreases when decreasing the amount of hydrogen in the fuel inlet, which leads to better performances. With reference to the ASR, the difference among points is due to the stack test temperature, which is a bit different in each test.

The conclusion of this essay is that less $H_2$ in the fuel inlet leads to better performances. But it is always necessary to introduce a low amount of hydrogen with the water to protect the cells.

SOFC SOEC operation

It is also interesting to make an analysis of test five (SOFC/SOEC 50-50%), because all of the input parameters are exactly the same in both operating modes. The only change is that the electronic load is working in SOFC and the power supply is working in SOEC. Both polarization curves can be illustrated together considering negative current to SOEC operation, stack temperature is also represented to analyse the thermal behaviour.

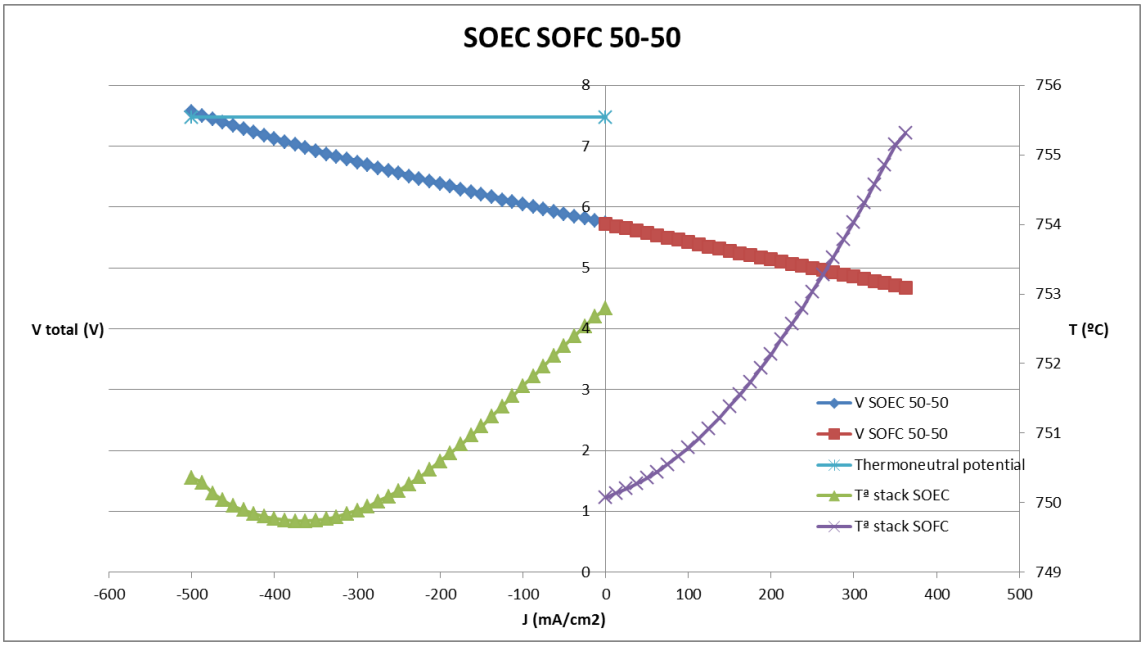


*Figure 64: Thermal behaviour and polarization curves test five*

Focusing on the polarization curves, the shape is the same as the theoretical one, which is represented and explained in the introduction. Voltage increases in the SOEC area and it decreases in the SOFC area due to irreversibilities.

Focusing on temperature, at the beginning of the SOEC area starting from the vertical axis, as the voltage is lower than the thermo-neutral, the stack is absorbing heat from the environment to complete the electrolysis reaction. Stack is cooling down so the stack temperature is decreasing in the graph. The necessary extra heat is produce by the furnace. From the thermo-neutral point, more heat than needed is produced, so in that point the stack temperature changes direction as stack is heating up. In the SOFC area, as the reaction is exothermic, the stack is heating up, so stack temperature increase almost linearly with current.

# 4.3. Constant utilization test results

The constant utilization test is the most realistic test, because it represents the real operation of the system better than the polarization curve tests. The flows change from one step to the next one while the utilizations are constant. In the safe area, the

operation mode change is produced with constant flow to prevent the cell from degradation.

The test was done with the more efficient compositions which have been demonstrated in the previous tests, 10% $H_2$ and 90% $H_2O$ in SOEC and 90% $H_2$ and 10% $H_2O$ in SOFC, the composition in the safe are is 50-50%. The test has started at 40 A in SOEC mode until 0 A, and then current has increased again until 40 A in SOFC operation. A general view of the test is represented in the following graph:

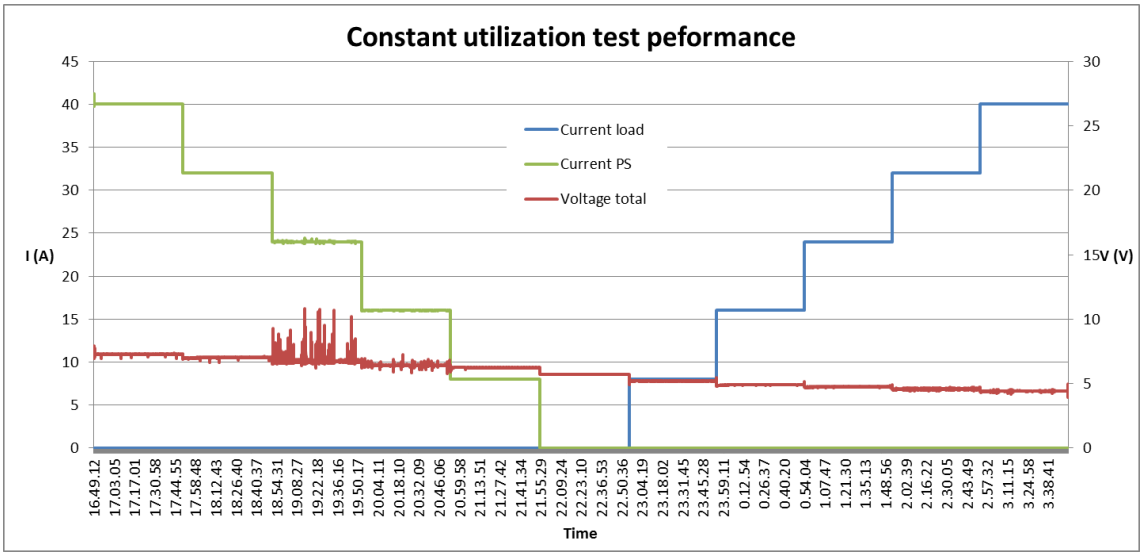


*Figure 65: Current and voltage behaviour Constant utilization test*

Each step was kept for one hour, as there are five steps in each operation mode and the OCV which is common, the total duration of the test has been of eleven hours. However, only the last five minutes of each step has been selected to be analysed, to evaluate data from stable operation. There have been some instabilities in the SOEC operation which were minimised introducing nitrogen with hydrogen into the fuel inlet to compensate the big amount of water and let the CEM work in better conditions.

Looking at the voltage, as in theoretical graphs, it increases in SOEC operation and decreases in SOFC operation, so each area can be clearly identified. To make a detailed analysis of the test, SOEC and SOFC operation has been analysed separately.

## SOFC operation

In the first graph, the voltage and the power are represented with reference to the current density for SOFC operation.

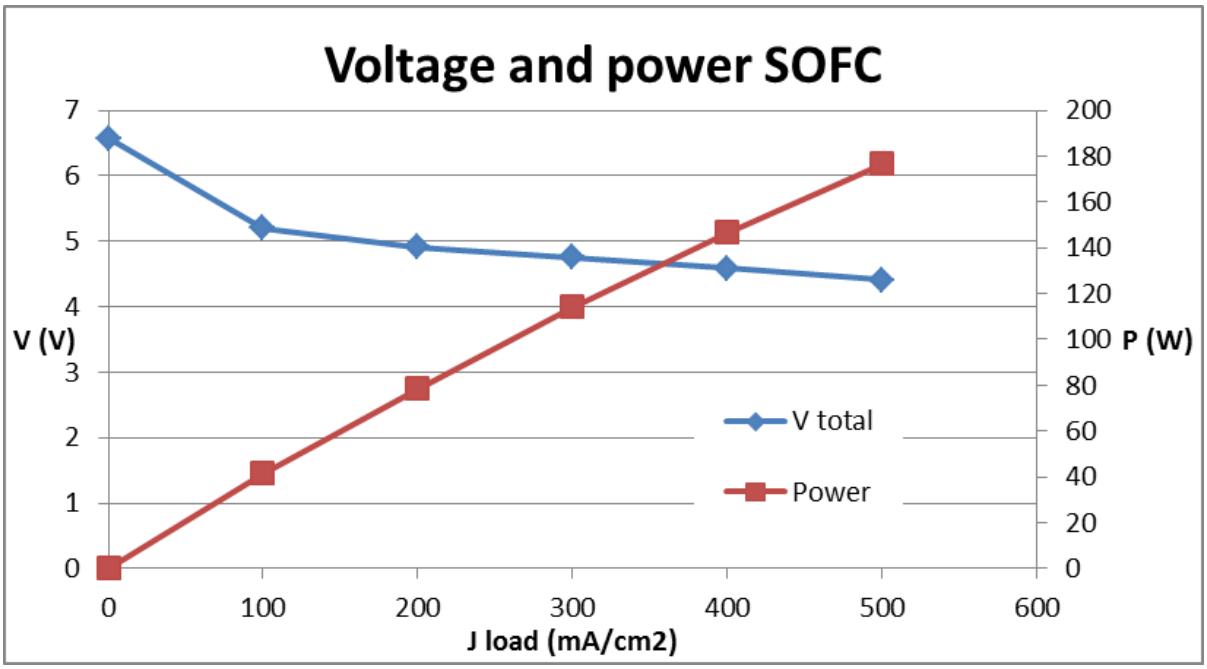


*Figure 66: SOFC voltage and power constant utilization test*

As a SOFC operation, the voltage decrease linearly with current due to the irreversibilities. There is a big difference in the pending between the first part and the rest of the straight, this difference is due to from 0 to 200 mA/cm$^2$ corresponds to the safe area, where the amount of water is higher than the rest. Maybe the safe area could be shorter because from 100 to 200 mA/cm$^2$ the behaviour is similar to the rest of steps, anyway, the system will only work in this area when passing from one operation mode to the other one, so it is not necessary to have optimized conditions. Power increases linearly with current density because voltage barely varies while current is increasing.

Regarding the thermal behaviour of the system, stack temperature is represented in figure 67. As in the previous tests, the cathode output thermocouple is the reference because there are not thermocouples inside the stack.

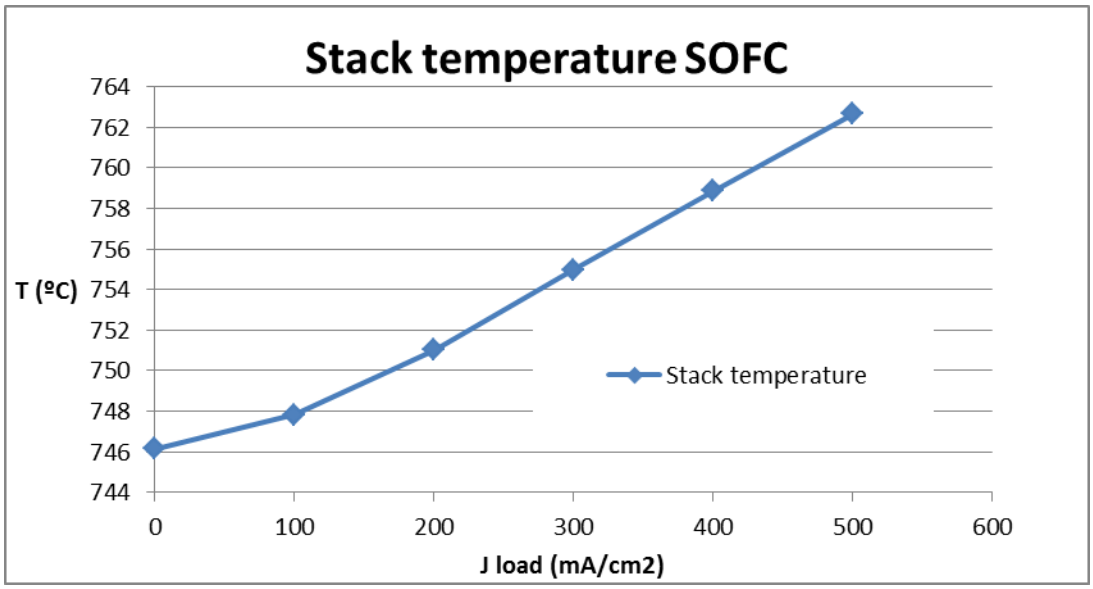


*Figure 67: SOFC thermal behaviour constant utilization test*

The thermal performance is in accordance to the theoretical behaviour of a SOFC operation. The temperature is increasing because heat is produced due to irreversibilities, the heat term (TΔS) increase if power increase. Heat produced was supposed to be countered with the air introduced in the air inlet, which varies respect current density according to a utilization of oxygen of 0,25. However, the graph indicates that a linear addition of air is not appropriate to keep constant temperature. What is clear is that SOFC air management is a really important parameter in terms of thermal behaviour of the system.

One of the most interesting analysis from an engineering point of view is the behaviour of the efficiency respect to the power produced by the system; this is represented in figure 68.

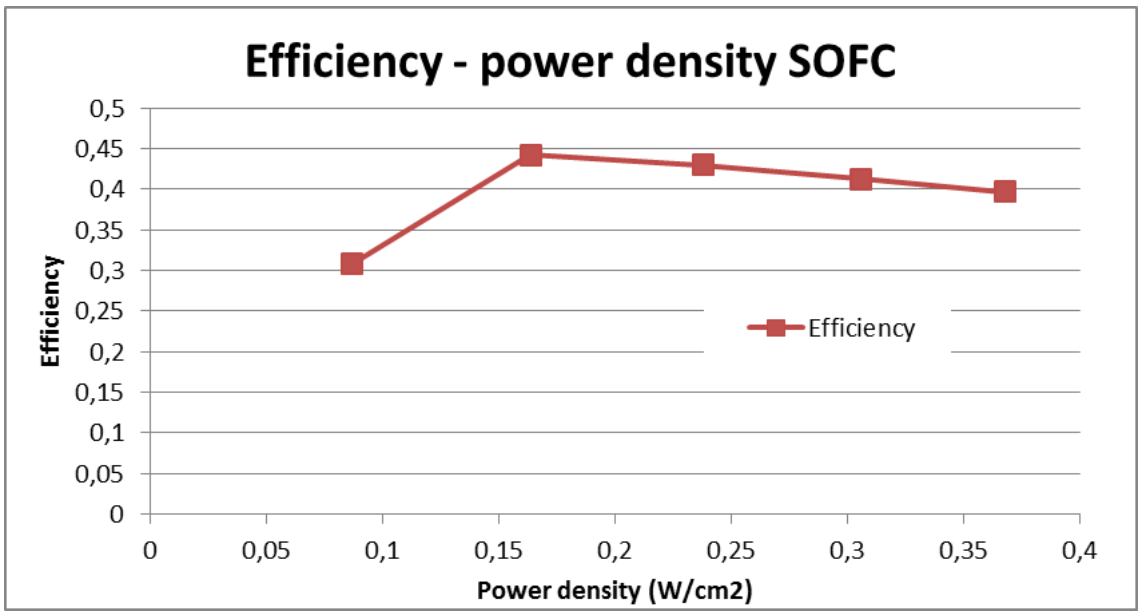


*Figure 68: SOFC efficiency - power density constant utilization test*

Unlike other power production systems, SOFC efficiency is not maximum at the maximum power. It is just the opposite; efficiency is higher at lower power level. The first part of the graph has a different shape because it corresponds to the safe area, where the utilization of fuel is lower. Efficiency is lower in the safe area because it depends on utilization of fuel and voltage, which practically does not vary in comparison with the Uf.

There is a trade-off between the operational cost and the technology cost (size of the stack). It is possible to work at high power and low efficiency with a small stack area (high operational cost and low technology cost). But it is also feasible to work at high power and high efficiency increasing the active area (low operational cost and high technology cost). The operational point can be chosen, which is a really advantage of this system.

## SOEC operation

The same analysis is also done is SOEC operation, although there are some particular aspect to be studied with reference to the hydrogen produced. The first graph showed is the same as in the previous test, voltage and power are represented:

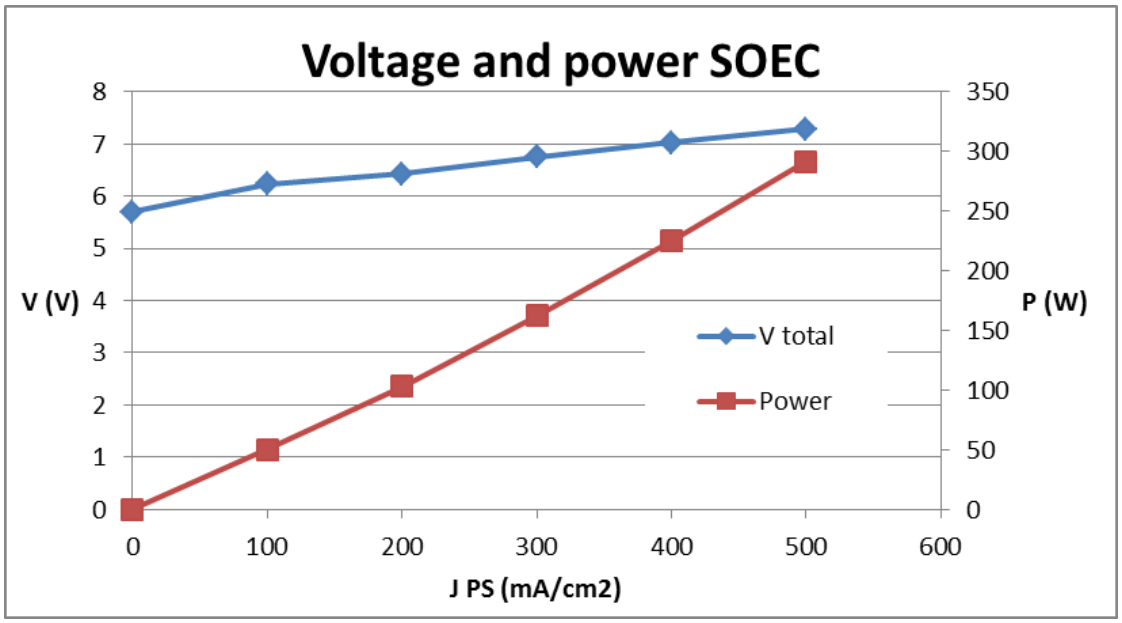


*Figure 69: SOEC voltage and power constant utilization test*

As in theoretical graphs, there are overpotentials, which represent irreversibilities during the operation of the system. The curve is a straight with a similar pending except in the first step, where the difference is due to the composition change in the safe area. Power applied to the stack increases in logic way because it is a product between voltage and current.

Regarding the thermal behaviour of the stack, it is represented in the following graph:

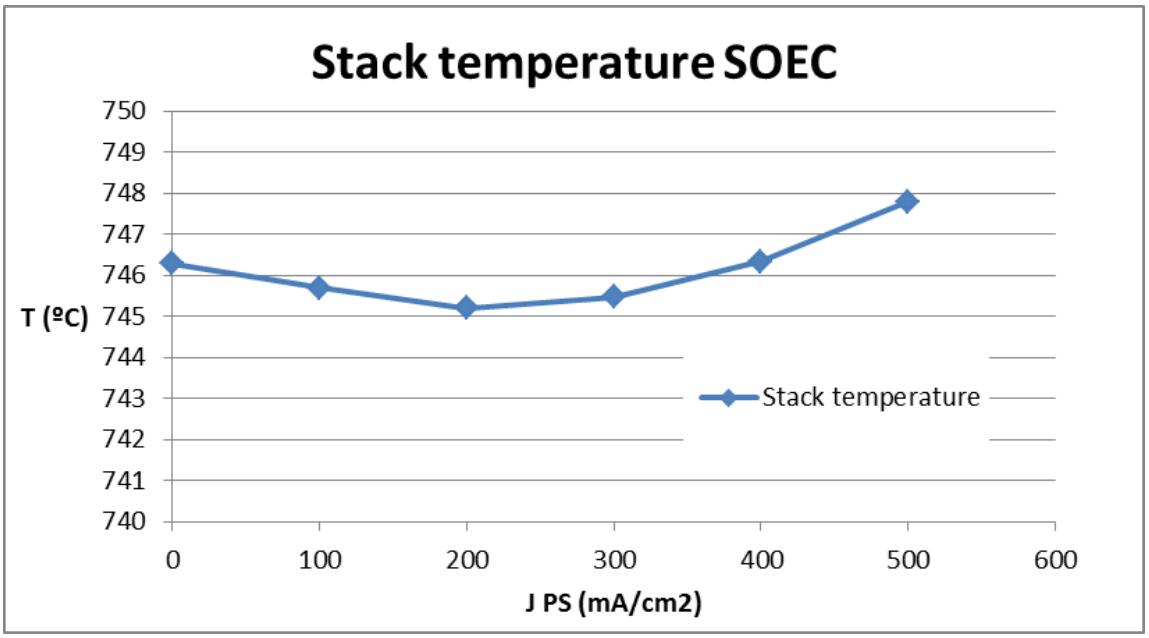


*Figure 70: SOEC thermal behaviour constant utilization test*

There are barely changes in stack temperature because the amount of air in the air inlet does not vary, as it is explained in the test plan. There is only a slightly decrease at the beginning because the stack is absorbing heat to complete the reaction until the thermo-neutral potential, which it is known that is achieved at 500 mA/cm$^2$. Near that point, a change is temperature is supposed to be produced due to the stack produce more energy than needed from that point.

With reference to the system efficiency, it is known that there are two ways of obtaining it; they are called efficiency one and two, the same as in the polarization curve tests. Both are represented with reference to the power density to check if the behaviour is the same as in SOFC operation.

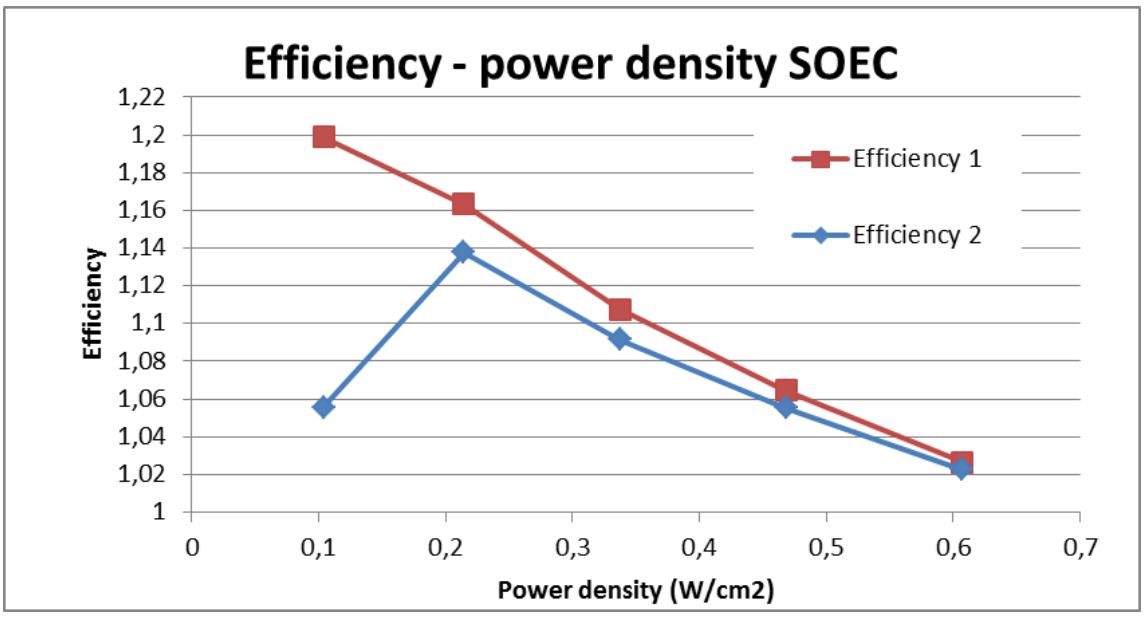


*Figure 71: SOEC efficiency - power density constant utilization test*

AS in SOFC, efficiency decreases with power density (except in the first part of the graph which corresponds to the safe area). So the maximum power is not the maximum efficiency, unlike the thermic power systems. There is not dependence between the size of the system and efficiency. In the last part of the graph, efficiency is almost 100% because the thermo-neutral potential is achieved and the heat produced and consumed are equal. Before that point, efficiency is higher than one due to heat is supplied to complete the electrolysis reaction and it does not appear in the efficiency equation. After that point, efficiency is supposed to be lower than 1 because some of the electric power applied to the system is being transformed into heat instead of producing hydrogen.

It is also quite interesting to represent efficiencies with reference to the hydrogen produced:

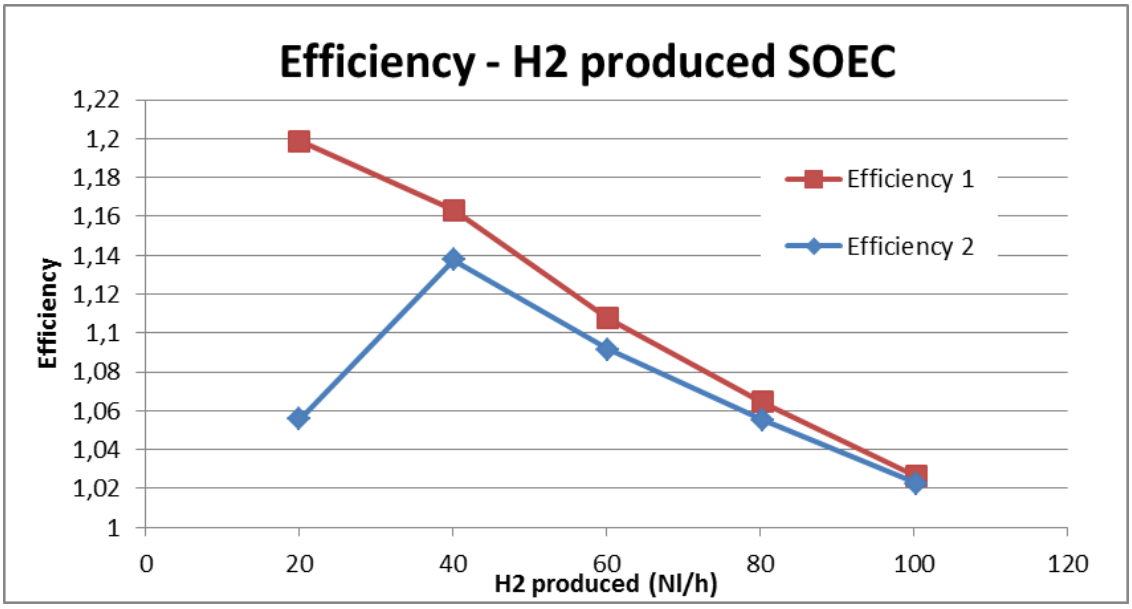


*Figure 72: SOEC efficiency - $H_2$ produced constant utilization test*

In the system studied, until 100 Nl/h $H_2$ can be produced with efficiency at least 100%. However, the system can be run at higher power to produce more hydrogen with less efficiency. The decision of the operating point is a trade-off between energies costs and operational costs.

## SOFC SOEC comparison

It is interesting to represent the power of both operating modes with reference to the current density.

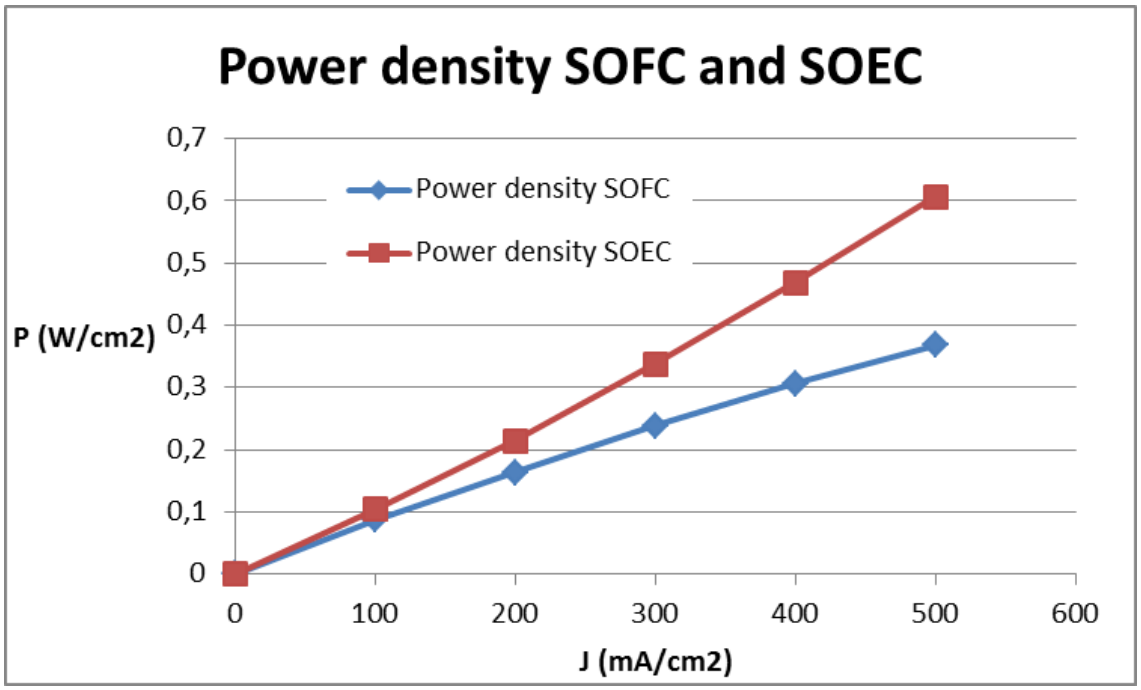


*Figure 73: SOFC and SOEC power density constant utilization test*

This graph is very representative. If the system is supposed to be run at the same power in both operating modes, there is one operating point (current) to each operating mode. So maybe it is better to work as a SOFC and SOEC at different power to be always in the same operating point correspondent to the best efficiency.

Efficiencies of both operating modes can be represented together with reference to the power density, as in the following graph:

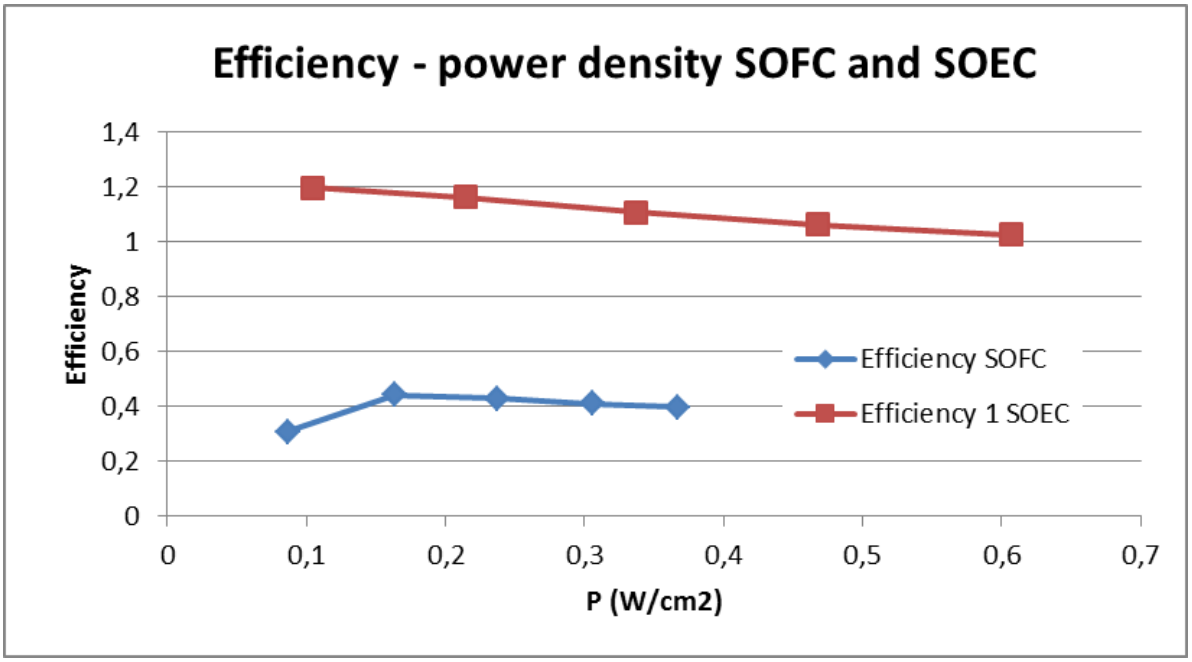


*Figure 74: SOFC and SOEC efficiency – power density constant utilization test*

Both efficiencies has the same shape in both operation modes, higher efficiency is not at higher current, this clearly set up the particularity of the system. SOEC efficiency is up to a higher value of power than the SOFC one because maximum power is not the same in SOFC and SOEC.

The following table represents the power density and the efficiency of each operating mode at the same operating point.

*Table 13: Numerical results of power density and efficiency*

| | SOFC | | SOEC | |
|---|---|---|---|---|
| J (mA/cm²) | Power density (W/cm²) | Efficiency | Power density (W/cm²) | Efficiency |
| 100 | 0,087 | 0,31 | 0.104 | 1.2 |
| 200 | 0,164 | 0,44 | 0.214 | 1.16 |
| 300 | 0,238 | 0,43 | 0,338 | 1,11 |
| 400 | 0,306 | 0,41 | 0,468 | 1,06 |
| 500 | 0,368 | 0,4 | 0,607 | 1,03 |

Considering the operating point of 500 mA/cm² (40 A) in both operating modes (different powers), the roundtrip efficiency can be calculated as the product of both efficiencies:

$$\eta_{rountrip,40A} = \eta_{SOFC,40A} * \eta_{SOEC,40A} = 0{,}4 * 1{,}03 = 0{,}436$$

The system efficiency at the selected working point is 43%, but it can be increased choosing the most efficient operating point in each operating mode:

$$\eta_{rountrip,max} = \eta_{SOFC,16A} * \eta_{SOEC,8A} = 0{,}44 * 1{,}2 = 0{,}528$$

The maximum system efficiency is 52%. This efficiency can be achieved at a higher power increasing the active area of the stack.

# 5. Conclusions

The main objective of this thesis is to verify the feasibility of running an oxide solid stack as a reSOC. As an electrolyser to produce hydrogen from water when there is electric energy excess (SOEC) and as a fuel cell to produce electric energy from the hydrogen produced previously (SOFC). This application is thought to be really useful in a near future, because of the need of suitable energy storage systems and reSOC has all the necessary requirements (efficiency, size, cost, life…). However, it is obvious that there are a lot of problems to be studied and solved to maximize the correct performance of this system, and some of them are analysed in this thesis.

One important issue of the system is the way to change from one operation mode to the other one, some problems were supposed to appear when passing from working with the load to working with the power supply. In this thesis it has been proved that the best way to operate is with both elements connected as in the electric scheme, and works the element necessary in accordance to the operation mode.

Another important issue to be studied is the fuel inlet composition; it is clear reading previous researches that it is always necessary to introduce a mix between steam and hydrogen in both operating modes, but the problem is to design what the best proportion is. After running the system in all modes with different inlet compositions, the conclusion is clear; In SOFC operation, the performance is better when the amount of steam in the inlet is lower. In SOEC operation, the performance is better when the amount of hydrogen in the inlet is lower. The best efficiencies achieved in this research are with a composition of 90% $H_2$ 10% $H_2O$ in SOFC mode and 10% $H_2$ 90% $H_2O$ in SOEC mode.

An important aspect which should be taken into account when running a stack is to avoid liquid water inside the system. To prevent that phenomenon, it is necessary the utilization of systems as the CEM and the heating line to ensure high temperature to prevent steam condensation before and after the reactions in the stack.

During SOEC operation, some instabilities appeared when the amount of hydrogen was very low. The problem was not in the stack but in the evaporator, the CEM had some problems to evaporate water when the amount of gas was not high, and it leaded to some voltage problems in the system. To solve this problem, a mix of hydrogen and nitrogen in the same proportion was introduced into the CEM to increase the amount of gas and evaporate the water easily. It is also quite important to adjust the CEM temperature, because low temperatures lead to water drops and very high temperature leads to pressure problems.

Also in SOEC operation, an important issue is to determine the operating point which corresponds to the thermo-neutral potential of the system. In this point, heat necessary to complete the reaction and heat produced coincide, so the efficiency is 100%. Thermo-neutral voltage is a theoretical value which does not depend on the system and it is 1,24 V. Looking at the polarization curves of the stack, it is possible to

determine the current value at which the cell voltage reaches that value. This happened at 40 A, the point that had been fixed as the operating point, so working at that point means high efficiency. However, it is also possible to apply more power and produce more hydrogen working less efficiently. Economic reasons have the key to determine the best operating point in each time.

During SOFC operation, temperature always increase with current because the reactions which takes place are exothermic, the only way to counter this temperature increase is managing the amount of air in the cathode, which is "free". Trying to keep the heat produced during this operation is a huge challenge, because as it is explained in the thermal behaviour section, SOEC performance will be improved by applying heat, getting even more than 100% efficiency.

One important conclusion with reference to both operating modes is the relation between efficiency and power. Results have demonstrated that there is an inverse relation between both terms. As the operational point can be chosen, efficiency can be increased not only reducing the power but also increasing the cell active area. There is a trade-off between the operational cost and the technology cost (size of the stack), and there is not dependence between efficiency and size.

After running the first essay, it was realised that there have been a problem with cell 6, whose behaviour was totally worse than the others. To solve it in the following essay, the utilization of oxygen was changed from 0,3 to 0,25. Doing so, the amount of air increased and the bad performance of the cell was minimised.

With all point explained above, it seems clear that reSOC has a huge potential in terms of energy storage. Above all, if reSOC works with a nuclear power plant to take advantage of the heat produced by it. Only stability problems and problems related to the balance of plant has to be solved to start commercialising this technology. The main problem is the lack of specific necessary elements to run the system due to the lack of market. However, they are thought to be solved in the near future.

# 6. References


[1] I. EG&G Technical Services, Fuel Cell Handbook (seventh edition), Morgantown, West Virginia 26507-0880: U.S. Department of Energy Office of Fossil Energy, National Energy Technology Laboratory, P.O. Box 880, November 2004.

[2] Ph.D, Giovanni Cinti, "fclab Universitá degli studi di Perugia Dipartimento di Ingegneria Industriale," [Online]. Available: http://www.fclab.unipg.it/download.html. [Accessed 16 03 2016].

[3] Byeong Wan Kwon, Caleb Ellefson, Joe Breit, Jinsoo Kim, M. Grant Norton, Su Ha, "Molybdenum dioxide-based anode for solid oxide fuel cell applications," Elsevier, 2013.

[4] Kendall, Subhash C Singhal and Kevin, High Temperature Solid Oxide Fuel Cells, Elsevier, 2003.

[5] Massimiliano Cimenti and Josephine M. Hill, "Direct Utilization of Liquid Fuels in SOFC for Portable Applications: Challenges for the Selection of Alternative Anodes," Energies, Department of Chemical and Petroleum Engineering, Schulich School of Engineering, University of Calgary, 2500 University Dr. NW, Calgary, AB T2N 1N4, Canada, 2009.

[6] A.H. Abdol Rahim, Alhassan Salami Tijani, S.K. Kamarudin, S. Hanapi, "An overview of polymer electrolyte membrane electrolyzer for hydrogen production: Modeling and mass transport," Elsevier, Malaysia, 2016.

[7] Daniele Penchini, Giovanni Cinti, Gabriele Discepoli, Umberto Desideri, "Theoretical study and performance evaluation of hydrogen production by 200 W solid oxide electrolyzer stack," Elsevier, University of Perugia, Department of Engineering, Via G. Duranti 67, 06125 Perugia, Italy, 2014.

[8] Lei Bi, Samir Boulfrad and Enrico Traversa, "Steam electrolysis by solid oxide electrolysis cells (SOECs) with proton-conducting oxides," Royal society of chemistry, 2014.

[9] Wikipedia, "Polymer electrolyte membrane electrolysis".

[10] M.A. Laguna-Bercero, "Recent advances in high temperature electrolysis using solid oxide fuel cells: A review," Elsevier, Instituto de Ciencia de Materiales de Aragón, ICMA, CSIC – Universidad de Zaragoza, 2012.

[11] Marcelo Carmo, David L. Fritz, Jürgen Mergel, Detlef Stolten, "A comprehensive review on PEM water electrolysis," Elsevier, Hydrogen Energy Publications, 2013.

[12] Christopher Graves, Sune D. Ebbesen, Mogens Mogensen, Klaus S. Lackner, “Sustainable hydrocarbon fuels by recycling CO2 and H2O with renewable or nuclear energy,” Elsevier, 500 West 120th Street, 918 S.W. Mudd MC4711, New York, NY 10027, USA, 2010.

[13] “hydrogenious technologies,” [Online]. Available: http://www.hydrogenious.net/en/energy-storage/. [Accessed 5 6 2016].

[14] P. D. Giorgio, “A new concept for ReSOC plant for EES,” Pisa, 2015.

[15] J. B. Hansen, “Syngas routes to alternative fuels,” 8 10 2014. [Online]. Available: http://www.slideshare.net/EBAconference/23-john-bogild-hansen. [Accessed 11 5 2016].

[16] “SOFC POWER,” [Online]. Available: http://www.htceramix.ch/upload/ASC-700_ASC-800.pdf. [Accessed 11 5 2016].

[17] [Online]. Available: http://www.testequipmentdepot.com/bk-precision/electronic-load/8510.htm. [Accessed 18 5 2016].

[18] [Online]. Available: http://www.keysight.com/en/pd-839148-pn-N5763A/power-supply-125v-120a-1500w?cc=IT&lc=ita. [Accessed 18 5 2016].

[19] B. high-tech, “Liquid Delivery System with Vapour Control CEM”.

[20] Domenico Ferrero, Andrea Lanzini, Massimo Santarelli, Pierluigi Leone, “A comparative assessment on hydrogen production from low- and high-temperature electrolysis,” Elsevier, Department of Energy (DENERG), Politecnico di Torino, Corso Duca degli Abruzzi 24, 10129 Turin, Italy, 2013.

[21] Frano Barbir, “PEM electrolysis for production of hydrogen from renewable energy sources,” Elsevier, Connecticut Global Fuel Cell Center, University of Connecticut, 44 Weaver Road, Unit 5233 Storrs, CT 06269-5233, United States, 2004.